AMADEUS results and future plan

Jagellonian University
Kraków 7 June 2017

Kristian Piscicchia*
Laboratori Nazionali di Frascati (INFN)
Museo Storico della Fisica e Centro Studi e Ricerche Enrico Fermi

kristian.piscicchia@lnf.infn.it

Low-energy QCD in the u-d-s sector

$$\mathcal{L}_{eff} = \mathcal{L}_{mesons}(\Phi) + \mathcal{L}_B(\Phi, \Psi_B)$$

- Chiral perturbation theory: interacting systems of N-G bosons (pions, kaons) coupled to baryons works well for ππ, πN, K^+N ..
  NOT for K^-N !!

- $K^- = (s\bar{u})$ strangeness = -1 , $K^+ = (\bar{u}s)$ strangeness = +1

  strange baryons stable respect to strong interaction all have s = -1

- the sub-threshold region is dominated by resonances → complex multichannel dynamics
  Λ(1405) just below $\bar{K}N$ threshold (1432 MeV)

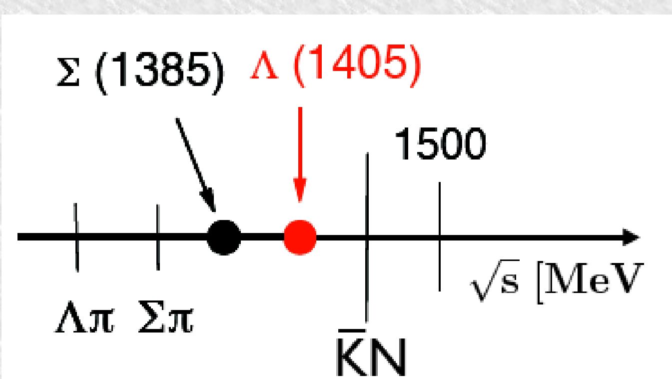

⟶

Possible solutions:

- Non-perturbative Coupled Channels approach: Chiral Unitary SU(3) Dynamics
- phenomenological $\bar{K}N$ and NN potentials

The Λ(1405) case

Mass = $1405.1^{+1.3}_{-1.0}$ MeV,
Width = 50.5 ± 2.0 MeV
$I = 0$, $S = -1$, $J^p = 1/2^-$,
Status: **** ,
strong **decay** into Σπ

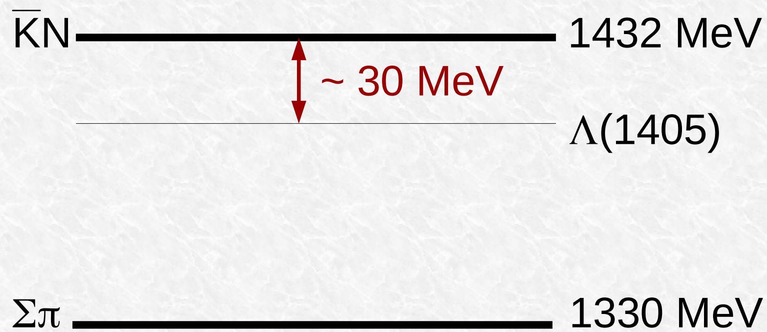

- 3 quark?
- **molecular?**
- **K̄N bound state?**
- pentaquark?

Theoretical prediction Dalitz-Tuan (1959)

First experimental evidence:

M. H. Alston, et al., Phys. Rev. Lett. 6 (1961) 698

$K^- p \rightarrow \pi\pi\pi\Sigma$

Λ(1405)

Λ(1116)

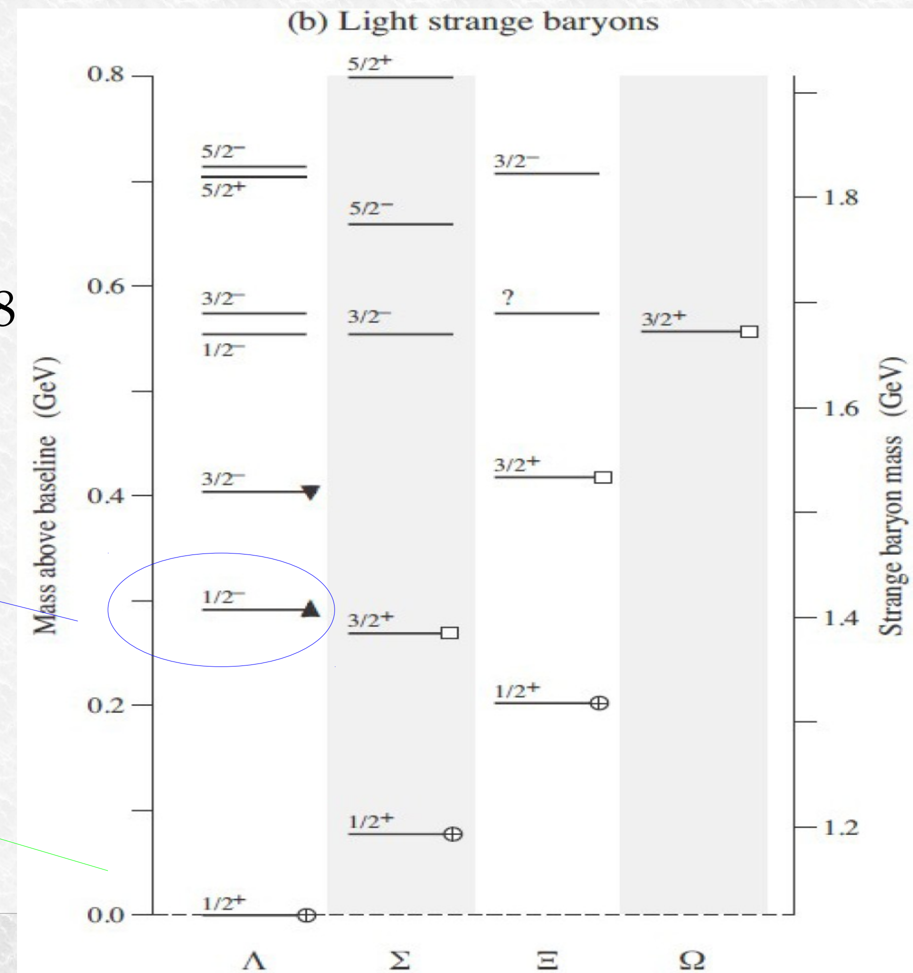

The Λ(1405) case

Λ(1405) is located slightly below the $\bar{K}N$ threshold (1432 MeV)

Three quark model picture difficulties to reproduce the Λ(1405):

- According to its negative parity, one of the quarks has to be excited to $l = 1$

- nucleon sector, we find the N(1535) → the expected mass of the Λ^* is around 1700 MeV

- too big energy splitting observed between the Λ(1405) and the Λ(1520) interpreted as the spin-orbit partner ($J^p = 3/2^-$).

- pentaquark (4q + qbar in $l = 0$), but also predicts other, unobserved, excited baryons,

R. Dalitz and collaborators first suggested to interpret Λ(1405) as an KN quasibound state.

R.H. Dalitz, T.C. Wong and G. Rajasekaran, Phys. Rev. **153** (1967) 1617.

The $\Lambda(1405)$ case

BUBBLE CHAMBER search of the $\Lambda(1405)$:

- O. Braun et al. Nucl. Phys. B129 (1977) 1

K- induced reactions on d $\rightarrow$ $\Sigma^- \pi^+ n$ the resonance is found & 1420 MeV

- D. W. Thomas et al., Nucl. Phys. B56 (1973) 15

pion induced reaction $\pi^- p \rightarrow K^+ \pi \Sigma$ the resonance is found & 1405 MeV

- R. J. Hemingway, Nucl. Phys. B253 (1985) 742

$K^- p \rightarrow \pi^- \Sigma^+(1660) \rightarrow \pi^- (\pi^+ \Lambda(1405)) \rightarrow \pi^- \pi^+ (\pi\Sigma)$ & 4.2 GeV

analysed by Dalitz and Deloff $M = 1406.5 \pm 4.0$ MeV, $\Gamma = 50 \pm 2$MeV

The Λ(1405) case

THE "LINE-SHAPE" OF THE Λ(1405) DEPENDS ON THE OBSERVED CHANNEL !!

$$\frac{d\sigma(\Sigma^-\pi^+)}{dM} \propto \frac{1}{3}\left|T^0\right|^2 + \frac{1}{2}\left|T^1\right|^2 + \frac{2}{\sqrt{6}} Re(T^0 T^{1*})$$

$$\frac{d\sigma(\Sigma^+\pi^-)}{dM} \propto \frac{1}{3}\left|T^0\right|^2 + \frac{1}{2}\left|T^1\right|^2 - \frac{2}{\sqrt{6}} Re(T^0 T^{1*})$$

$$\frac{d\sigma(\Sigma^0\pi^0)}{dM} \propto \frac{1}{3}\left|T^0\right|^2$$

The Λ(1405) case

THE "LINE-SHAPE" OF THE Λ(1405) DEPENDS ON THE OBSERVED CHANNEL !!

$$\frac{d\sigma(\Sigma^-\pi^+)}{dM} \propto \frac{1}{3}\left|T^0\right|^2 + \frac{1}{2}\left|T^1\right|^2 + \frac{2}{\sqrt{6}}Re(T^0T^{1*})$$

$$\frac{d\sigma(\Sigma^+\pi^-)}{dM} \propto \frac{1}{3}\left|T^0\right|^2 + \frac{1}{2}\left|T^1\right|^2 - \frac{2}{\sqrt{6}}Re(T^0T^{1*})$$

$$\frac{d\sigma(\Sigma^0\pi^0)}{dM} \propto \frac{1}{3}\left|T^0\right|^2$$

IS DIFFERENT IN $\Sigma^+\pi^-$ VS $\Sigma^-\pi^+$

DUE TO ISOSPIN INTERFERENCE

The Λ(1405) case

THE "LINE-SHAPE" OF THE Λ(1405) DEPENDS ON THE OBSERVED CHANNEL !!

$$\frac{d\sigma(\Sigma^-\pi^+)}{dM} \propto \frac{1}{3}\left|T^0\right|^2 + \frac{1}{2}\left|T^1\right|^2 + \frac{2}{\sqrt{6}} Re(T^0 T^{1*})$$

$$\frac{d\sigma(\Sigma^+\pi^-)}{dM} \propto \frac{1}{3}\left|T^0\right|^2 + \frac{1}{2}\left|T^1\right|^2 - \frac{2}{\sqrt{6}} Re(T^0 T^{1*})$$

$$\frac{d\sigma(\Sigma^0\pi^0)}{dM} \propto \frac{1}{3}\left|T^0\right|^2$$

IS DIFFERENT IN $\Sigma^+\pi^-$ VS $\Sigma^-\pi^+$

DUE TO ISOSPIN INTERFERENCE

THE CLEANEST SIGNATURE OF THE Λ(1405) IS GIVEN BY THE NEUTRAL CHANNEL:

- is free from isospin interference
- is purely I = 0, no Σ(1385) contamination.

Λ(1405) .. the golden channel

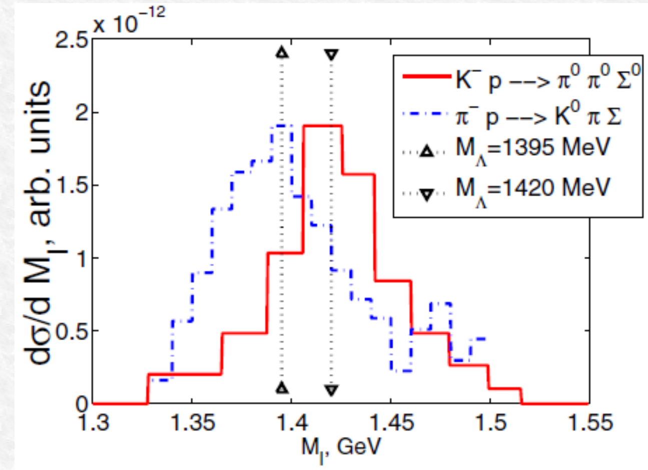

Crystall Ball: K-p $\rightarrow$ **$\Sigma^0\pi^0\pi^0$** for kaon momentum in the range (514-750 MeV/c). S. Prakhov et al. Phys Rev. C70 (2004) 03465

(**interpreted by Magas et al. PRL 95, 052301 (2005)**)

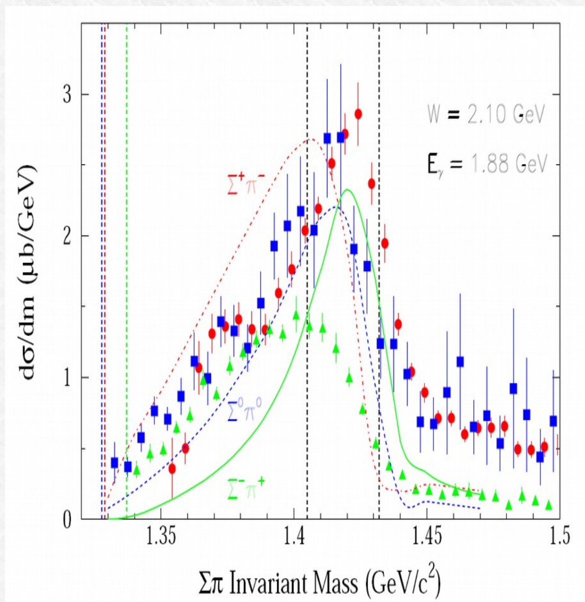

CLAS: γ p $\rightarrow$ K+ **Σπ**

AIP Conf.Proc. 1441 (2012) 296-298

COSY julich: pp $\rightarrow$ pK+ **$\Sigma^0\pi^0$**

(I. Zychor et al., Phys. Lett. B 660 (2008) 167)

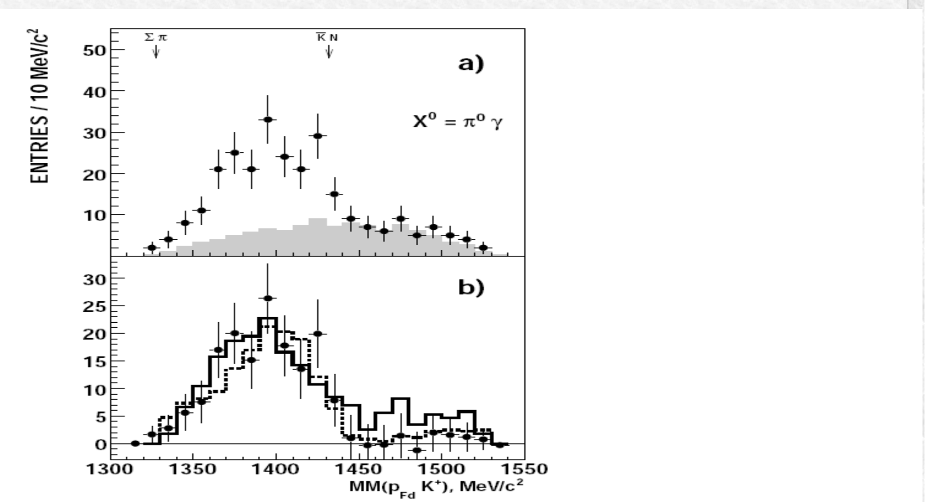

Fig. 4. a) Missing–mass $MM(p_{Fd}K^+)$ distribution for the $pp \rightarrow pK^+p\pi^-X^0$ reaction for events with $M(p_{Sd}\pi^-) \approx m(\Lambda)$ and $MM(pK^+p\pi^-) > 190\,\mathrm{MeV/c^2}$. Exper-

Λ(1405) .. the golden channel

Crystall Ball: K-p $\rightarrow \Sigma^0\pi^0\pi^0$ for kaon momentum in the range (514-750 MeV/c). S. Prakhov et al. Phys Rev. C70 (2004) 03465

(Magas et al. PRL 95, 052301 (2005))

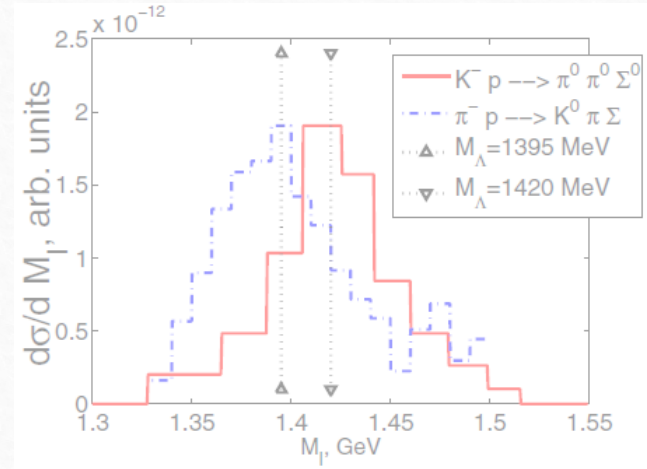

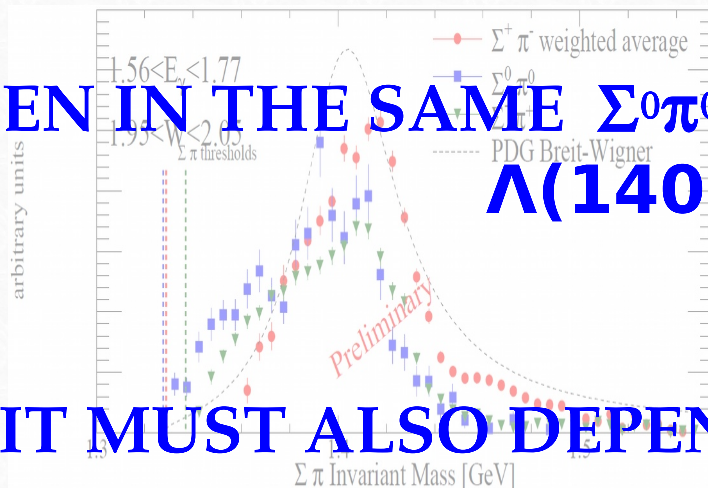

EVEN IN THE SAME $\Sigma^0\pi^0$ THE "LINE-SHAPE" OF THE Λ(1405) CHANGES

CLAS: $\gamma p \rightarrow pK^+ \Sigma\pi$

AIP Conf.Proc. 1441 (2012) 296-298

IT MUST ALSO DEPEND ON THE PRODUCTION MECHANISM

COSY julich: pp $\rightarrow$ pK+ $\Sigma^0\pi^0$

(I. Zychor et al., Phys. Lett. B 660 (2008) 167)

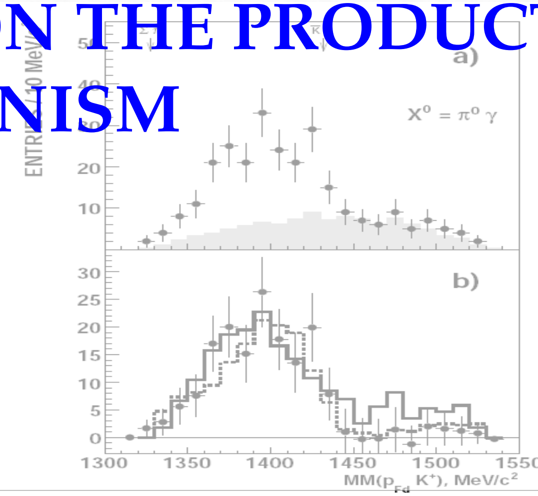

Fig. 4. a) Missing–mass $MM(p_{Fd}K^+)$ distribution for the $pp \rightarrow pK^+p\pi^-X^0$ reaction for events with $M(p_{Sd}\pi^-) \approx m(\Lambda)$ and $MM(pK^+p\pi^-) > 190\,\mathrm{MeV/c^2}$. Exper-

The Λ(1405) case

- Chiral unitary models: Λ(1405) is an I = 0 quasibound state emerging from the coupling between the $\bar{K}N$ and the Σπ channels. Two poles in the neighborhood of the Λ(1405):

two poles: about 1420 ; about = 1380 MeV

Phys. Lett. B 500 (2001), Phys. Rev. C 66 (2002), (Nucl. Phys. A 725(2003) 181) .. many others .. (Nucl. Phys. A881, 98 (2012)) .. others

mainly coupled to $\bar{K}N$ mainly coupled to Σπ → line-shape depends on production mechanism

- Akaishi-Esmaili-Yamazaki phenomenological potential

Phys. Lett. B 686 (2010) 23-28 Confirmation of single pole ansatz?

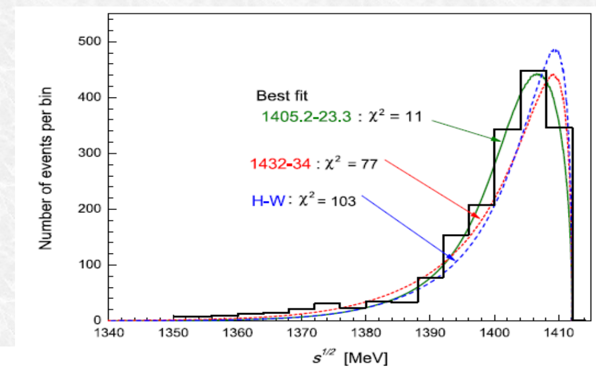

Fig. 6. Detailed differences in $M_{\Sigma\pi}$ spectra among the Hyodo–Weise prediction and the present model predictions.

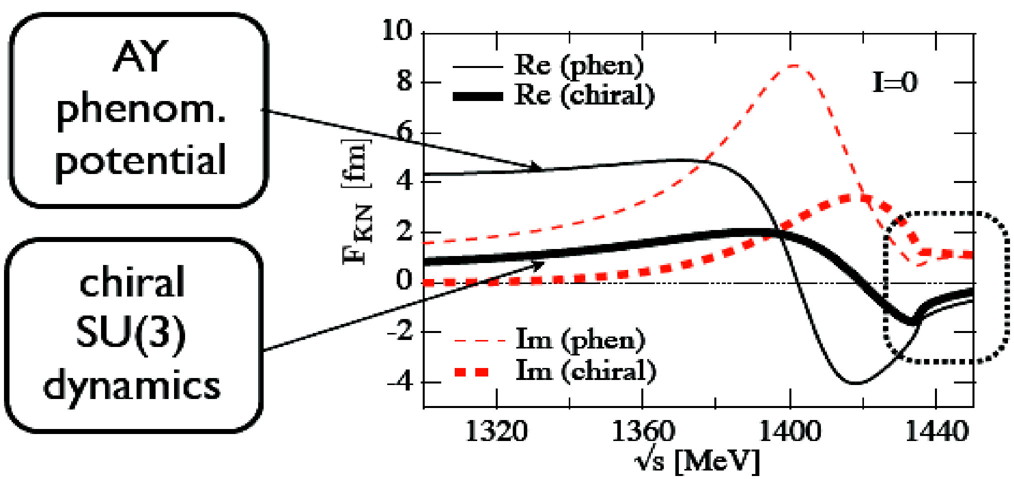

large differences in **subthreshold** extrapolations

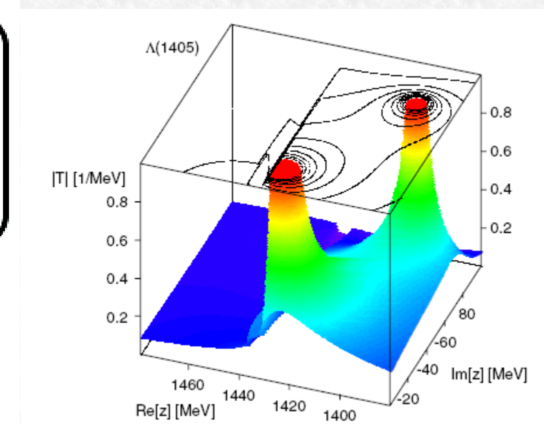

- **Chiral dynamics** predicts significantly **weaker attraction** than AY (local, energy independent) potential in **far-subthreshold** region

The Λ(1405) case

Two main biases:

- the kinematical energy threshold 1412 MeV

($M_K + M_p$ - | BE_p |) the high pole energy region is closed,

- The shape and the amplitude of the NON-RESONANT

$\Sigma\pi$ production below KbarN threshold is unknown.

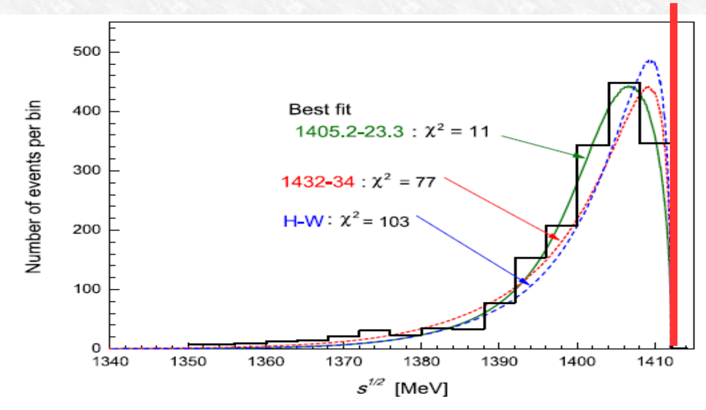

Fig. 6. Detailed differences in $M_{\Sigma\pi}$ spectra among the Hyodo–Weise prediction and the present model predictions.

An ideal experiment:

- Λ(1405) is produced in K- p absorption → mainly coupled to the high mass pole,
- Λ(1405) is observed in the $\Sigma^0\pi^0$ decay channel (pure isospin 0),
- K- is absorbed in-flight on a bound proton with p_K ~ 100 MeV, $\Sigma\pi$ invariant mass gain of ~ 10 MeV to open an energy window to the high mass pole.
- Knowledge of the $\Sigma\pi$ NON-RESONANT production amplitude.

AMADEUS & DAΦNE

DAΦNE

- double ring e^+e^- collider working at C.M. energy of ϕ, producing **≈ 1000 ϕ /s**

$\phi \rightarrow K^+K^-$ (BR = (49.2 ± 0.6)%)

- **low momentum** Kaons ≈ 127 Mev/c
- **back to back** K^+K^- topology

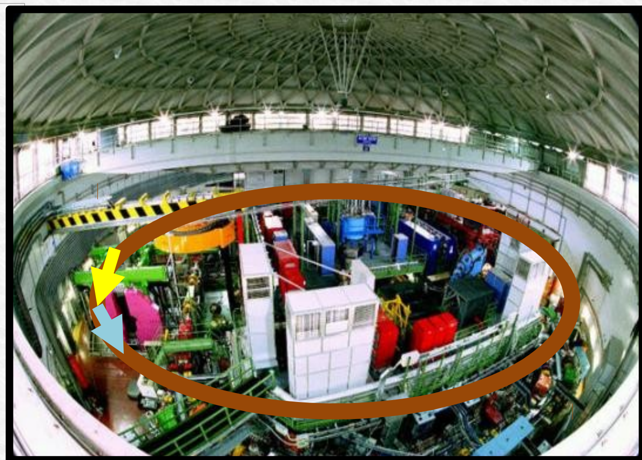

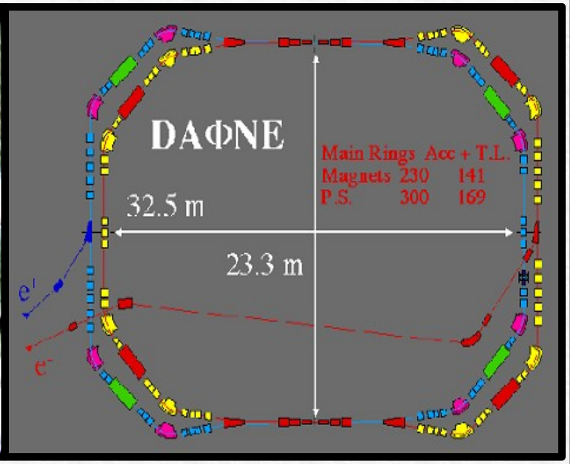

AMADEUS step 0 → KLOE 2004-2005 dataset analysis ($\mathscr{L}$ = 1.74 pb^{-1})

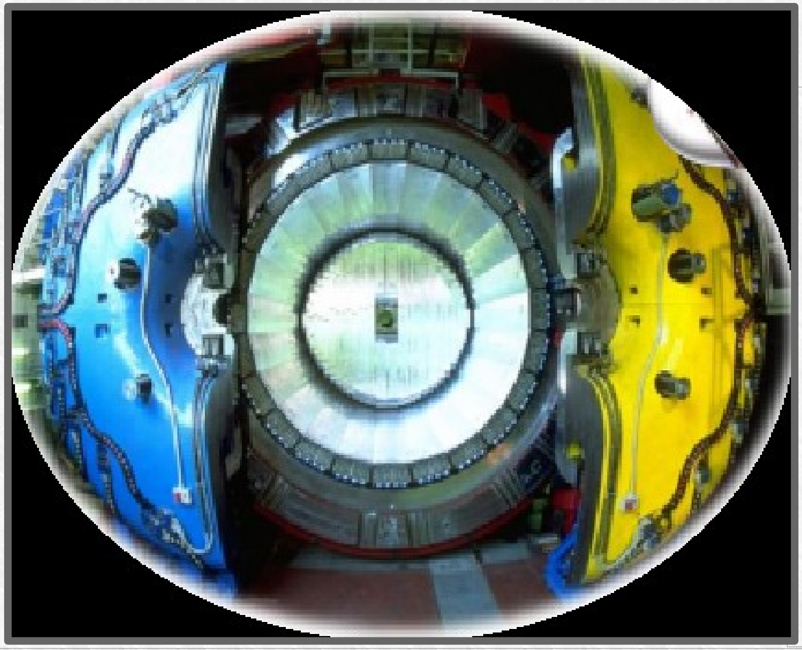

KLOE

- Cilindrical drift chamber with a **4π geometry** and electromagnetic calorimeter
- **96% acceptance**
- optimized in the energy range of all **charged particles** involved
- **good performance** in detecting **photons and neutrons** checked by kloNe group [M. Anelli et al., Nucl Inst. Meth. A 581, 368 (2007)]

K^- absorption on light nuclei

from the materials of the KLOE detector

DC gas (90% He, 10% C_4H_{10}) & DC wall (C + H)

AT-REST (K^- absorbed from atomic orbit) or IN-FLIGHT (p_K~100MeV)

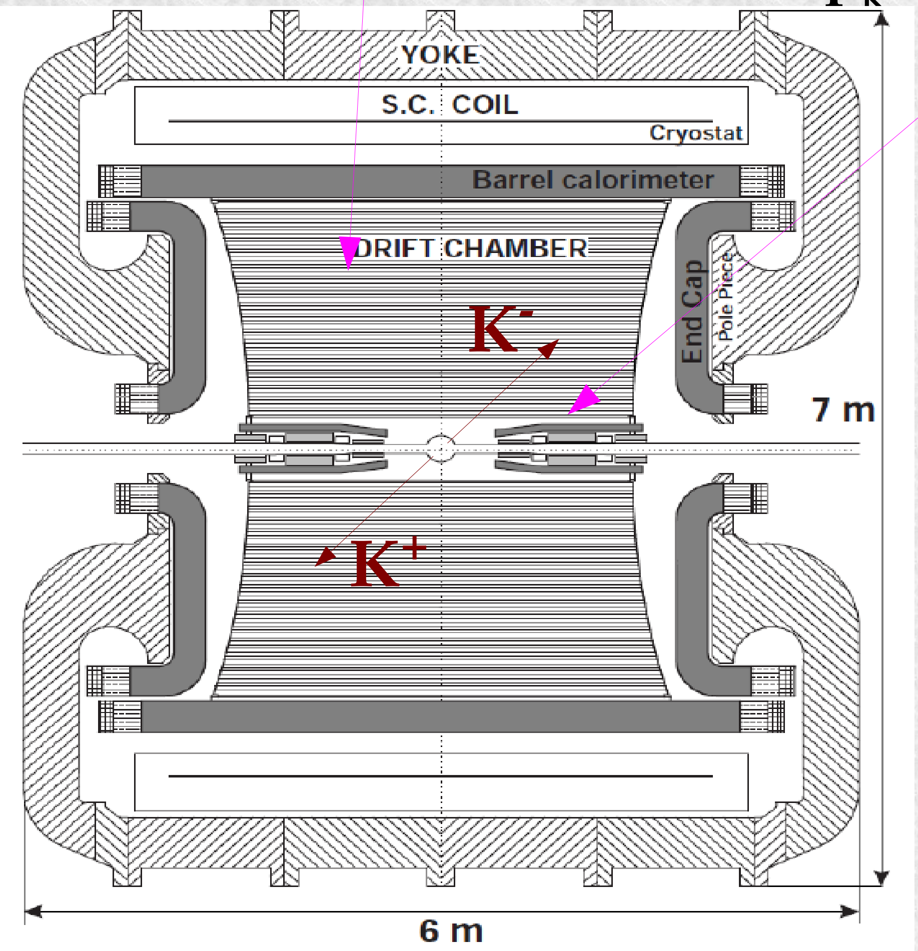

Advantage:
excellent resolution ..
$\sigma_{p\Lambda}$ = 0.49±0.01 MeV/c in DC gas
$\sigma_{m\gamma\gamma}$ = 18.3±0.6 MeV/c^2

Disadvantage:
Not dedicated target → different nuclei contamination → complex interpretation .. but → new features .. K^- in flight absorption.

At-rest VS in-flight K^- captures

AT-REST

K^- absorbed from atomic orbit

($p_K \sim$ 0 MeV)

IN-FLIGHT

($p_K \sim$100MeV)

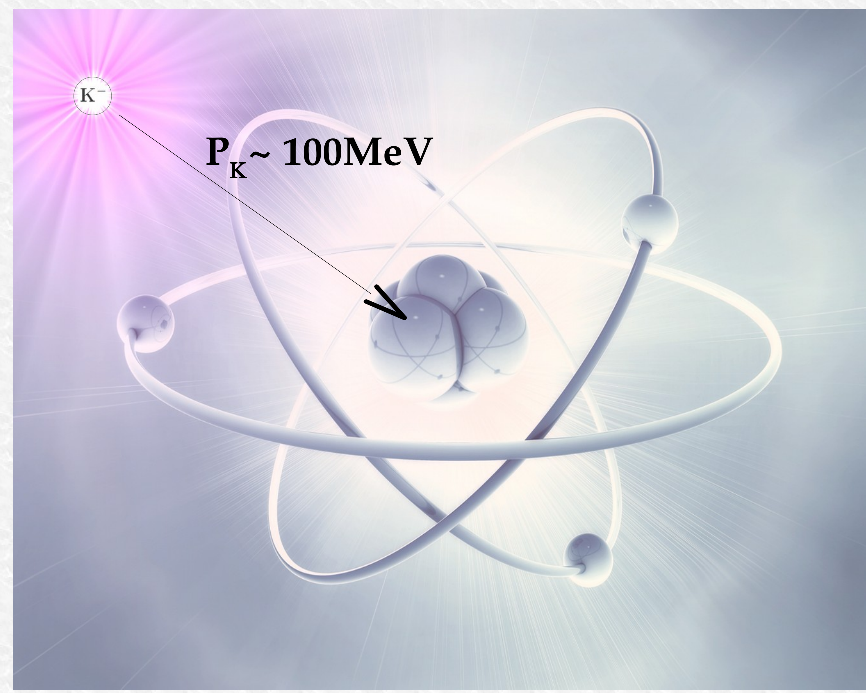

The scientific goal of AMADEUS

Low energy QCD in strangeness sector is still waiting for experimental conclusive constrains on:

1) $\bar{K}$-N potential → how deep can an antikaon be bound in a nucleus?

- U_{KN} strongly affects the position of the $\Lambda(1405)$ state → we investigate it through $(\Sigma\text{-}\pi)^0$ decay --- Y π CORRELATION

- if U_{KN} is strongly attractive then K^- NN bound states should appear → we investigate through (Λ/Σ-N) decay --- Y N CORRELATION

2) Y-N potential → extremely poor experimental information from scattering data

- U_{YN} determines the strength of the final state YN (elastic & inelastic) scattering in nuclear environment → could be tested by Y N CORRELATION

The scientific goal of AMADEUS

Low energy QCD in strangeness sector is still waiting for experimental conclusive constrains on:

1) $\bar{K}$-N potential → how deep can an antikaon be bound in a nucleus?

- U_{KN} strongly affects the position of the $\Lambda(1405)$ state → we investigate it through $(\Sigma\text{-}\pi)^0$ decay --- Y π CORRELATION

- if U_{KN} is strongly attractive then K^- NN bound states should appear → we investigate through (Λ/Σ-N) decay --- Y N CORRELATION

2) Y-N potential → extremely poor experimental information from scattering data

- U_{YN} determines the strength of the final state YN (elastic & inelastic) scattering in nuclear environment → could be tested by Y N CORRELATION

K^- - N single nucleon absorption the case of the $\Lambda(1405)$

Λ(1405) case

Phys.Rev.Lett.95:052301,2005

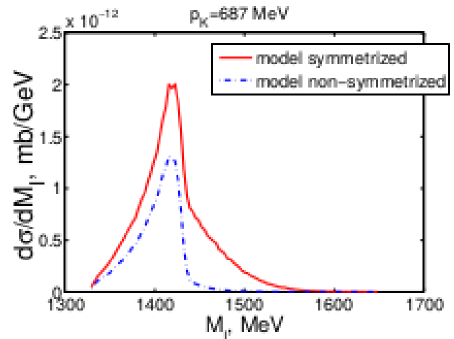

FIG. 4: Theoretical $(\pi^0\Sigma^0)$ invariant mass distribution for an initial kaon lab momenta of 687 MeV. The non-symmetrized distribution also contains the factor 1/2 in the cross section.

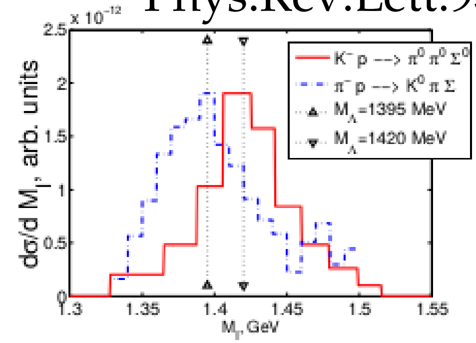

FIG. 5: Two experimental shapes of Λ(1405) resonance. See text for more details.

$p_{\pi 0}$ **resolution**: $\sigma_p \approx 12$ MeV/c

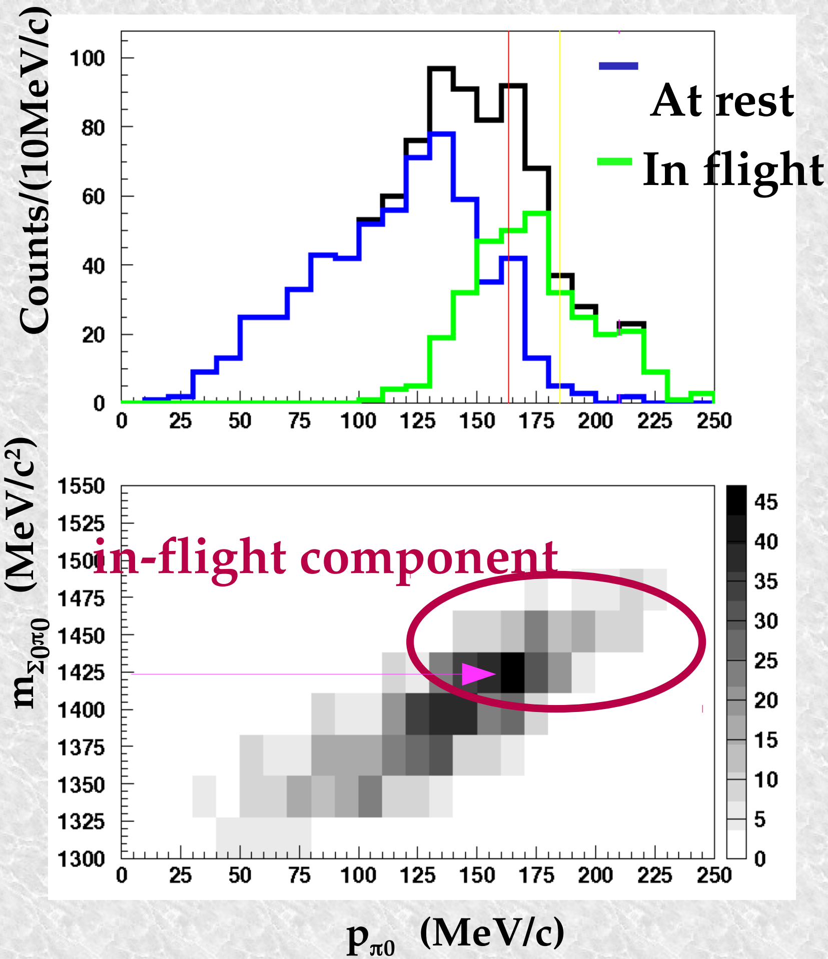

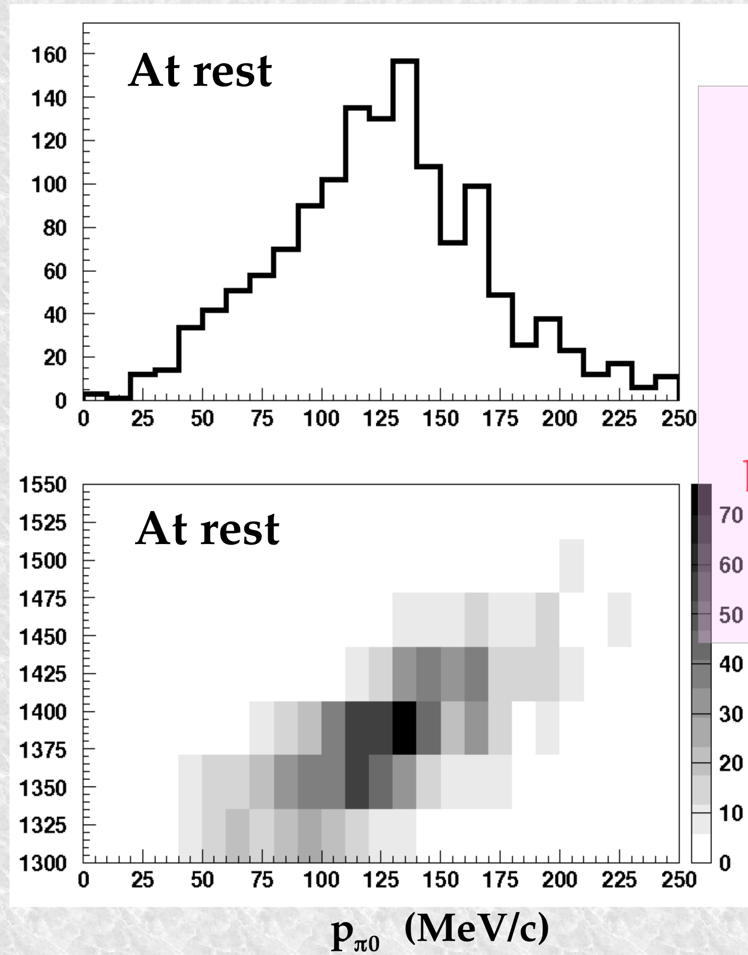

IN-FLIGHT

K- 12C

opens a window

between 1416 MeV

and K-Nth

Complex interpretation due to K- H absorptions ongoing with the collaboration of A. Cieply (UJF, Prague)

$p_{\pi 0}$ **resolution**: $\sigma_p \approx 12$ MeV/c

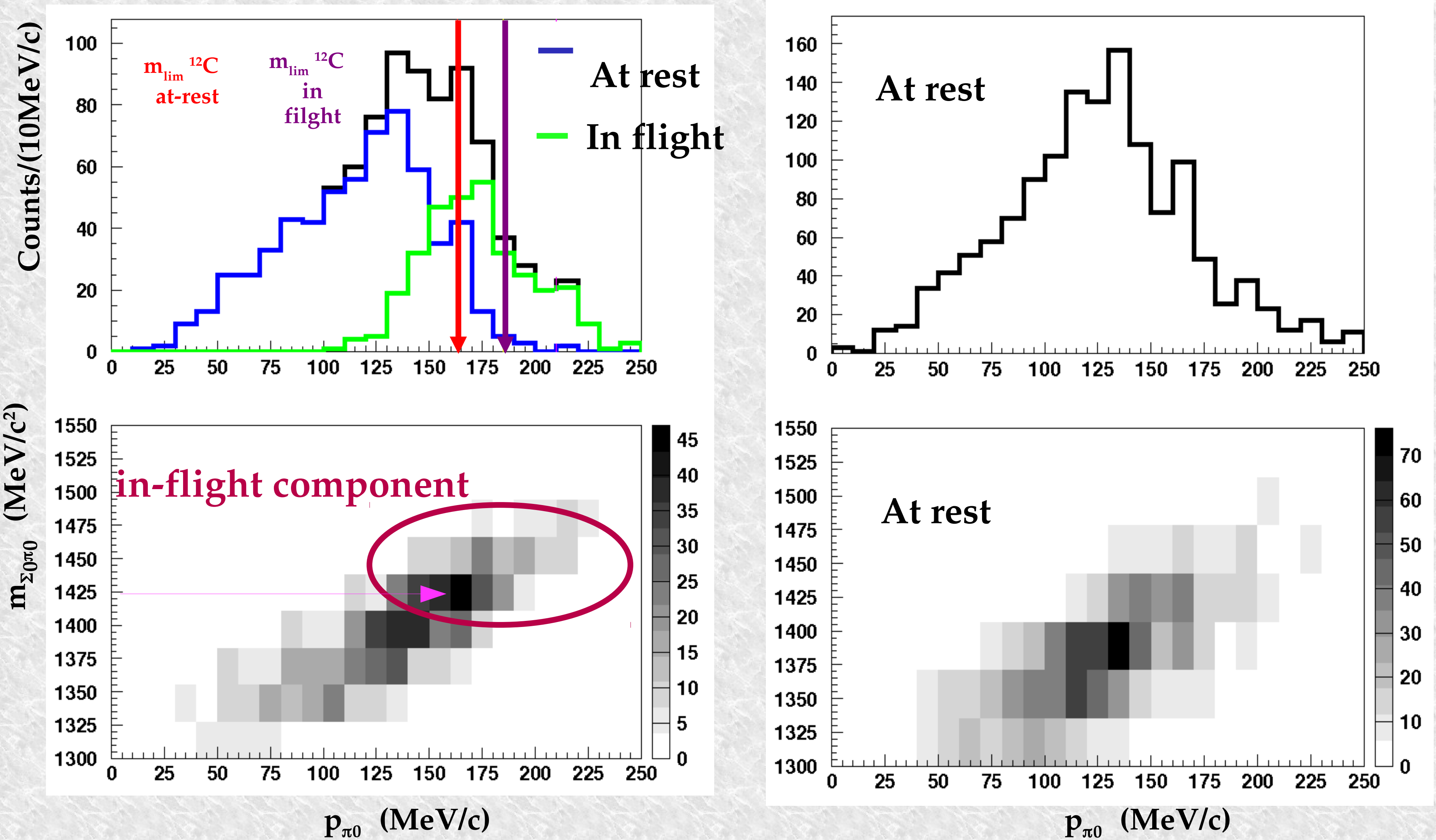

$\Sigma^+\pi^-$ correlation

$K^- p \rightarrow \Sigma^+ \pi^-$ detected via: $(p\pi^0)\ \pi^-$

Possibility to disentangle: Hydrogen, in-flight, at-rest, K^- capture

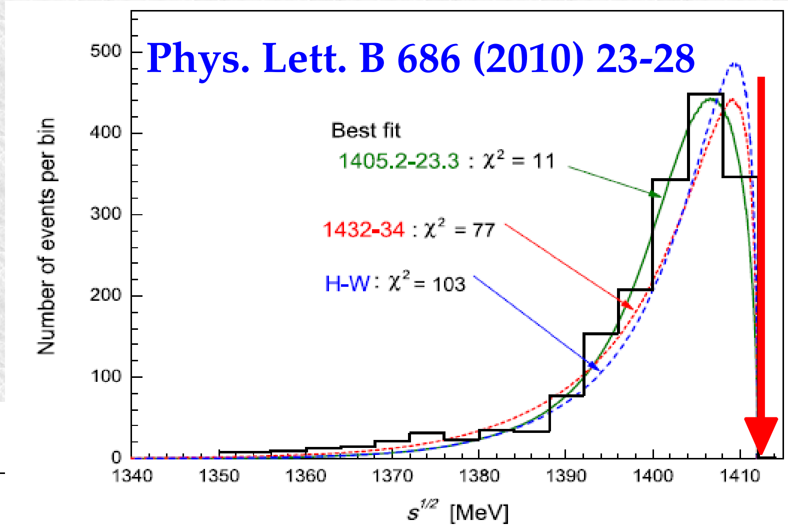

Fig. 6. Detailed differences in $M_{\Sigma\pi}$ spectra among the Hyodo–Weise prediction and the present model predictions.

$p_{\pi-}$ resolution: $\sigma_p \approx 1$ MeV/c

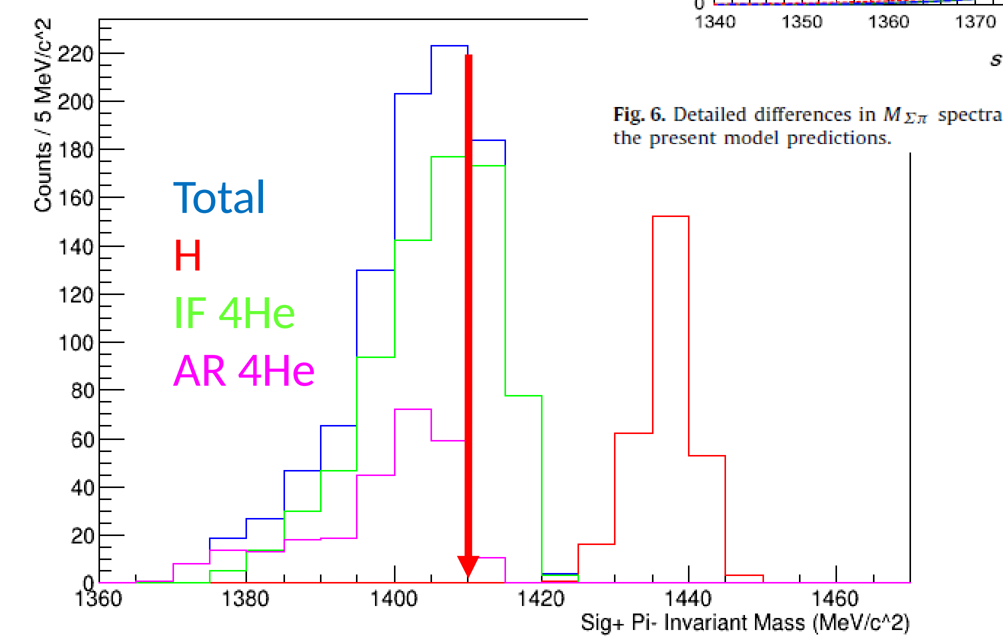

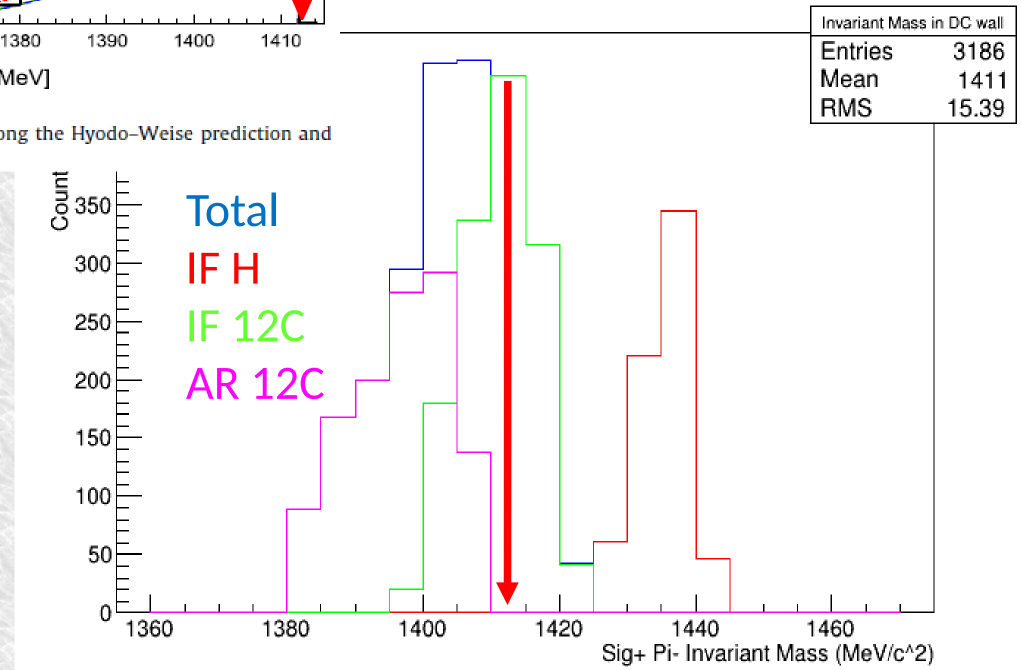

$\Sigma^+\pi^-$ correlation

$K^- p \rightarrow \Sigma^+ \pi^-$ detected via: $(p\pi^0)\ \pi^-$

Possibility to disentangle: Hydrogen, in-flight, at-rest, K^- capture

if resonant production contribution is important a high mass component appears!

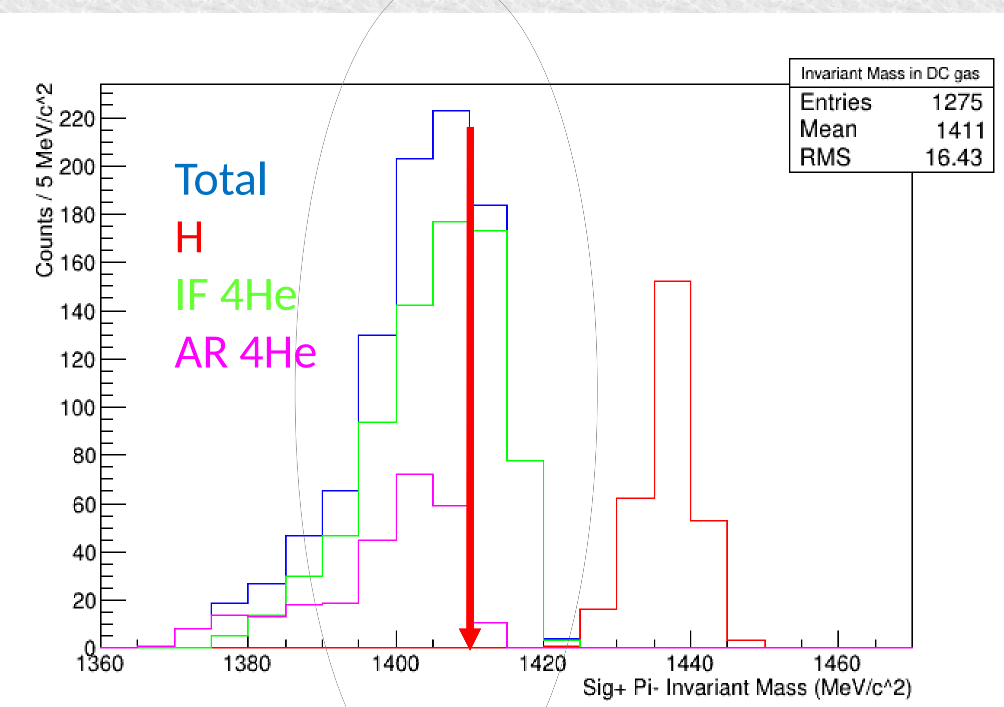

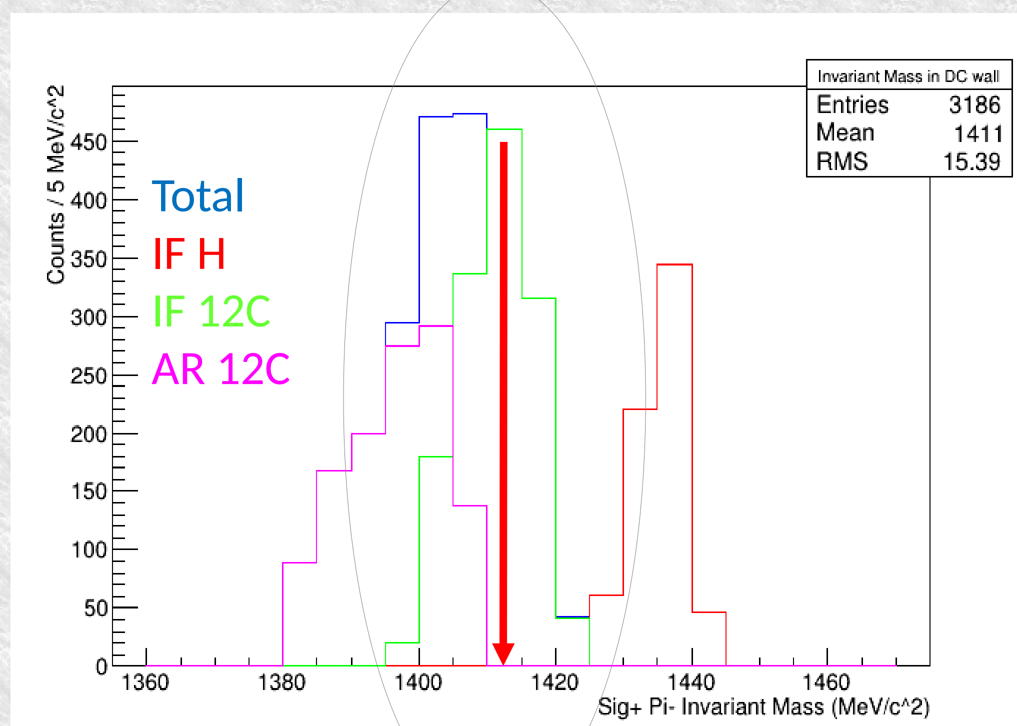

Resonant VS non-resonant

$K^- N \rightarrow (Y^* ?) \rightarrow Y \pi$

in medium, how much comes from resonance ?

Non resonant transition amplitude:

- Never measured before below threshold

(33 MeV below threshold):

$$E_{Kn} = -|B_n| - \frac{p_3^2}{2\mu_{\pi,\Lambda,3He}},$$

- few, old theoretical calculations

(Nucl. Phys. B179 (1981) 33-48)

Resonant VS non-resonant

Investigated using:

K^{-} "n" → $\Lambda\pi^{-}$ direct formation in ^{4}He

the goal is to measure **$|f^{N-R}_{\Lambda\pi}(I=1)|$**

to get information on **$|f^{N-R}_{\Sigma\pi}(I=0)|$**

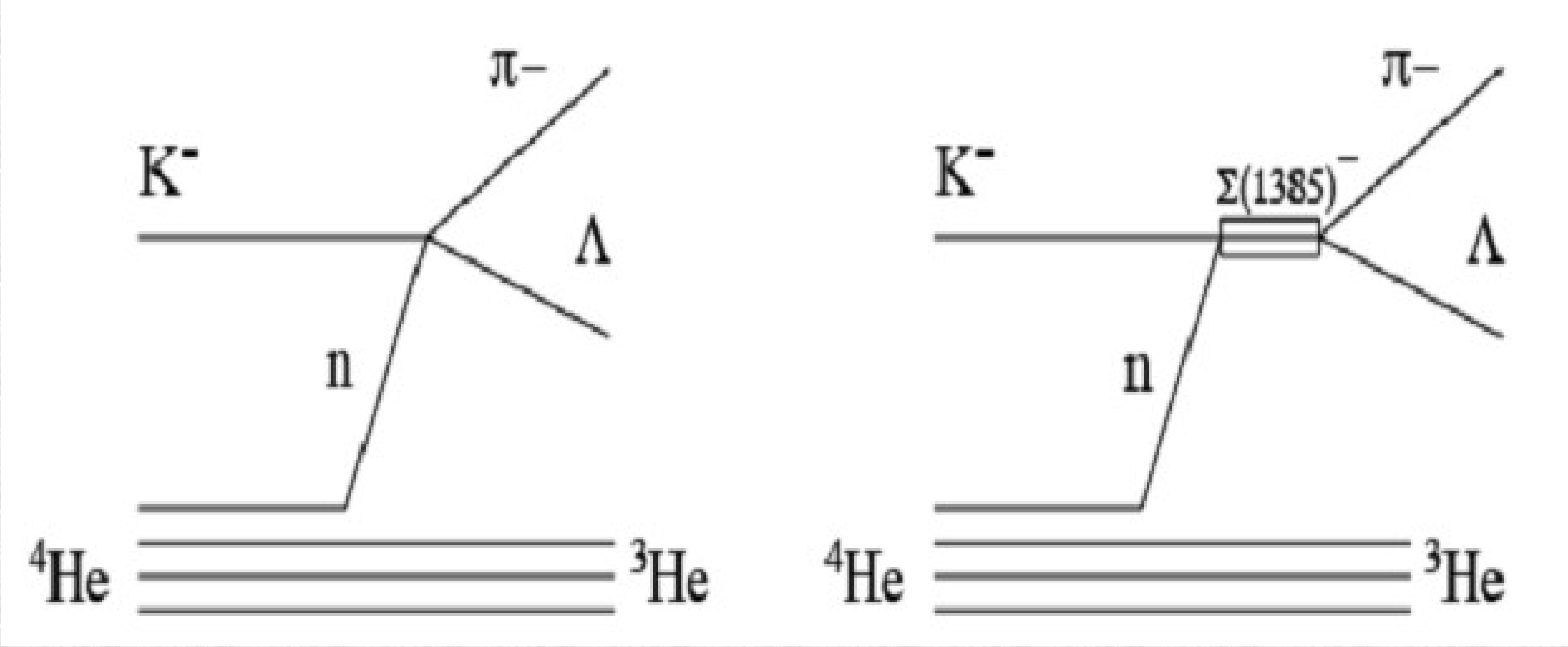

$K^- \, ^4He \rightarrow \Lambda p^- \, ^3He$ resonant and non-resonant processes

Nucl. Phys. A954 (2016) 75-93

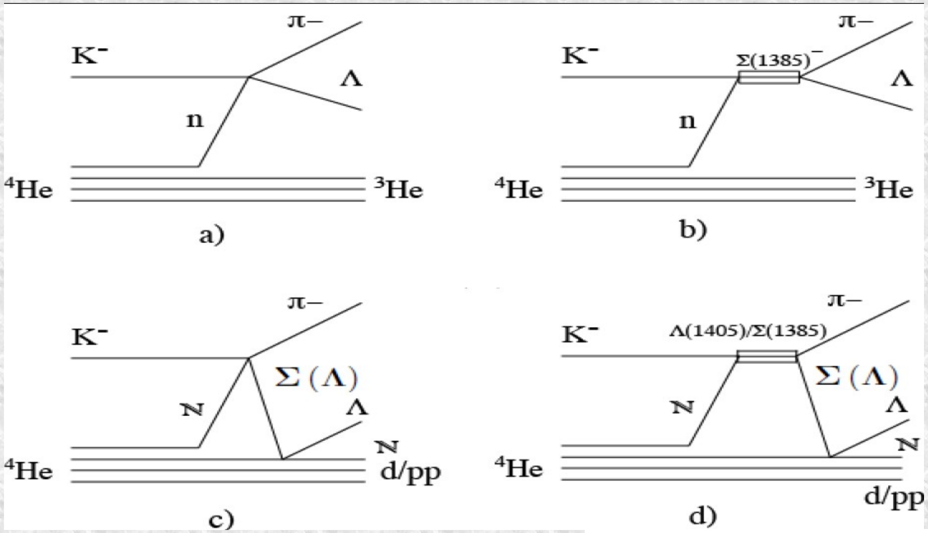

Theoretical shapes for :

total $\Lambda\pi^-$ momentum spectra for the resonant (Σ^{*-}) and non-resonant (I = 1) processes were calculated, for both S-state and P-state K^- capture at-rest and in-flight. Corrections to the amplitudes due to Λ/π final state interactions were estimated.

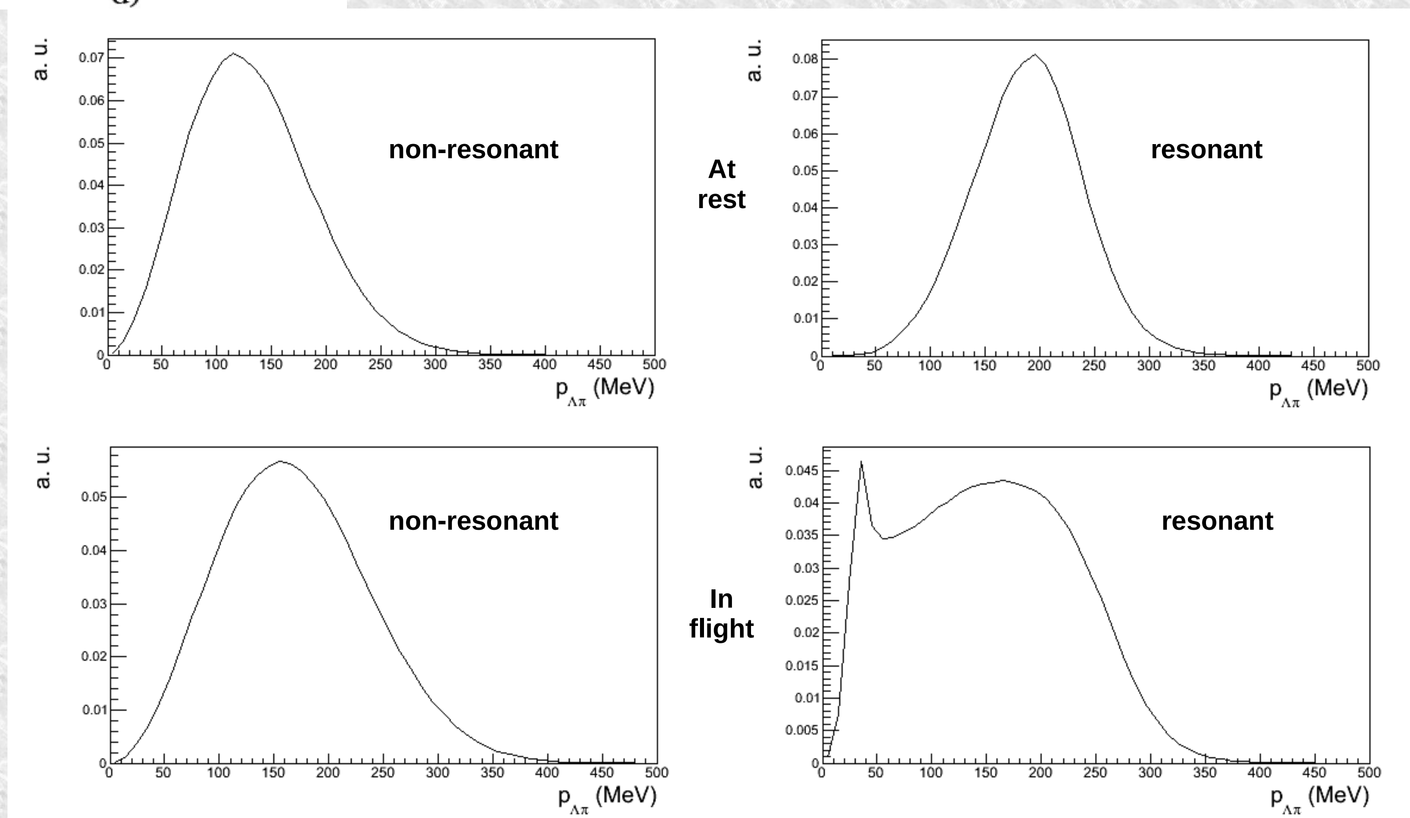

Collaboration with S. Wycech

How to extract the $K^- n \rightarrow \Lambda\pi^-$ non resonant transition amplitude

simultaneous fit ($p_{\Lambda\pi^-}$ - $m_{\Lambda\pi^-}$ - $\cos(\theta_{\Lambda\pi^-})$) with signal and background processes :

- non resonant K^- capture at-rest from S states in ^{4}He
- resonant K^- capture at-rest from S states in ^{4}He
- non resonant K^- capture in-flight in ^{4}He
- resonant K^- capture in-flight in ^{4}He

- primary $\Sigma\pi^-$ production followed by the $\Sigma N \rightarrow \Lambda N'$ conversion process
- K^- capture processes in ^{12}C giving rise to $\Lambda\pi^-$ in the final state

In order to extract:

NR-ar/RES-ar & NR-if/RES-if

Results for the $K^- n \rightarrow \Lambda\pi^-$ non resonant transition amplitude

Channels	Ratio/Amplitude	σ_{stat}	σ_{syst}
RES-ar/NR-ar	0.39	$\pm$ 0.04	$^{+0.18}_{-0.07}$
RES-if/NR-if	0.23	$\pm$ 0.03	$^{+0.23}_{-0.22}$
NR-ar	12.00 %	$\pm$ 1.66 %	$^{+1.96}_{-2.77}$ %
NR-if	19.24 %	$\pm$ 4,38 %	$^{+5.90}_{-3.33}$ %
$\Sigma \rightarrow \Lambda$ conv.	2.16 %	$\pm$ 0.30 %	$^{+1.62}_{-0.83}$ %
K^{-12}C capture	57.00 %	$\pm$ 1.23 %	$^{+2.21}_{-3.19}$ %

TABLE I. Resonant to non-resonant ratios and amplitude of the different channels extracted from the fit of the $\Lambda\pi^-$ sample. The statistical and systematic errors are also shown. See text for details.

Preliminary

extracted:

NR-ar/RES-ar & NR-if/RES-if

Simultaneous momentum – angle – mass fit

Light band sys err.
Dark band stat. Err.

Σ/Λ nuclear conversion

K-N→Σ π

└→ ΣN→ΛN'

Absorptions in 12C
(from Carbon wall data)

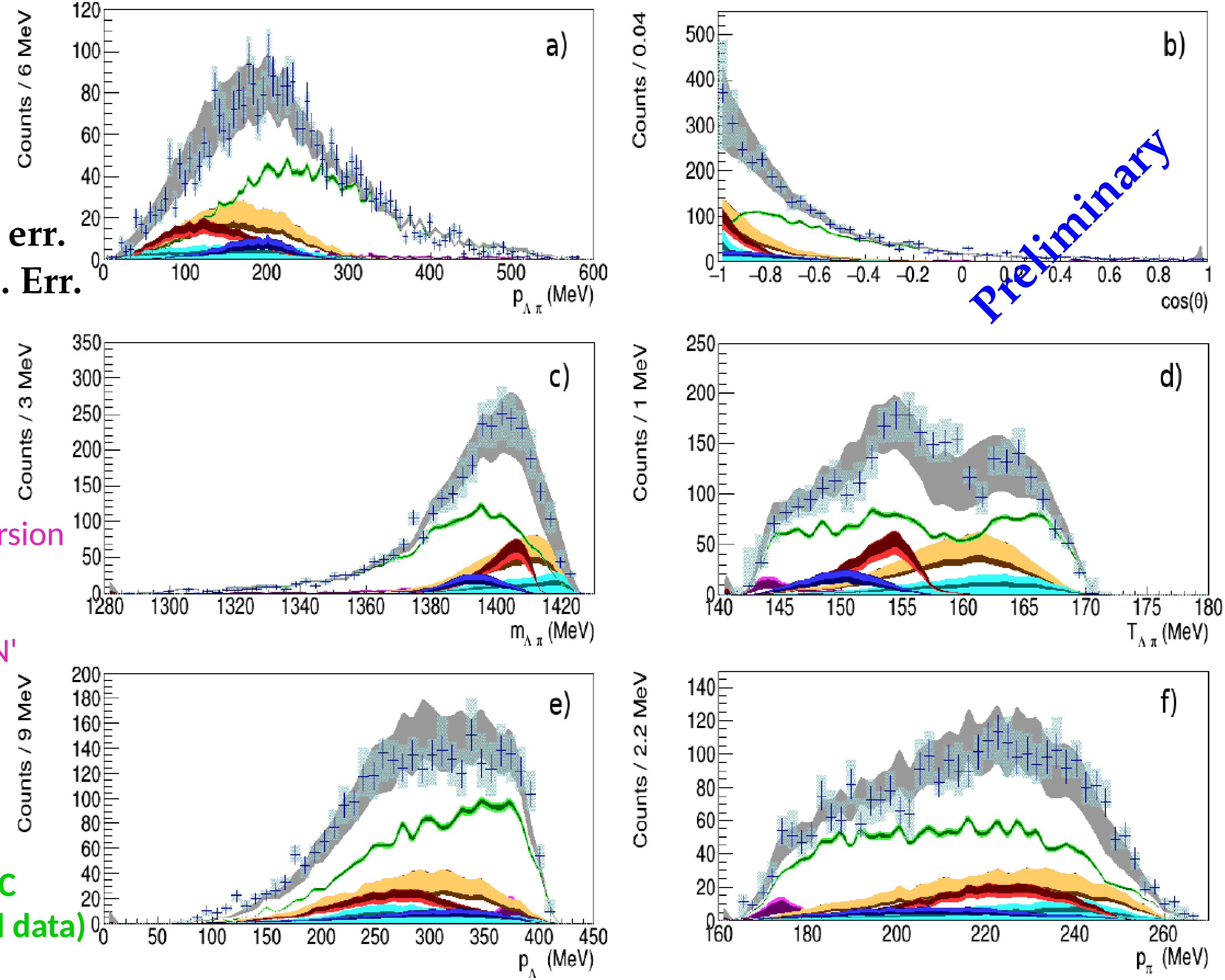

Simultaneous momentum – angle – mass fit

Light band sys err.
Dark band stat. Err.

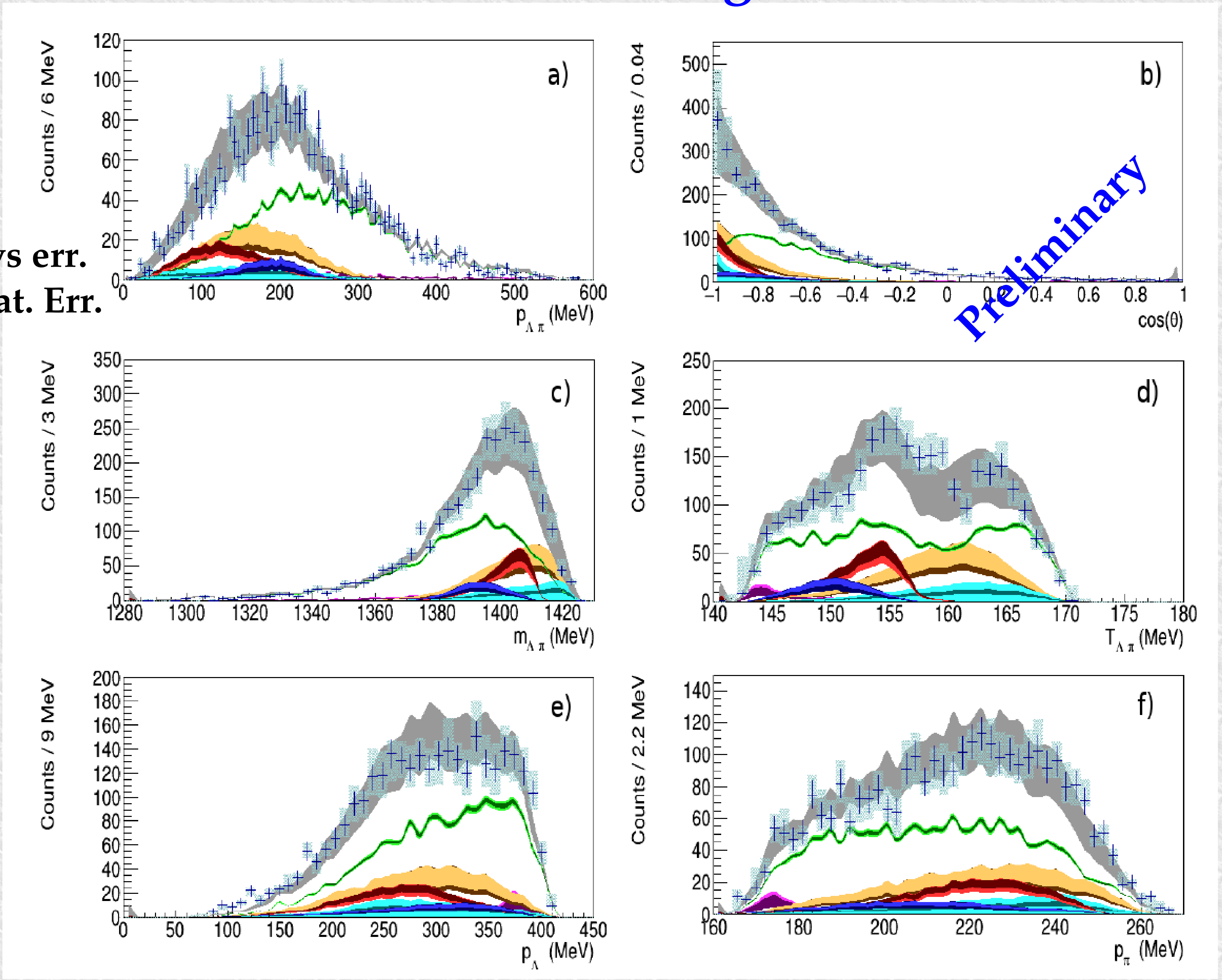

Non-Resonant
(at-rest)
(in-flight)

Resonant Σ∗
(at-rest)
(in-flight)

Comparison

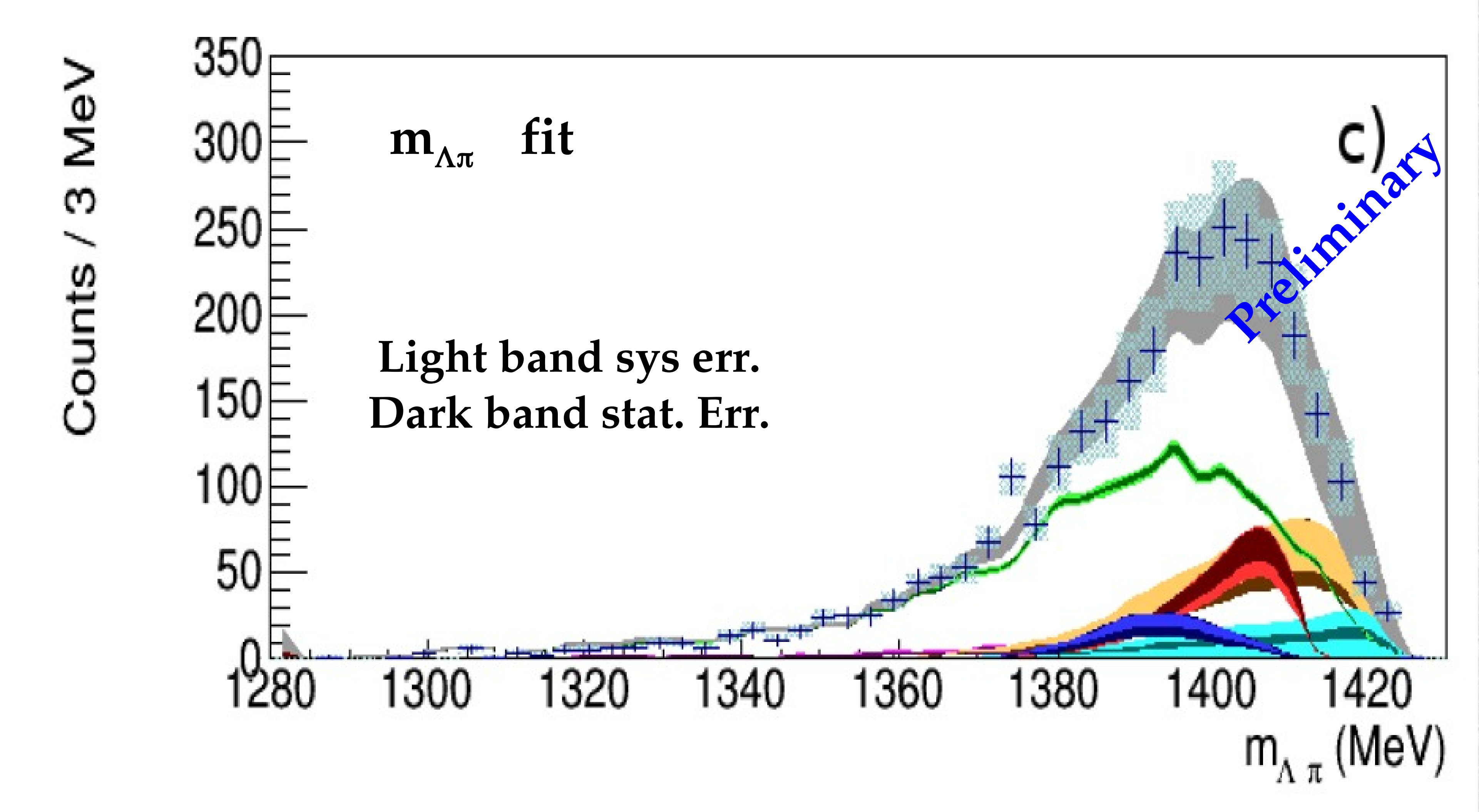

Non-Resonant
(at-rest)
(in-flight)

Resonant Σ*
(at-rest)
(in-flight)

Outcome of the measurement

From the well known Σ* transition probability:

Preliminary

$$\frac{\mathrm{NR-ar}}{\mathrm{RES-ar}} = \frac{\int_0^{pmax} P_{ar}^{nr}(p_{\Lambda\pi})\, dp_{\Lambda\pi}}{\int_0^{pmax} P_{ar}^{res}(p_{\Lambda\pi})\, dp_{\Lambda\pi}} =$$

$$= |f_{ar}^s|^2 \cdot 8,94 \cdot 10^5 \mathrm{MeV}^2 \, .$$

$$\rightarrow |f_{ar}^s| = (0.334 \pm 0.018\,\mathrm{stat}^{+0.034}_{-0.058}\mathrm{syst})\ \mathrm{fm}\, .$$

The sub-threshold result is compatible with corresponding values extracted from $K^- p \rightarrow \Lambda \pi^0$ cross sections above threshold

J. K. Kim, Columbia University Report, Nevis 149 (1966)

J. K. Kim, Phys Rev Lett, 19 (1977) 1074:

$E = -33$ MeV	$p_{lab} = 120$ MeV	160 MeV	200 MeV	245 MeV
$0.334 \pm 0.018\,\mathrm{stat}^{+0.034}_{-0.058}\mathrm{syst}$	0.33(11)	0.29(10)	0.24 (6)	0.28(2)

K^- - multiN absorption and search for bound states

How deep can an antikaon be bound in a nucleus?

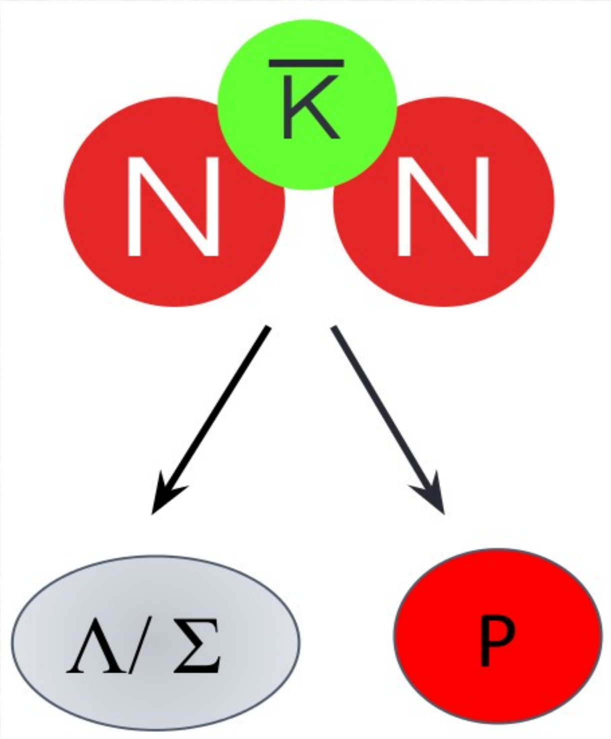

Possible Bound States:

$(K^- pp) \rightarrow \Lambda\, p$
$\rightarrow \Sigma^0\, p$

$(K^- ppn) \rightarrow \Lambda\, d$
$\rightarrow \Sigma^0\, d$

predicted due to the strong $\bar{K}N$ interaction in the I=0 channel.

[Wycech (1986) - Akaishi & Yamazaki (2002)]

K^-pp bound state

....at the end of 2015

	Dote,Hyodo, Weise	Akaishi, Yamazaki	Barnea, Gal, Liverts	Ikeda, Sato	Ikeda, Kamano,Sato	Schevchenko ,Gal, Mares	Revai, Schevchenko	Maeda, Akaishi, Yamazaki
B (MeV)	17-23	48	16	60-95	9-16	50-70	32	51.5
Γ(MeV)	40-70	61	41	45-80	34-46	90-110	49	61
Method	Variational	Variational	Variational	Faddeev-AGS	Faddeev-AGS	Faddeev-AGS	Faddeev-AGS	Faddeev-Yakubovsky
Interaction	Chiral	Phenom.	Chiral	Chiral	Chiral	Phenom.	Chiral	Phenom.

Experiments reporting DBKNS		
KEK-PS E549	T. Suzuki at al. MPLA23, 2520-2523 (2008)	
FINUDA	M. Agnello et al. PRL94, 212303 (2005)	Extraction of a **signal**
DISTO	T. Yamazaki et al. PRL104 (2010)	Extraction of a **signal**
OBELIX	G. Bendiscioli et al. NPA789, 222 (2007)	Extraction of a **signal**
HADES	G. Agakishiev et al. PLB742, 242-248 (2015)	**Upper limit**
LEPS/SPring-8	A.O. Tokiyasu et al. PLB728, 616-621 (2014)	**Upper limit**
J-PARC E15	T. Hashimoto et al. PTEP, 061D01 (2015)	**Upper limit**
J-PARC E27	Y. Ichikawa et al. PTEP, 021D01 (2015)	Extraction of a **signal**

How deep can an antikaon be bound in a nucleus?

$K^{-}pp$ bound state.....the theory

Chiral SU(3)-based (Energy dependent) → Shallow~20 MeV

Phenomenological (Energy independent) → Deep~40-70 MeV

	Dote, Hyodo, Weise	Akaishi, Yamazaki	Barnea, Gal, Liverts	Ikeda, Sato	Ikeda, Kamano, Sato	Schevchenko, Gal, Mares	Revai, Schevchenko	Maeda, Akaishi, Yamazaki
B (MeV)	17-23	48	16	60-95	9-16	50-70	32	51.5
Γ(MeV)	40-70	61	41	45-80	34-46	90-110	49	61
Method	Variational	Variational	Variational	Faddeev-AGS	Faddeev-AGS	Faddeev-AGS	Faddeev-AGS	Faddeev-Yakubovsky
Interaction	Chiral	Phenom.	Chiral	Chiral	Chiral	Phenom.	Chiral	Phenom.

Large width means short-life state → hard to measure
Small width means long-life state → easy to measure

How deep can an antikaon be bound in a nucleus?

$K^{-}pp$ bound state

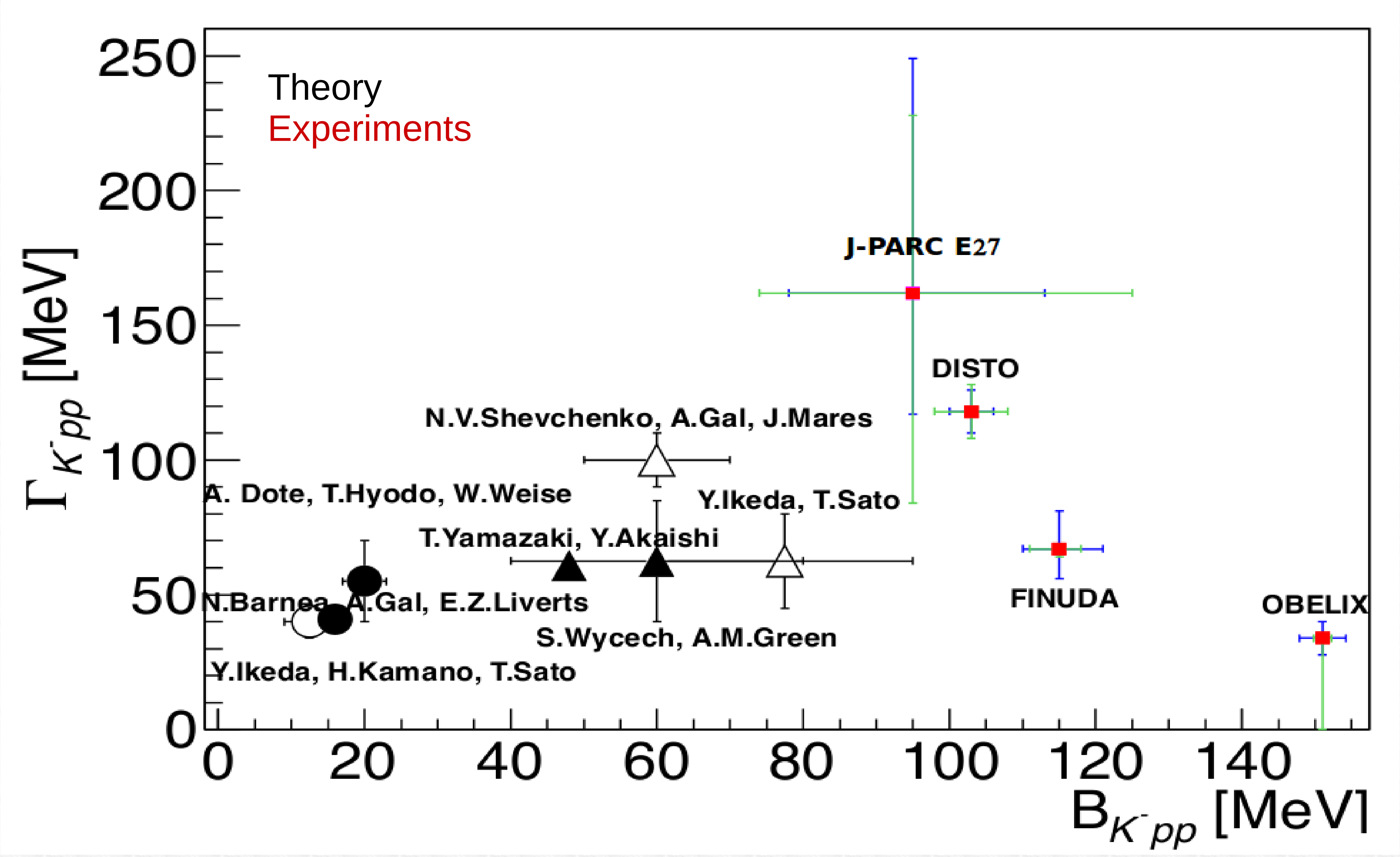

How deep can an antikaon be bound in a nucleus?

interpreted in

T. Sekihara, E. Oset, A. Ramos, Prog. Theor. Exp. Phys (2016) (12): 123D03

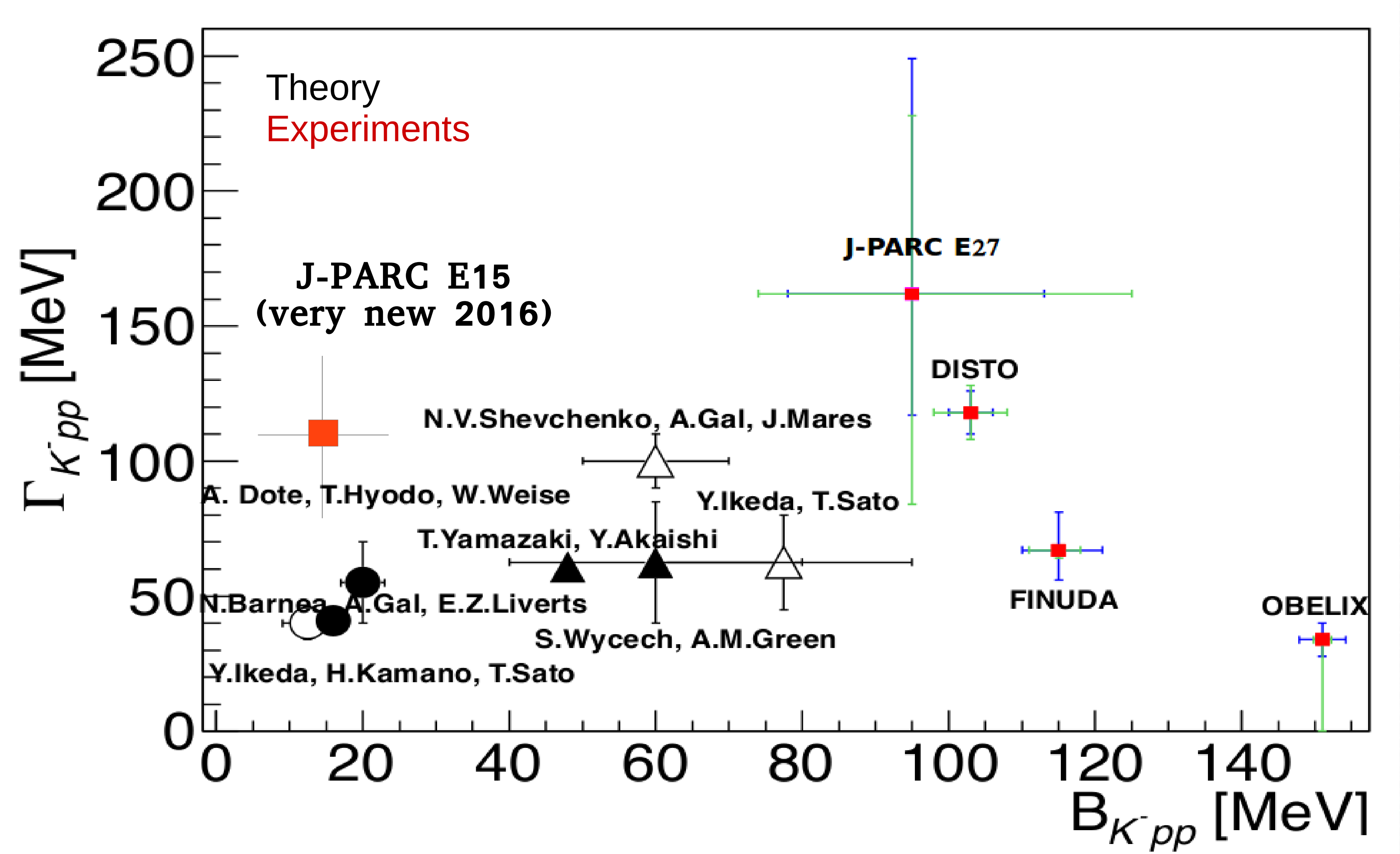

[from the talk of T. Nagae at HYP2015, Sep. 10, 2015]

J-PARC E15

$K^- + {}^3He \rightarrow \Lambda + p + n$

Invariant mass spectroscopy

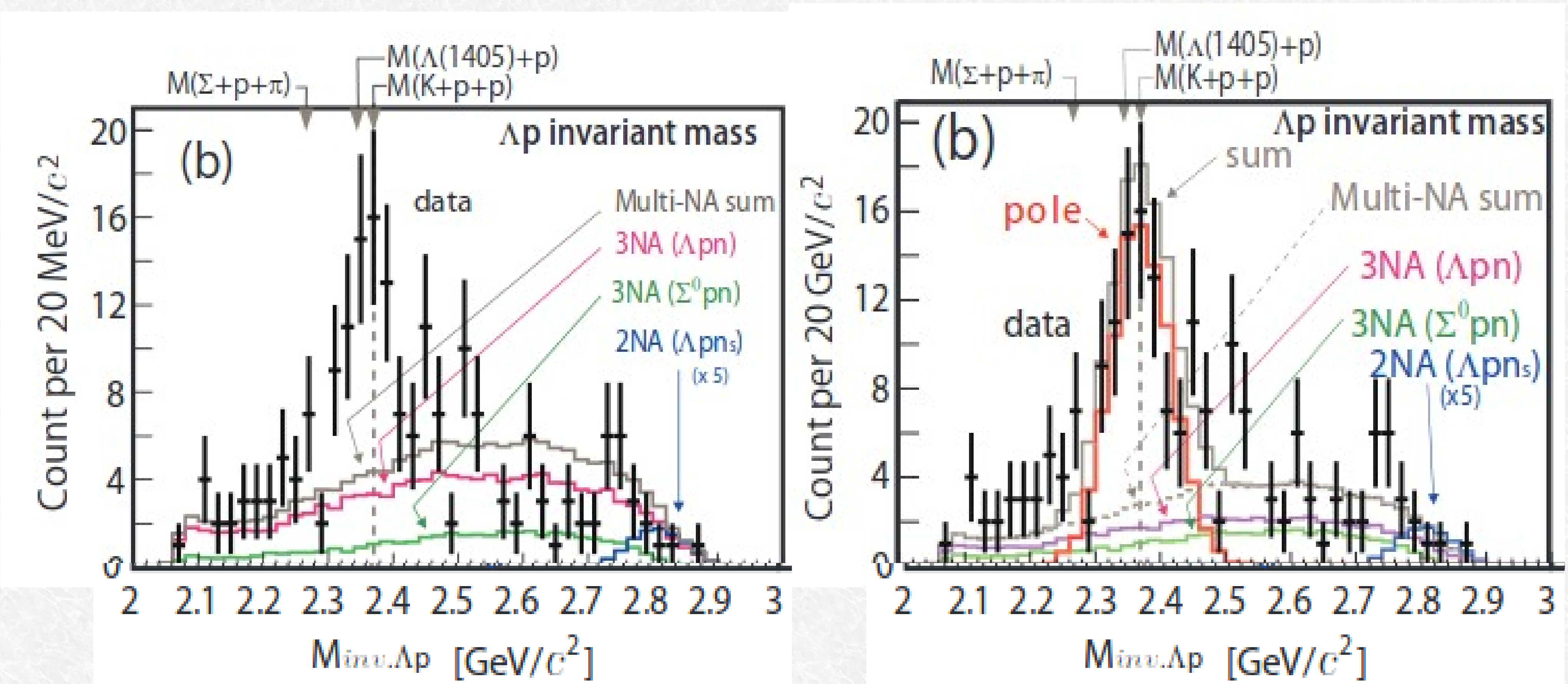

[J-PARC E15 Collaboration: arXiv:1601.06876 [nucl-ex]]

M = 2355 +6 −8 (stat.) ± 12 (syst.) MeV/c2
Γ = 110 +19 −17 (stat.) ± 27 (syst.) MeV/c2

BE = 15 MeV

Σ0 p correlated production, goals of this analysis

K- Absorption

- Pin down the contribution of the process:

$$K^- + NN \rightarrow \Sigma^0 + p$$

with respect to processes as:

$$K^- + NN \rightarrow \Sigma^0 + p \rightarrow p\text{''} + \Sigma^0\text{''}\ (FSI)$$

$$K^- + NNN \rightarrow \Sigma^0 + p + X$$

$$K^- + NNNN \rightarrow \Sigma^0 + p + X$$

Kaonic Bound States

$$ppK^- \rightarrow \Sigma^0 + p$$

- Yield Extraction and Significance

Final fit

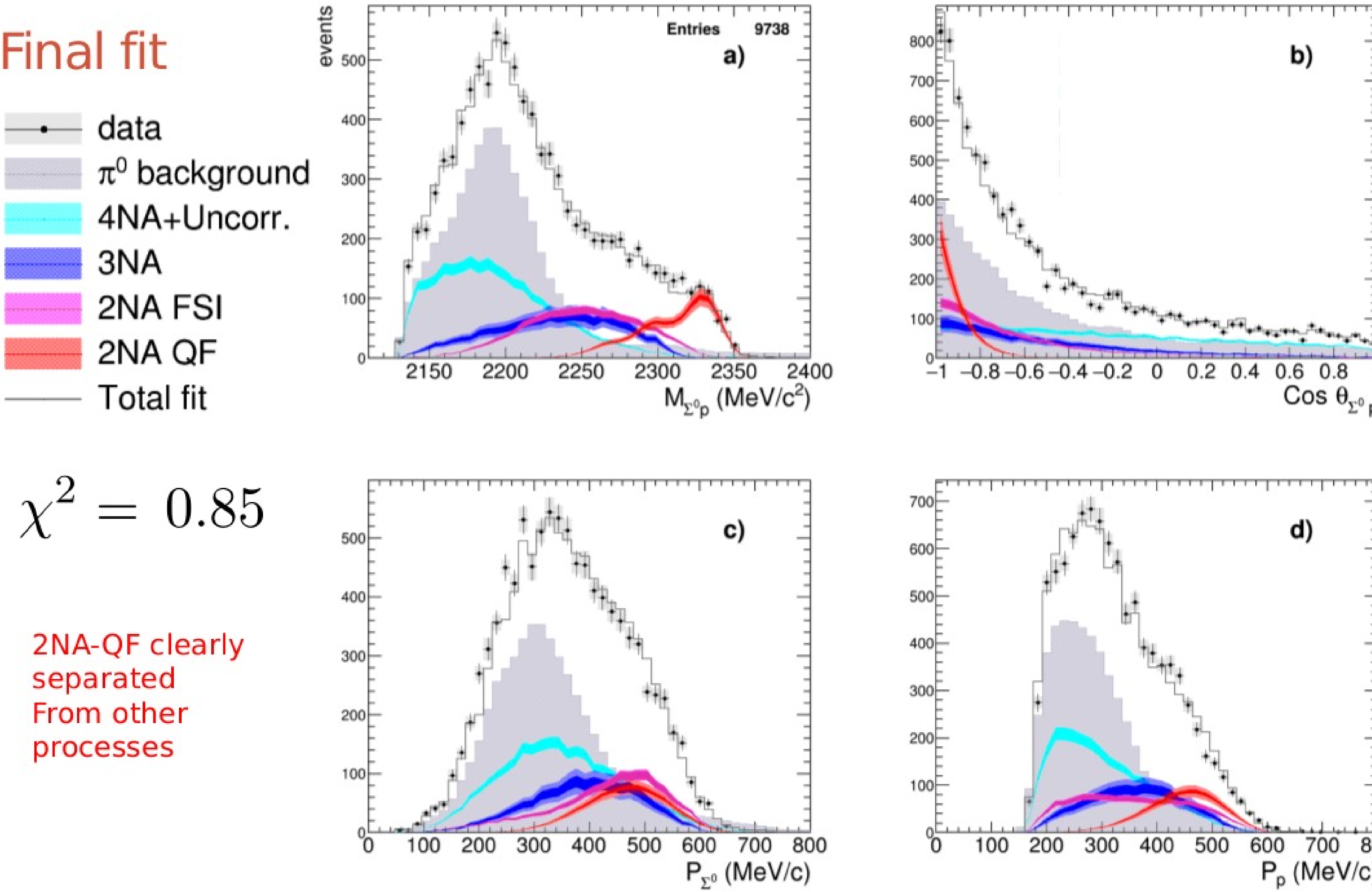

$$\chi^2 = 0.85$$

2NA-QF clearly separated From other processes

From the contributions to the fit, the yields are extracted for K- stop

Absorption results

	yield / $K^-_{stop} \cdot 10^{-2}$	$\sigma_{stat} \cdot 10^{-2}$	$\sigma_{syst} \cdot 10^{-2}$
2NA-QF	0.127	$\pm$ 0.019	$^{+0.004}_{-0.008}$
2NA-FSI	0.272	$\pm$ 0.028	$^{+0.022}_{-0.023}$
Tot 2NA	0.376	$\pm$ 0.033	$^{+0.023}_{-0.032}$
3NA	0.274	$\pm$ 0.069	$^{+0.044}_{-0.021}$
Tot 3body	0.546	$\pm$ 0.074	$^{+0.048}_{-0.033}$
4NA + bkg.	0.773	$\pm$ 0.053	$^{+0.025}_{-0.076}$

…is there room for the signal of a **ppK- bound state**?

Fit with ppK-

Best solution:

- B.E. = 45 MeV/c2
- Width = 30 MeV/c2

$$\chi^2 = 0.807$$

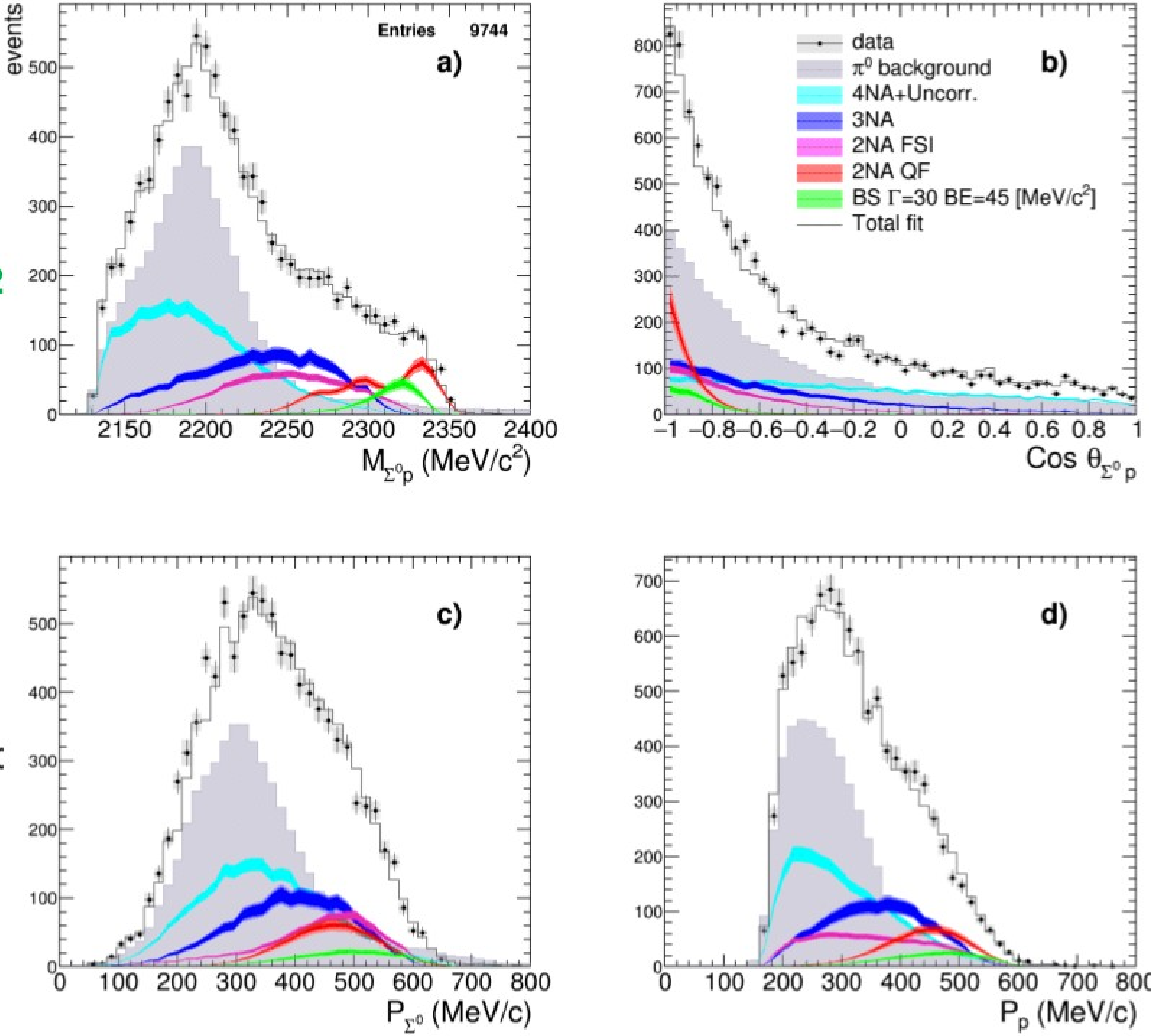

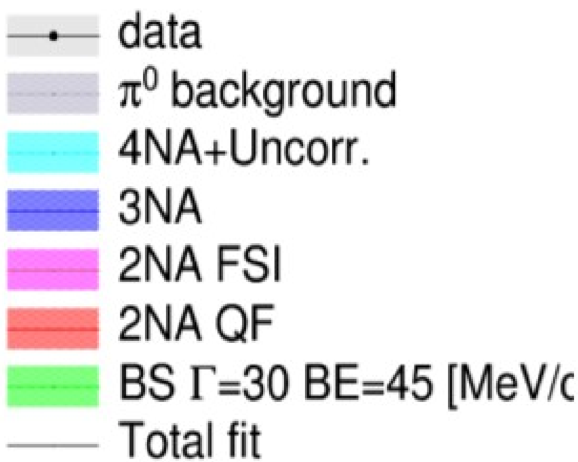

Evaluation of the significance of the ppK- signal

For B.E. = 45 MeV/c2, Width = 30 MeV/c2

$$Yield/K^{-}_{stop} = (0.044 \pm 0.009 stat^{+0.004}_{-0.005} syst) \cdot 10^{-2}$$

F-test to evaluate the addition of an extra parameter to the fit:

Significance of “signal” hypothesis w.r.t “Null-Hypothesis” (no bound state)

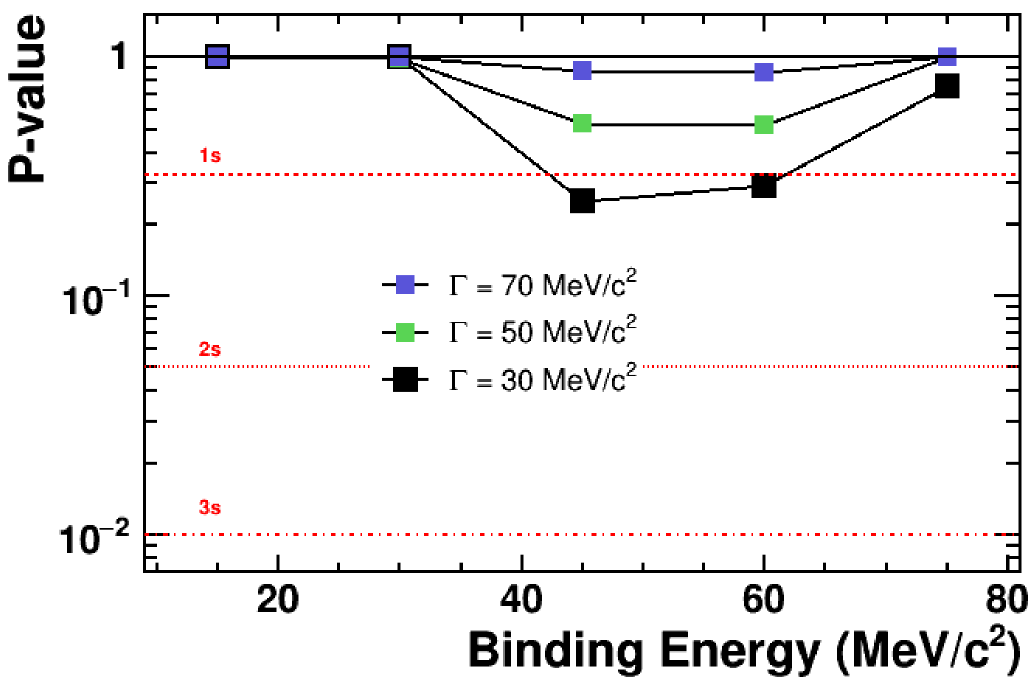

Conclusions

- 2NA-QF yield

	yield / $K^-_{stop} \cdot 10^{-2}$	$\sigma_{stat} \cdot 10^{-2}$	$\sigma_{syst} \cdot 10^{-2}$
2NA-QF	0.127	$\pm$ 0.019	$^{+0.004}_{-0.008}$

- No significant detection of ppK- bound state

O. Vazquez Doce et al., Physics Letters B 758 (2016) 134

$K^- \, {}^4He \rightarrow \Lambda t$

4NA cross section and yield

Λt available data

Available data:

- in Helium :

  - bubble chamber experiment
  [M.Roosen, J.H. Wickens, Il Nuovo Cimento 66, (1981), 101]
  K^- stopped in liquid helium, Λ dn/t search. 3 events compatible with the Λt kinematics were found

  BR($K^{-4}He \rightarrow \Lambda t$) **= (3 ± 2) × 10^{-4} /K_{stop}** global, no 4NA

- Solid targets

  - FINUDA [Phys.Lett. B669 (2008) 229]
  (40 events in different solid targets)

Λt available data

FINUDA presented [Phys.Lett.B (2008) 229]:

- a study of Λ vs t momentum correlation and an opening angle distribution
- **40 events** collected and added together coming from different targets ($^{6,7}Li$, ^{9}Be)

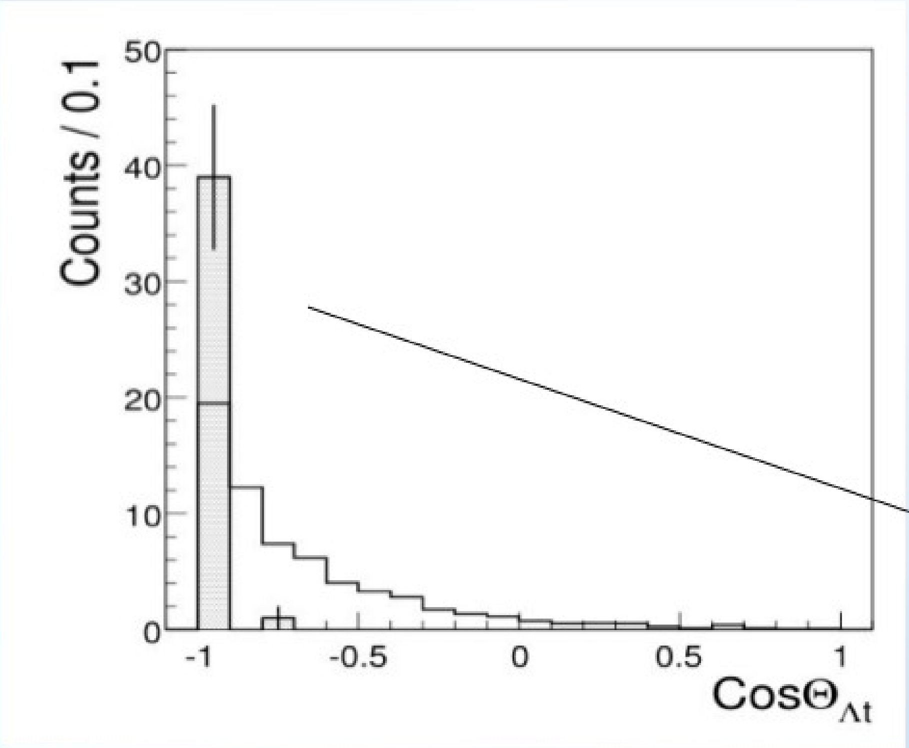

Filled histogram= data

Open histogram = Phase space simulation

$$K^- A \rightarrow \Lambda\, t\, A'$$

Unclear back to back topology

Λt emission yield → $10^{-3} - 10^{-4} / K^-_{stop}$

global, no 4NA

Experimental data only back-to-back

Λt correlation studies in ^4He from the DC gas : contributing processes

single nucleon absorption (1NA)

$$K^- \, ^4He \rightarrow \Lambda \, \pi^0 \, t_{res}$$

$$K^- \, ^4He \rightarrow \Sigma^0 \pi^0 \, t_{res} \quad , \quad \Sigma^0 \rightarrow \Lambda\gamma$$

conversion on triton:

$$K^- \, ^4He \rightarrow \Sigma^0 \pi^0 \, t \quad , \quad \Sigma^0 t \, / \, \Lambda t$$

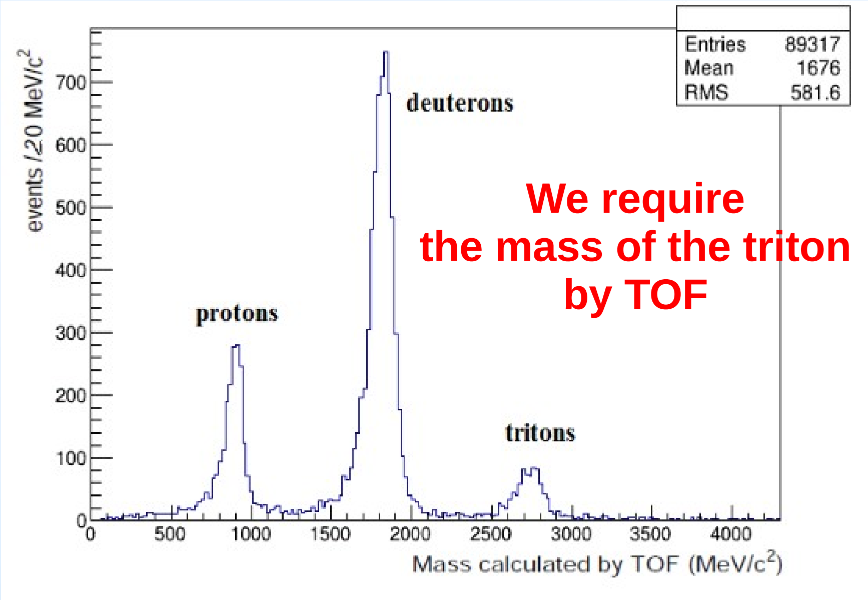

We require the mass of the triton by TOF

Tritons are spectators, **too low momentum:** p_t ~ Fermi momentum

<u>lower then the calorimeter threshold</u> (p_t ~ 500 MeV/c)

<u>checked by MC simulations</u>

4NA processes – K⁻ absorbed by the **α particle:**

$$K^- \, ^4He \rightarrow \Lambda t$$

$$K^- \, ^4He \rightarrow \Sigma^0 t \quad , \quad \Sigma^0 \rightarrow \Lambda\gamma$$

conversion is suppressed by the Σ^0- t Back to back topology!

MC simulations: efficiency & resolution

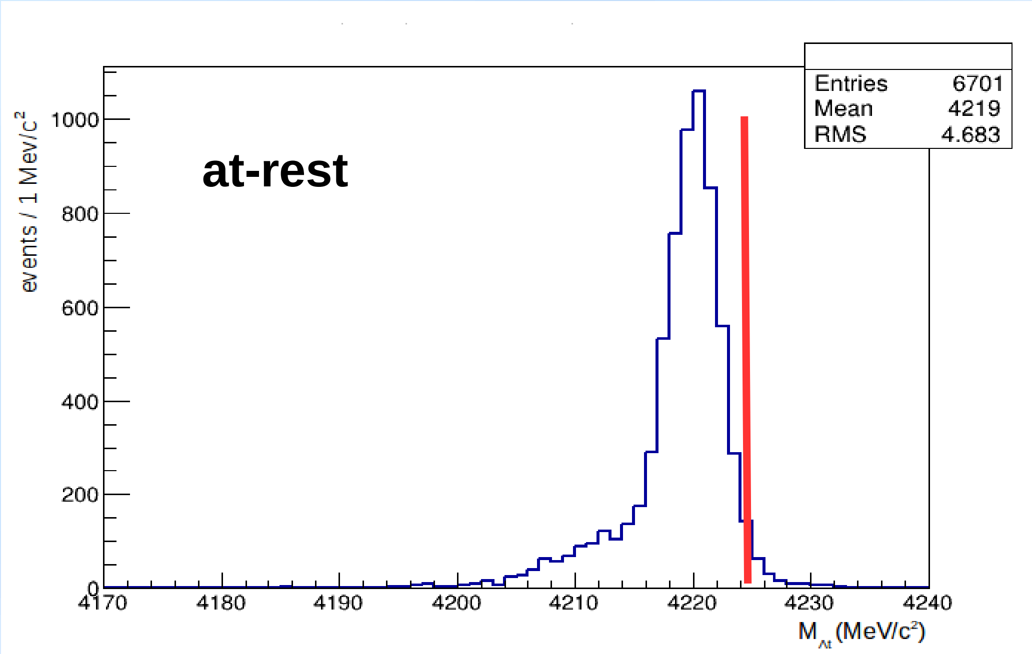

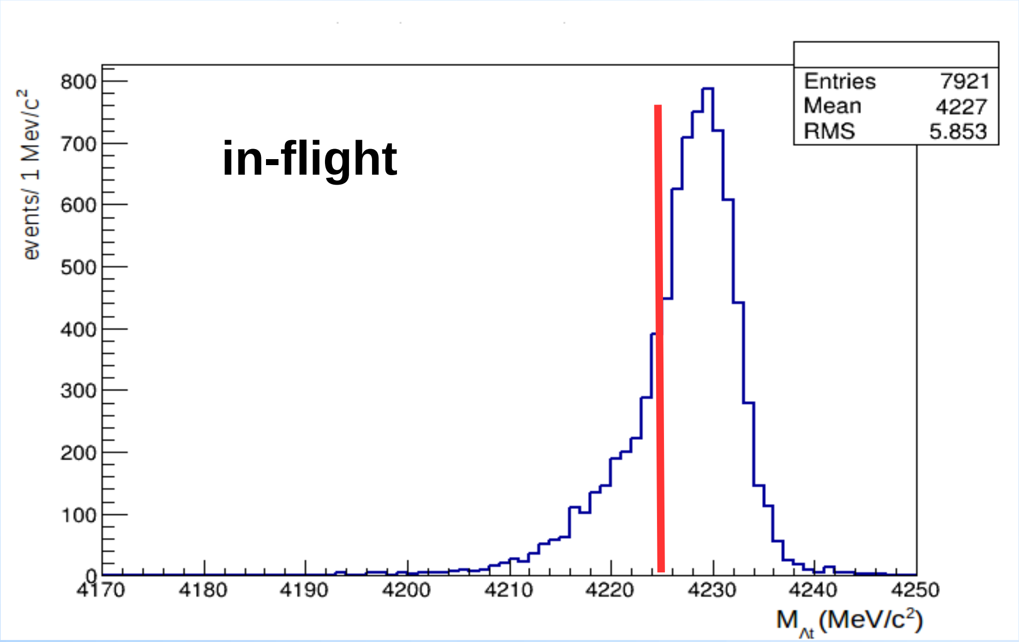

mass threshold at-rest

$M_{\Lambda t}$ invariant mass resolution = 2.2 MeV/c^2

overall detection + reconstruction efficiency for 4NA direct Λt production :

$$\epsilon_{4NA,ar,\Lambda t} = 0.0493 \pm 0.0006 \quad ; \quad \epsilon_{4NA,if,\Lambda t} = 0.0578 \pm 0.0006,$$

at-rest in-flight

K- ^{4}He → Λt 4NA cross section

Preliminary

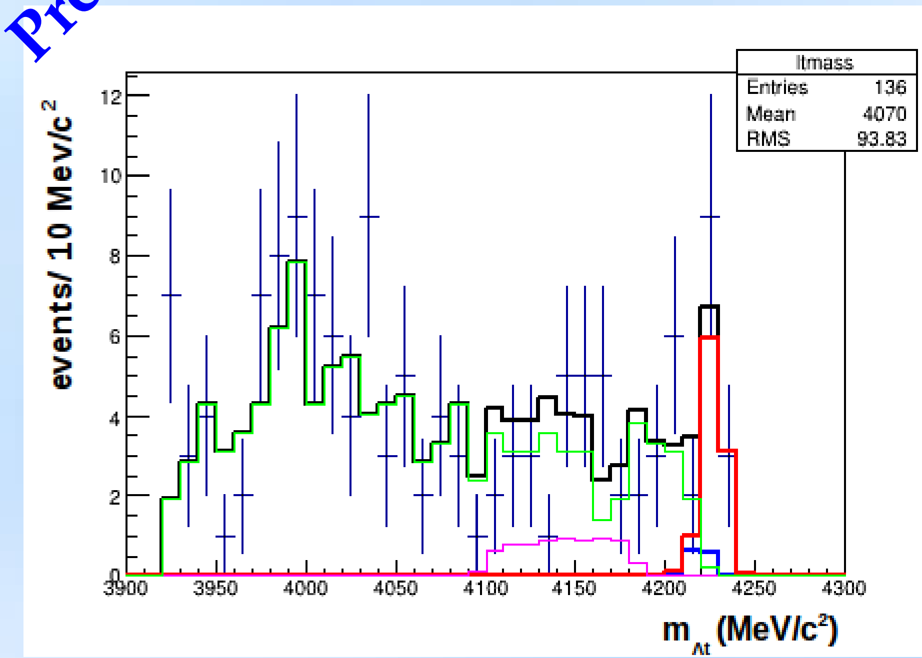

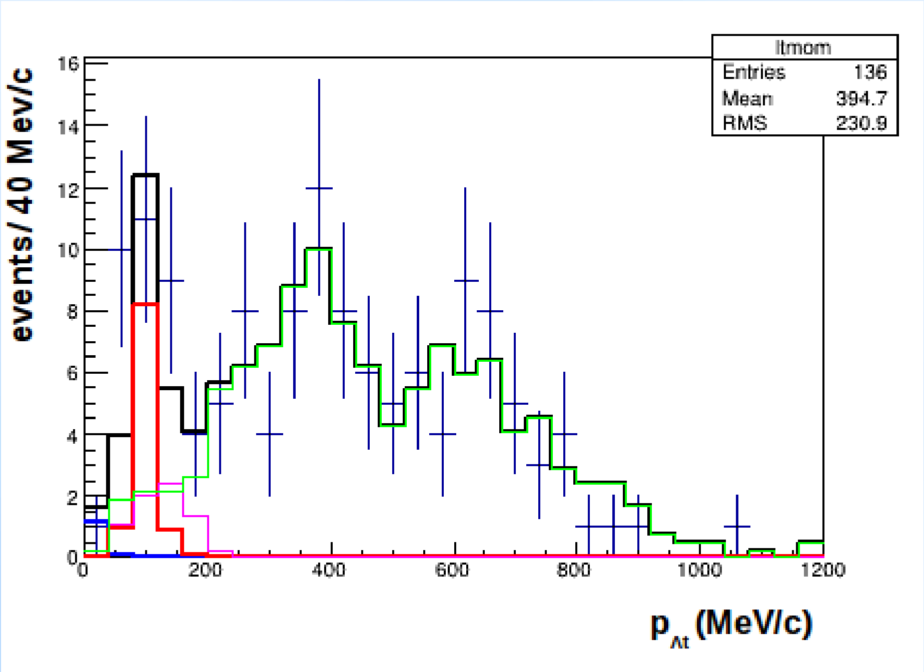

data

--- carbon data from DC wall

--- 4NA K^{-} ^{4}He → Λt in flight MC

--- 4NA K^{-} ^{4}He → Λt at rest MC

--- 4NA K^{-} ^{4}He → Σ^0t , Σ^0 → Λγ MC

--- 4NA K^{-} ^{4}He → Σ^0t , Σ^0 → Λγ MC

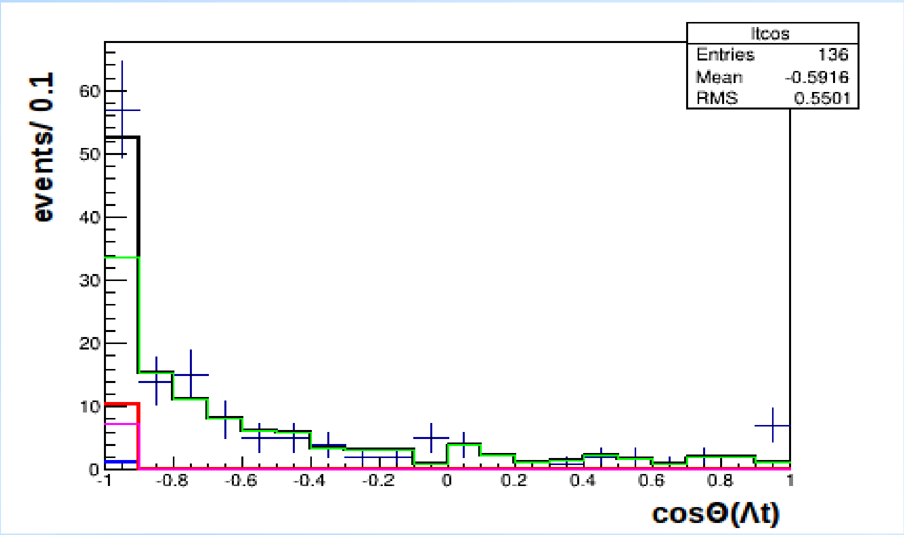

Preliminary

$K^- \, {}^4He \rightarrow \Lambda t$ 4NA cross section

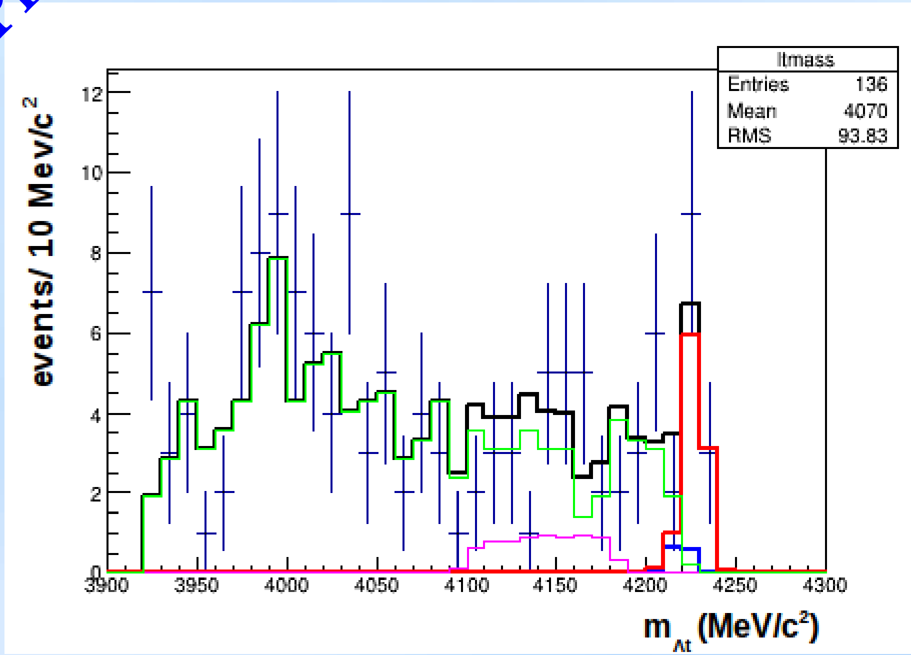

data

--- carbon data from DC wall

--- 4NA $K^- \, {}^4He \rightarrow \Lambda t$ in flight MC

--- 4NA $K^- \, {}^4He \rightarrow \Lambda t$ at rest MC

--- 4NA $K^- \, {}^4He \rightarrow \Sigma^0 t$, $\Sigma^0 \rightarrow \Lambda\gamma$ MC

--- 4NA $K^- \, {}^4He \rightarrow \Sigma^0 t$, $\Sigma^0 \rightarrow \Lambda\gamma$ MC

Contribution to the spectra	Parameter value
K^{-4}He $\rightarrow \Lambda t$ at rest	0.01 ± 0.01
K^{-4}He $\rightarrow \Lambda t$ in-flight	0.09 ± 0.02
K^{-4}He $\rightarrow \Sigma^0 t$ in-flight	0.05 ± 0.03
K^{-12}C $\rightarrow \Lambda t$ experimental distribution from the carbon DC wall	0.85 ± 0.06
χ^2 / ndf	0.654

Total number of events = 136

4NA $K^- \, {}^4He \rightarrow \Lambda t$ at rest $\rightarrow$ 1 ± 1 events

4NA $K^- \, {}^4He \rightarrow \Lambda t$ in flight $\rightarrow$ 12 ± 3 events

BR($K^- \, {}^4He$(4NA) $\rightarrow \Lambda t$) **< 1.3 × 10^{-4} /K$_{stop}$**

σ(100 ± **19** MeV/c) ($K^- \, {}^4He$(4NA) $\rightarrow \Lambda t$) **=**

= (0.42 ± 0.13(stat) $^{+0.01}_{-0.02}$ (syst)) mb

perspectives:

- **Sub-threshold K- n → Λ π⁻ non resonant amplitude**

Nucl. Phys. A954 (2016) 75-93

$$|f^s_{ar}| = (0.334 \pm 0.018\,\mathrm{stat}^{+0.034}_{-0.058}\mathrm{syst})\,\mathrm{fm}\,.$$

experimental paper finalised

next step extract the same info in I = 0 to interpret the $\Sigma^0\pi^0$ spectra

- **K- multiN absoption yields in Σ^0 p** Physics Letters B 758 (2016) 134

	yield / $K^-_{stop} \cdot 10^{-2}$	$\sigma_{stat} \cdot 10^{-2}$	$\sigma_{syst} \cdot 10^{-2}$
2NA-QF	0.127	$\pm$ 0.019	$^{+0.004}_{-0.008}$

Same analysis is ongoing in Λ p (R. Del Grande PhD thesys)

- **K- ^{4}He → Λt 4NA cross section** σ(100 **± 19** MeV/c) (K^- ^{4}He(4NA) → Λt) **=**

= (0.42 ± 0.13(stat) $^{+0.01}_{-0.02}$ (syst)) mb **paper in preparation**

- **feasibility study of the Σ^0 - N/NN *two* and *three body forces* measurement from K-absoption in ^{4}He**

Low-energy QCD in the u-d-s sector

- strong interaction is governed by QCD (color SU(3) gauge theory)

- fundamental matter fields are quarks (6 flavors & 3 colors R , G , B)

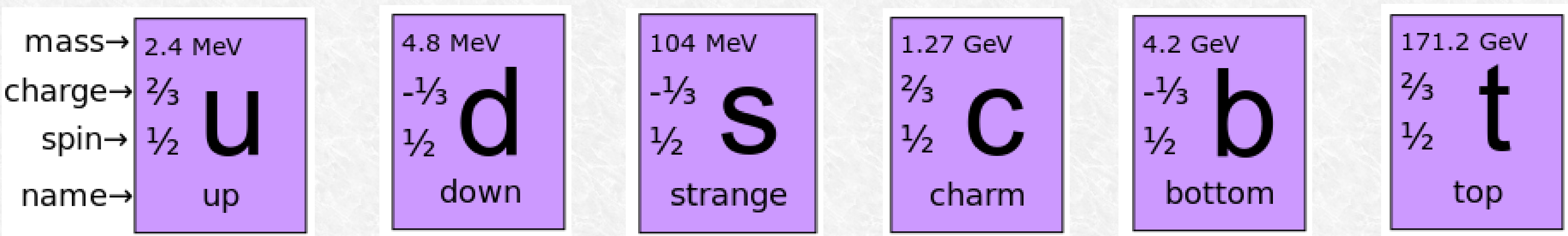

- gauge fields are 8 gluons

- in the massless limit ..

quark fields

gluon fields

$$\mathcal{L}^0_{\mathrm{QCD}} = -\frac{1}{2}\mathrm{tr}\,[G_{\mu\nu}G^{\mu\nu}] + \bar{q}i\gamma^{\mu}D_{\mu}q,$$

$$G_{\mu\nu} = \partial_{\mu}A_{\mu} - \partial_{\nu}A_{\mu} - ig[A_{\mu}, A_{\nu}], \qquad D_{\mu} = \partial_{\mu} - igA_{\mu}, \quad A_{\mu} = \sum_{a} T^{a}A^{a}_{\mu},$$

Low-energy QCD in the u-d-s sector

- CHIRAL PERTURBATION THEORY

a chiral Lagrangian with effective degrees of freedom *U* takes the place of the QCD Lagrangian:

$$\exp\{iZ\} = \int \mathcal{D}q\mathcal{D}\bar{q}\mathcal{D}A_\mu \exp\left\{i\int d^4x\mathcal{L}_{QCD}\right\} = \int \mathcal{D}U \exp\left\{i\int d^4x\mathcal{L}_{eff}\right\}$$

lowest excitations (pseudoscalar mesons):

$$\Phi = \begin{pmatrix} \frac{1}{\sqrt{2}}\pi^0 + \frac{1}{\sqrt{6}}\eta & \pi^+ & K^+ \\ \pi^- & -\frac{1}{\sqrt{2}}\pi^0 + \frac{1}{\sqrt{6}}\eta & K^0 \\ K^- & \bar{K}^0 & -\frac{2}{\sqrt{6}}\eta \end{pmatrix}$$

with chiral field $U(\Phi) = \exp\left\{\frac{i\sqrt{2}\Phi}{f}\right\}$

the counting rule is defined considering the meson momentum small respect to the ch. sy. Breaking scale $4\pi f \sim 1$ GeV.

Similar for the baryon fields:

$$B = \begin{pmatrix} \frac{1}{\sqrt{2}}\Sigma^0 + \frac{1}{\sqrt{6}}\Lambda & \Sigma^+ & p \\ \Sigma^- & -\frac{1}{\sqrt{2}}\Sigma^0 + \frac{1}{\sqrt{6}}\Lambda & n \\ \Xi^- & \Xi^0 & -\frac{2}{\sqrt{6}}\Lambda \end{pmatrix}$$

Why AMADEUS & DAΦNE?

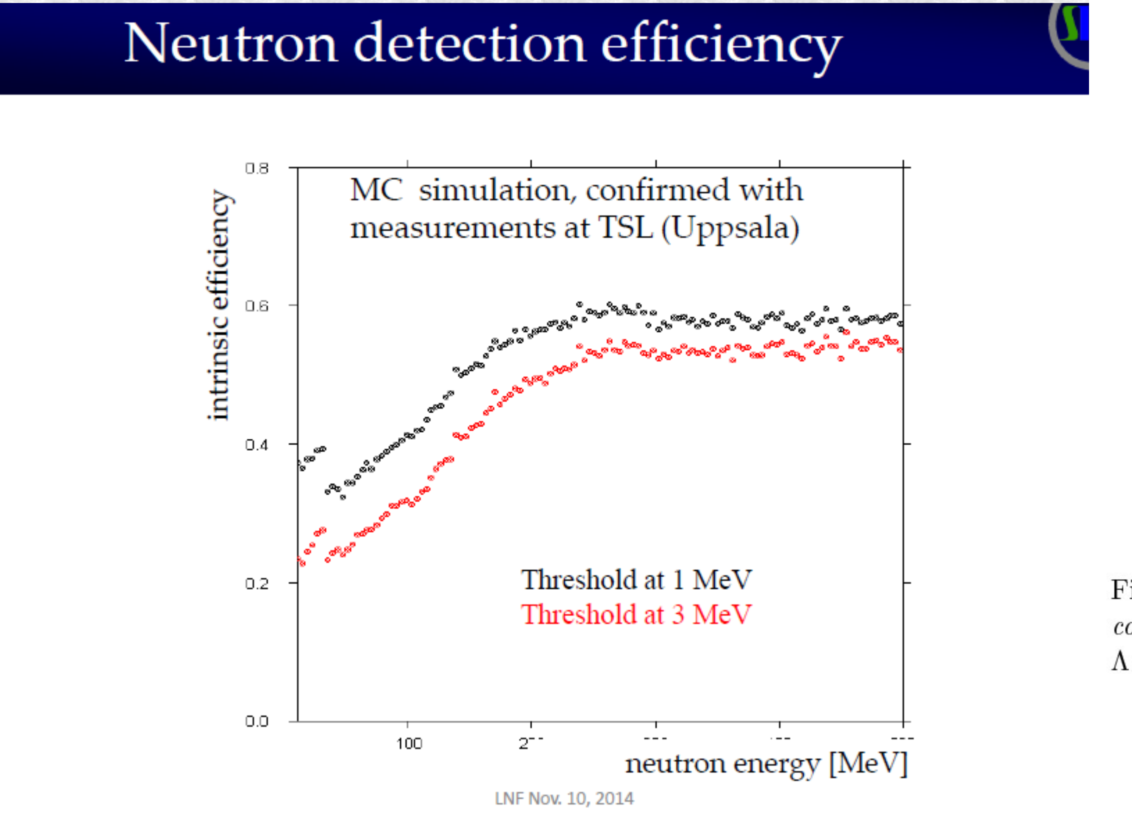

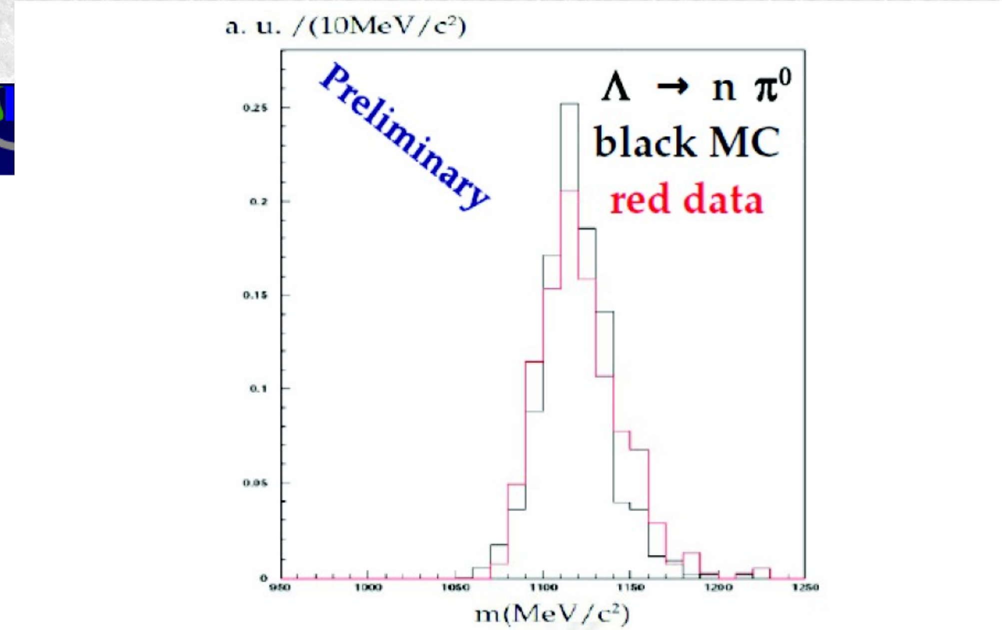

Fig. 1. $n\pi^0$ *invariant mass spectrum measured by the KLOE EMC, the red line corresponds to data, the black one corresponds to a Monte Carlo simulation of the* $\Lambda \to n\pi^0$ *decay, reconstructed in the KLOE calorimenter.*

KLOE

- 96% acceptance,
- optimized in the energy range of all charged particles involved
- good performance in detecting photons (and neutrons checked by kloNe group (M. Anelli et al., Nucl Inst. Meth. A 581, 368 (2007)))

Λ(1116) the signature of K$^-$ hadronic interaction

The **presence of a Λ(1116) is the signature of K$^-$ absorption** and is the starting point of the performed analysis:

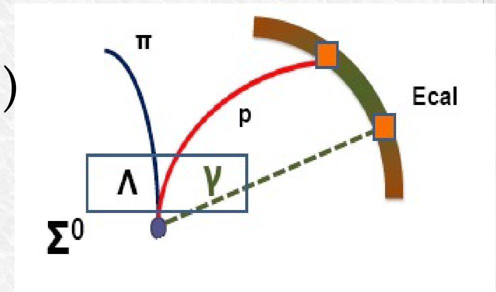

reconstruction of the Λ decay vertex: Λ(1116) → pπ^- (BR ~ 64 %)

requests:

- vertex with at least two opposite charged particles
- spatial position of vertex inside DC, or in DC entrance wall
- tracks with dE/dx > 95 ADC counts.

First positive tracks are requested to have an associated cluster in the calorimeter and the correct *E* - *p* relation, lack of low momentum protons!

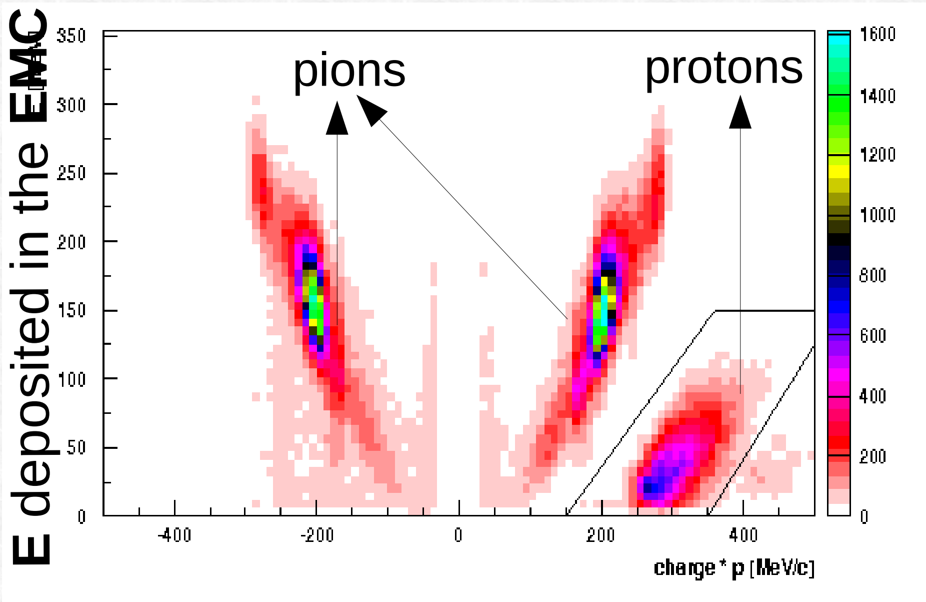

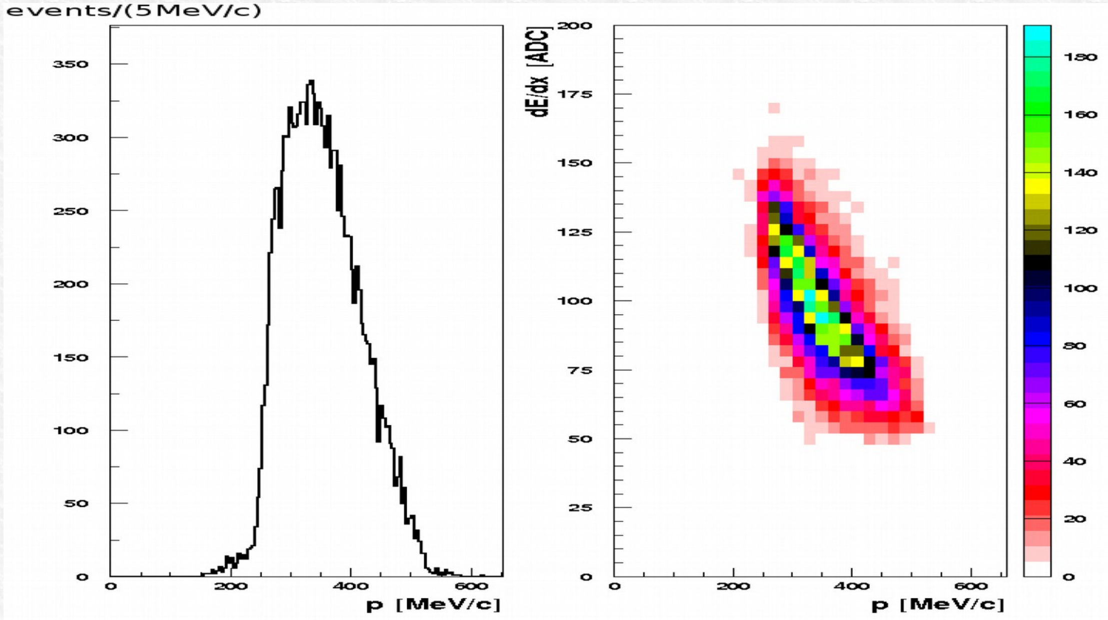

Λ(1116) the signature of K^- hadronic interaction

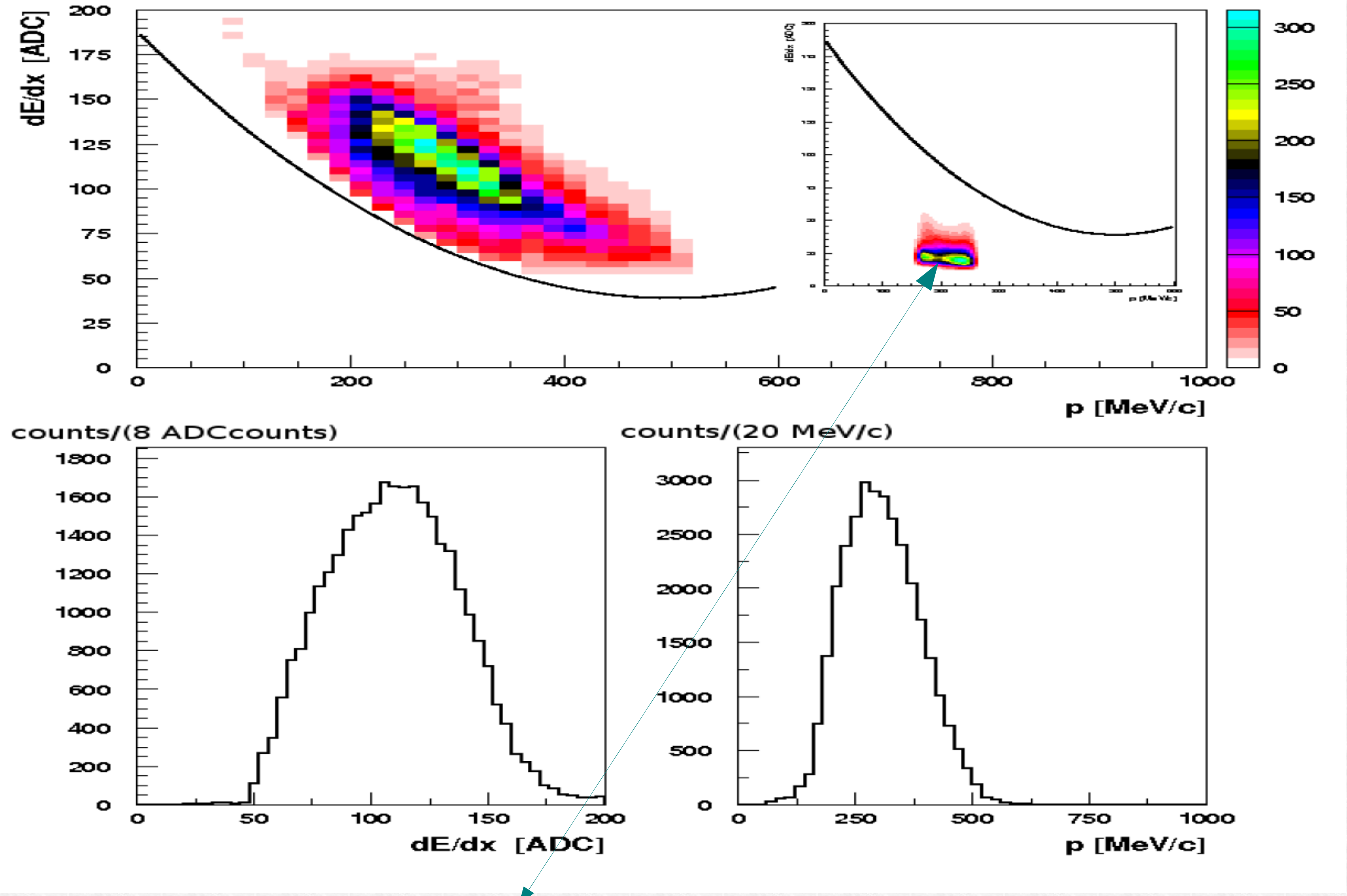

A clear separation with respect to pions (from K^+ two body decay) is evident.

Λ(1116) the signature of K⁻ hadronic interaction

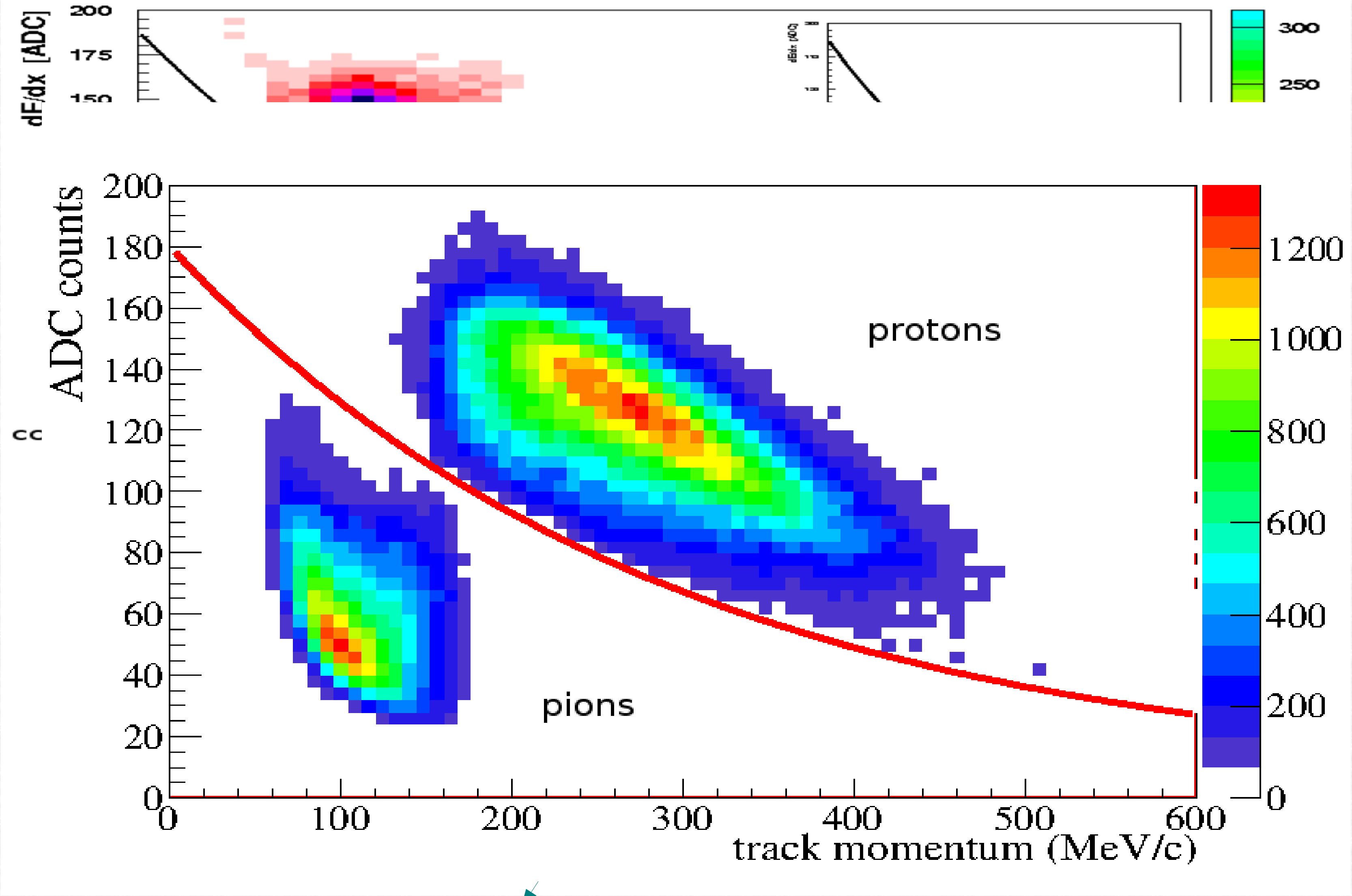

A clear separation with respect to pions (from K^+ two body decay) is evident.

Λ(1116) the signature of K^- hadronic interaction

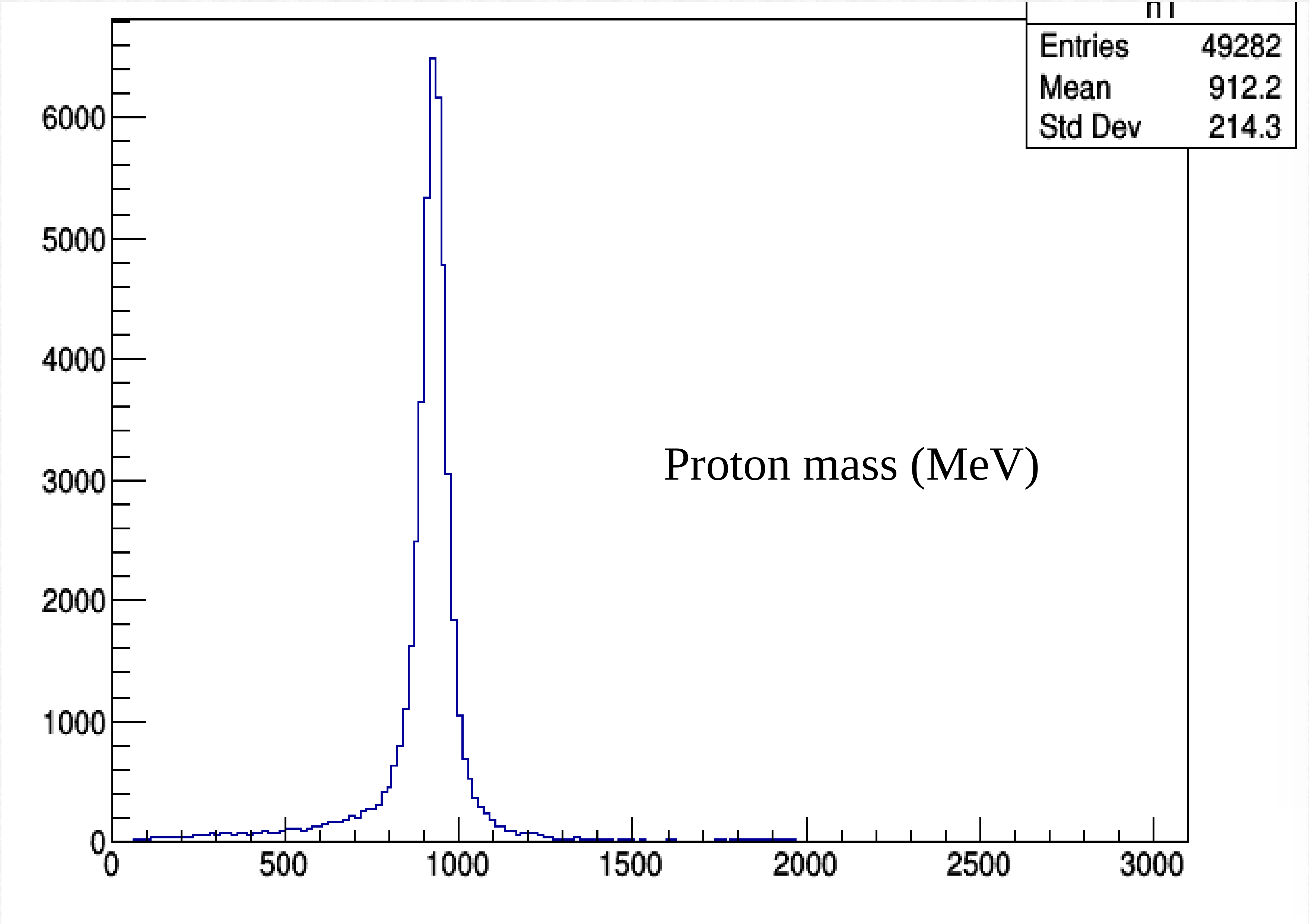

Λ(1116) the signature of K^- hadronic interaction

1^{st} Step: $\Lambda \rightarrow p + \pi^-$ identification (BR = 63.9 ± 0.5 %)

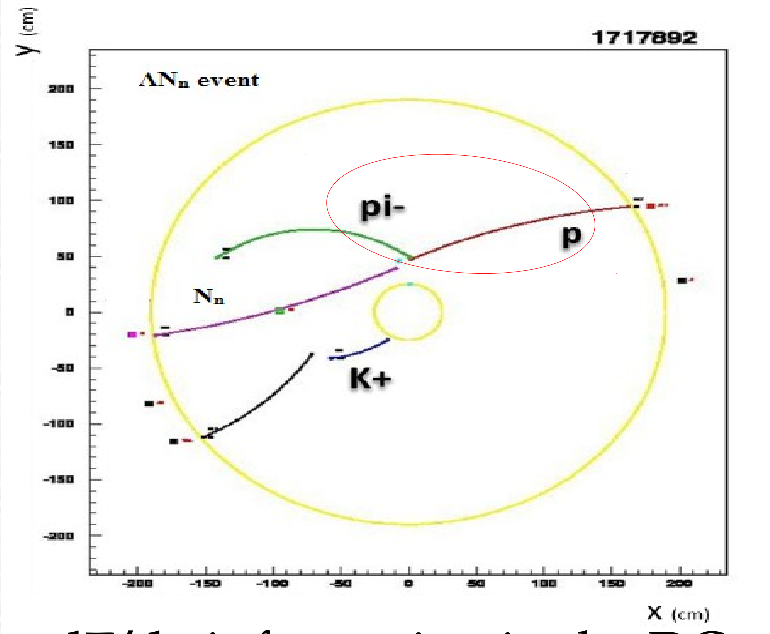

dE/dx information in the DC wires

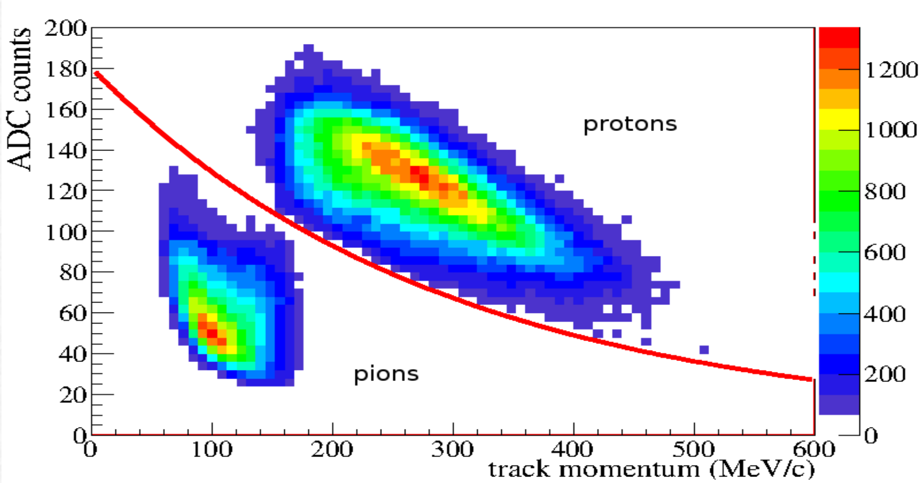

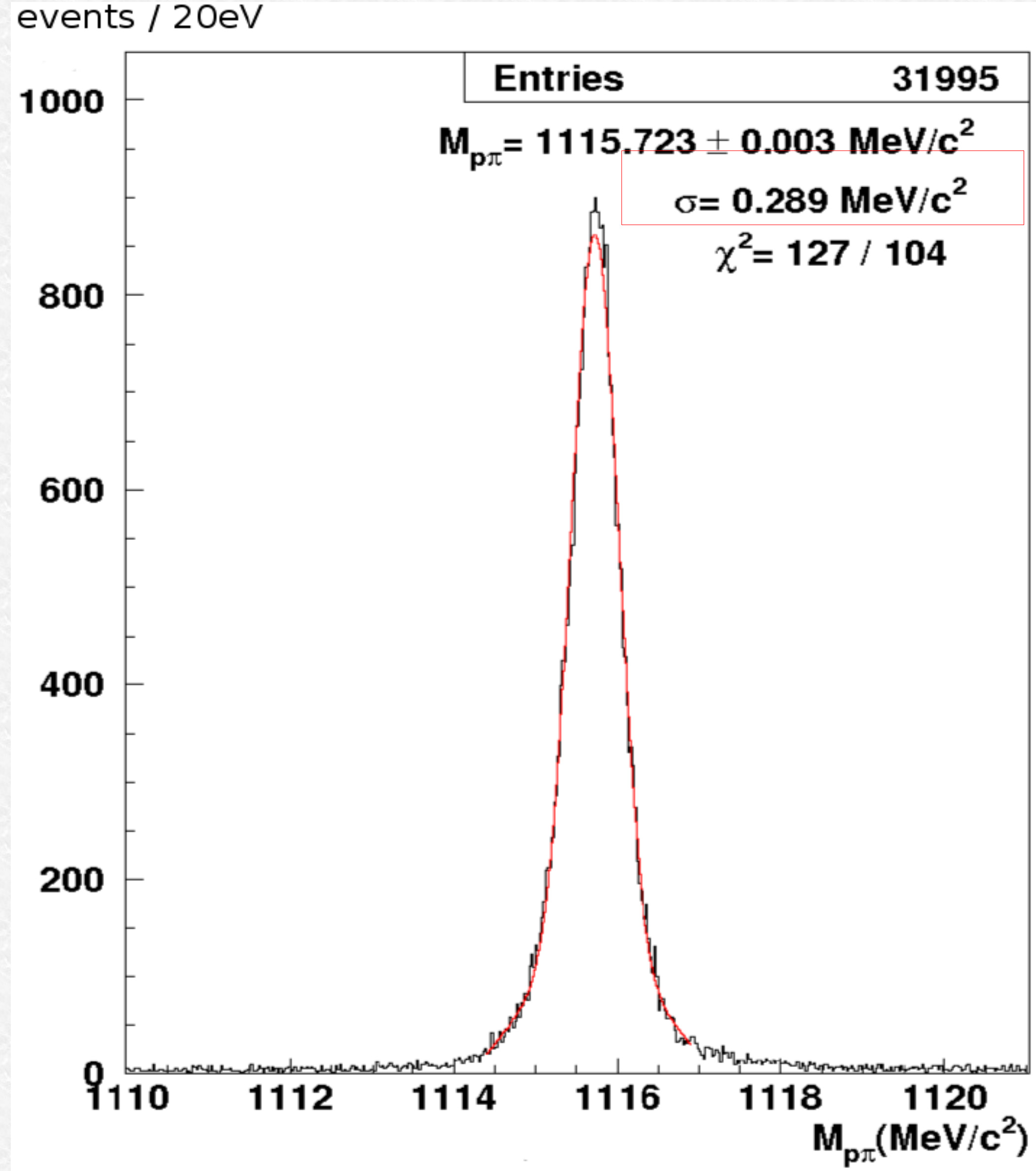

Photons selection

1) Select events with at least three neutral clusters (E_{c1} > 20 MeV) not from K decay ($K^+ \to \pi^+ \pi^0$)

2) **photon clusters selection**: a first minimization is performed $\chi_t^2 = t^2/\sigma_t^2$ where $t = t_i - t_j$ is the difference between time of flights in light speed hypothesis. This selects three photon clusters in time from the Λ decay vertex $\mathbf{r}_\Lambda$.

3) **photon clusters identification**: to distinguish photon clusters from π^0 decay, from γ_3 (due to Σ^0 decay) a second minimization is performed on $\chi_{\pi\Sigma}^2$:

$$\chi^2_{\pi\Sigma} = \frac{(m_{\pi^0} - m_{ij})^2}{\sigma^2_{ij}} + \frac{(m_{\Sigma^0} - m_{k\Lambda})^2}{\sigma^2_{k\Lambda}}$$

i,j and *k* represent one of the previously selected candidate photon cluster.

4) Cuts on χ_t^2 and $\chi_{\pi\Sigma}^2$ variables were optimized using MC simulations. Specific cuts are introduced in order to avoid the selection of splitted clusters or background for π^0

The algorithm has (from true MC information) an efficiency (98±1)% to identify photons and (78±2)% to select the correct triple of neutral clusters.

Photons selection

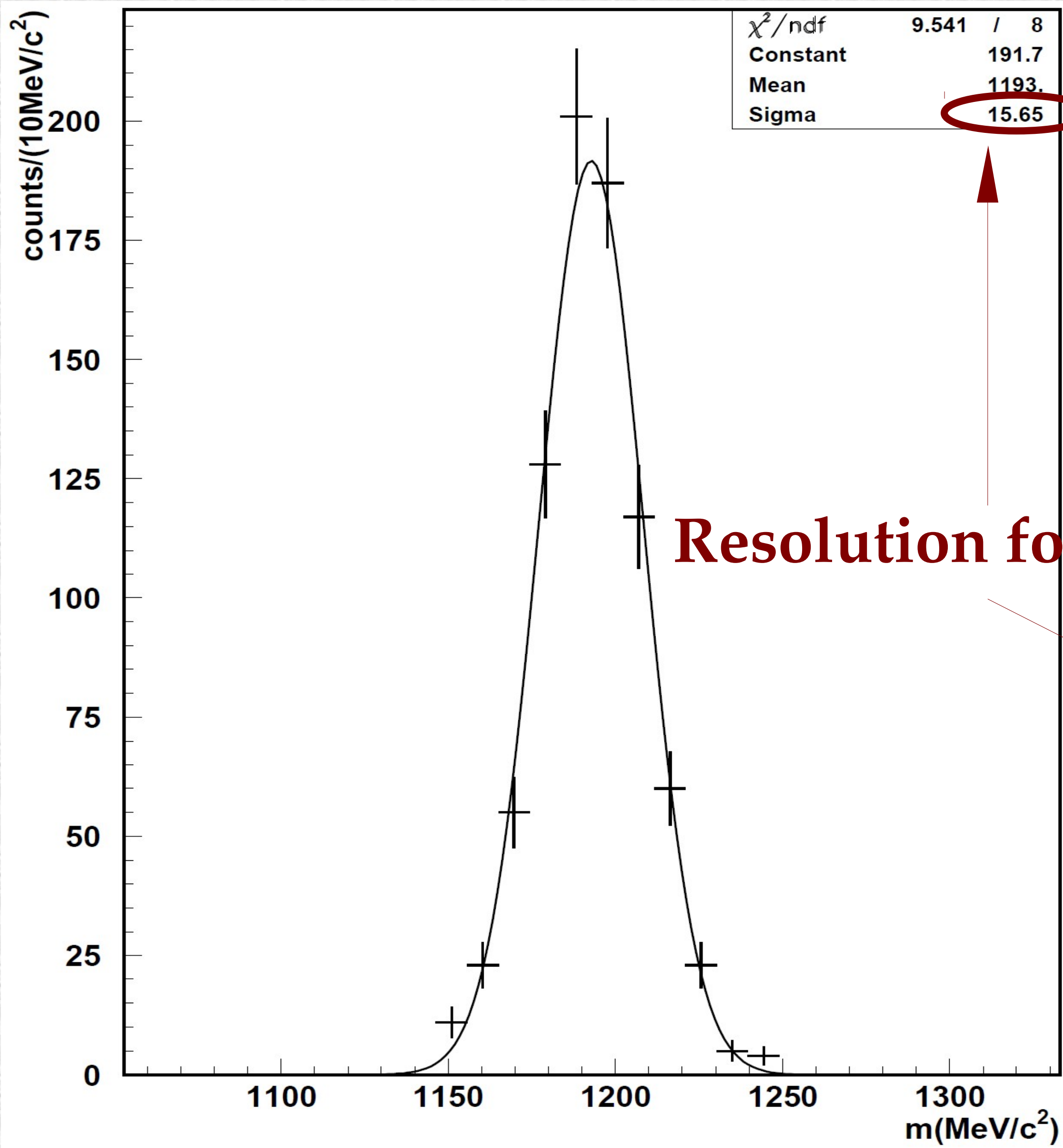

$m_{\Lambda\gamma 3}$

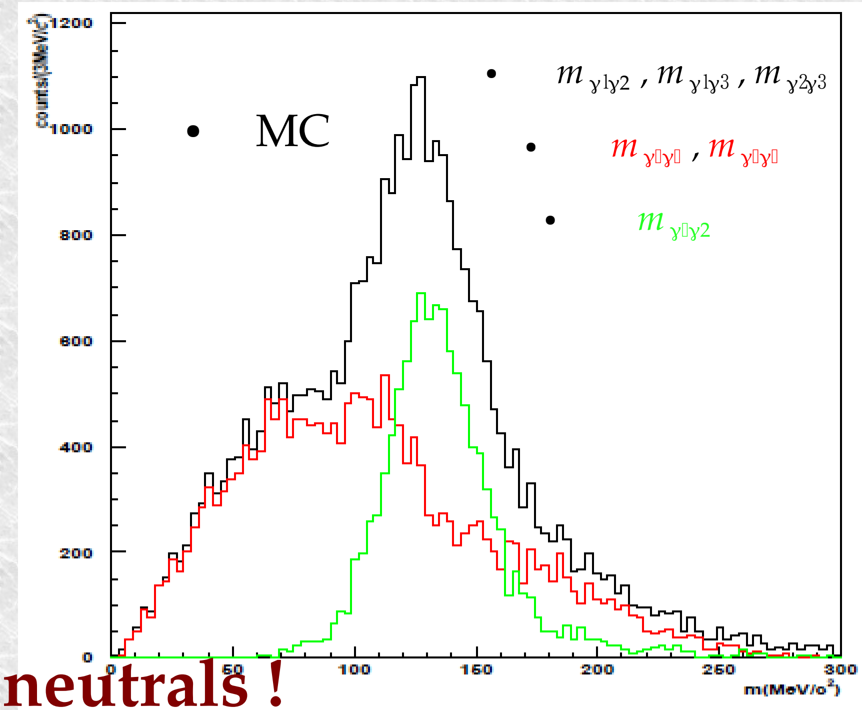

Resolution for neutrals !

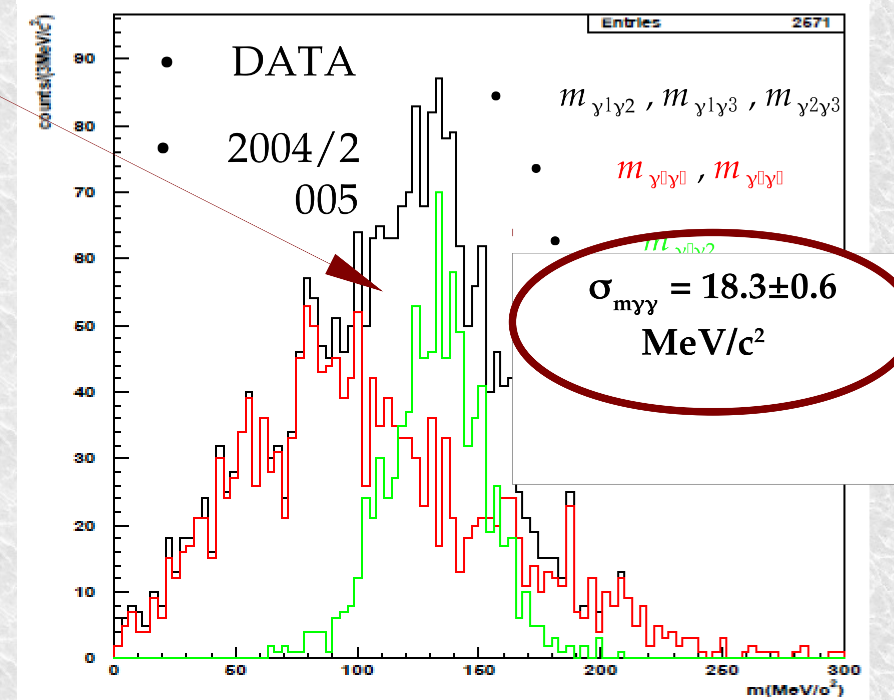

$K^- \ {}^4He \rightarrow \ \Lambda \ \pi^- \ {}^3He$ events selection

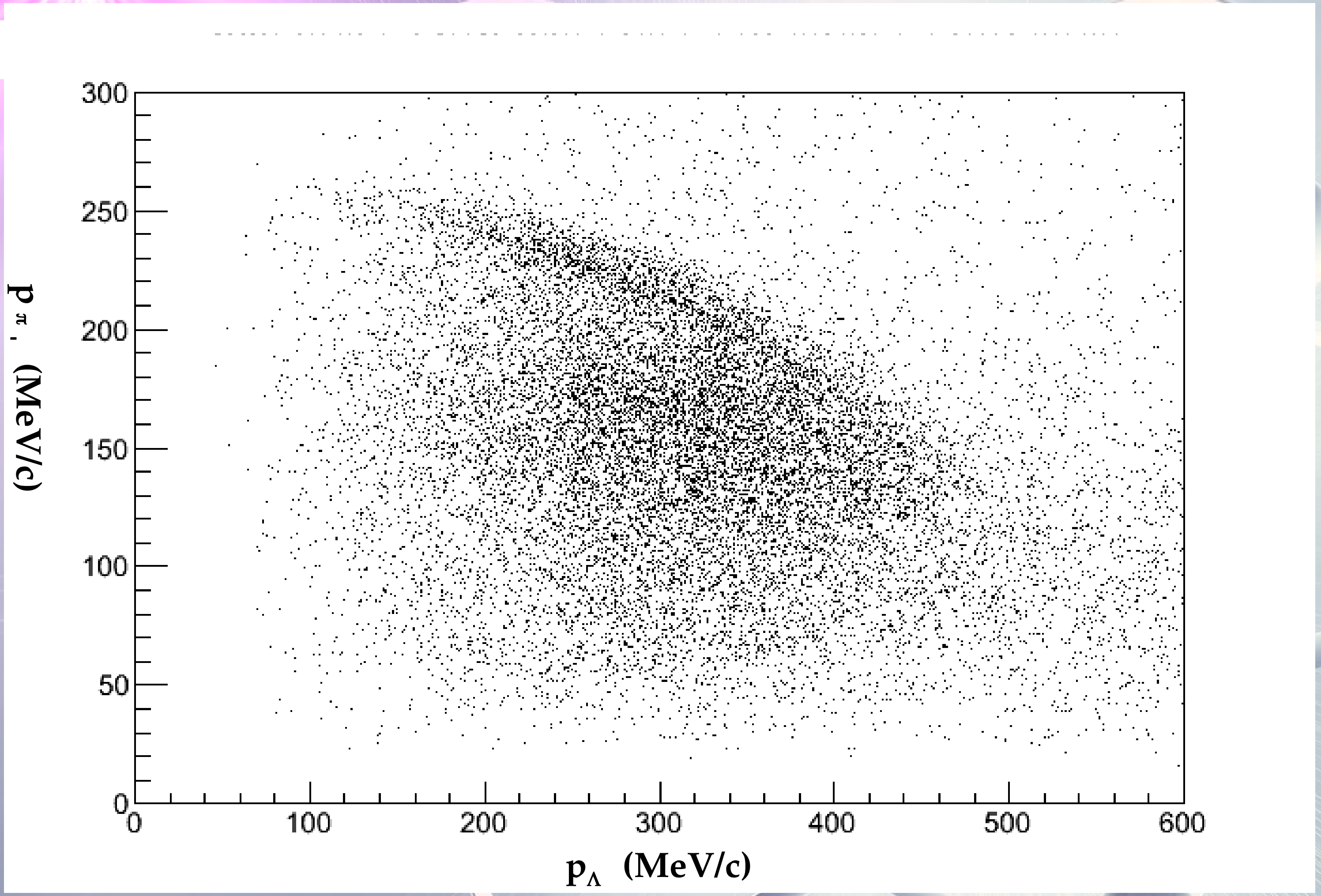

$K^- \ ^4He \rightarrow \Lambda \pi^- \ ^3He$ events selection

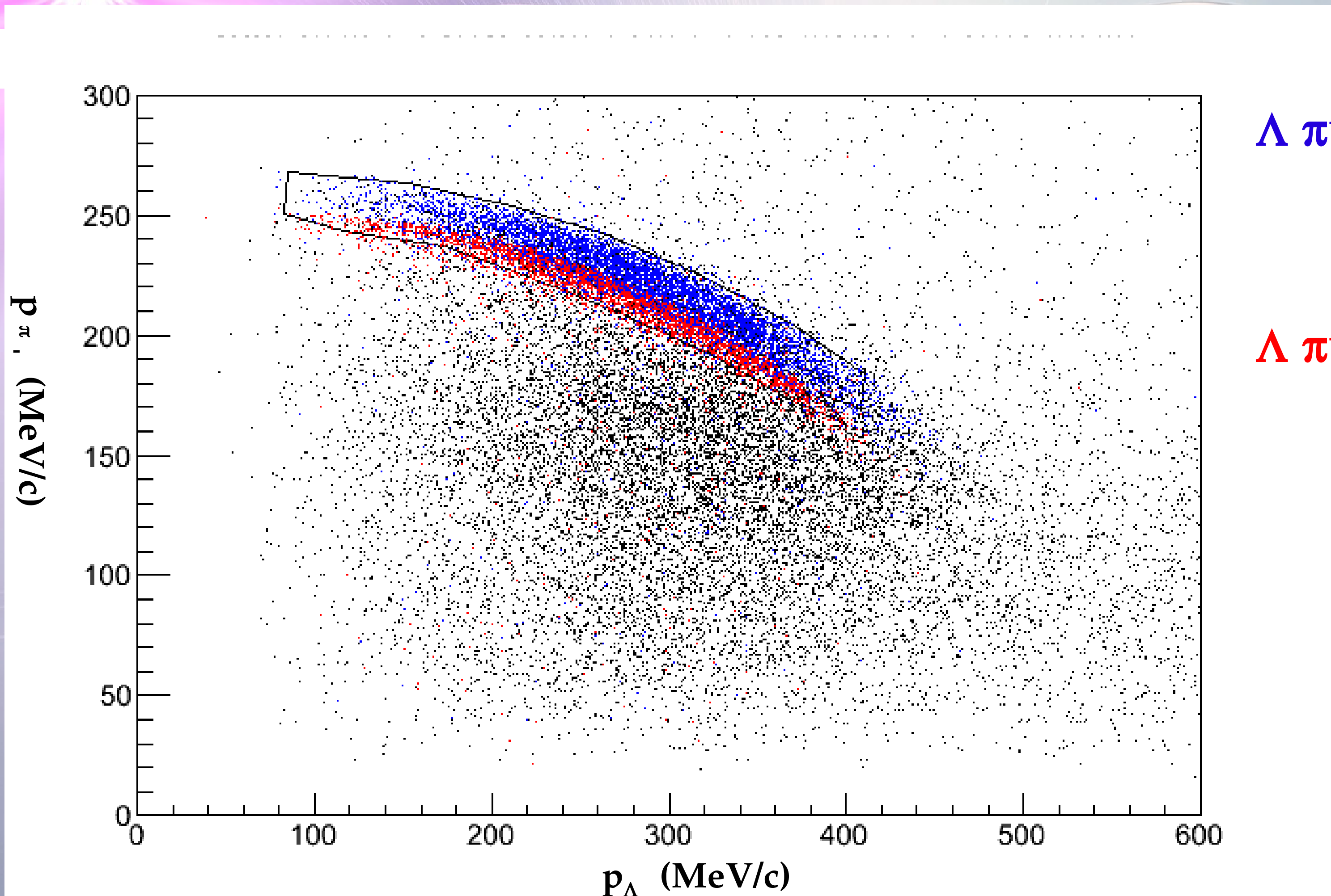

$\Lambda \pi^-$ direct production In-flight RES + NR

$\Lambda \pi^-$ direct production At-rest RES + NR

Background sources: - $\Lambda \pi^-$ events from Σ p/n $\rightarrow$ Λ p/n conversion

- $\Lambda \pi^-$ events from $K^- \ ^{12}C$ absorptions in Isobutane

Further background sources

K$^-$

a) FSI of the Λ was found to introduce a correction to the amplitude < 3%.

b) FSI of the π is found to be negligible.

K^- $^4He \rightarrow$ $\Lambda \pi^-$ ^3He background

- Σ p/n $\rightarrow$ Λ p/n conversion:

  Each possible conversion channel was simulated

  Σ^0 p / Σ^0 n / Σ^+ n / At-rest / In-flight / from RES and N-R produced Σs

- $\Lambda \pi^-$ events from K^- ^{12}C absorptions in Isobutane (90% He, 10% C_4H_{10}):

  K^- ^{12}C DATA in the KLOE DC wall are used

  estimated contribution: $\%(K^- \, ^{12}C) = 0.44 \pm 0.13$

  $N_{KC}/N_{KHe} = (n_{KC}/n_{KHe}) \cdot (\sigma_{KC}/\sigma_{KHe}) \cdot (BR_{KC}(\Lambda \pi^-)/BR_{KHe}(\Lambda \pi^-))$

  Nuovo Cimento 39 A 338-347 (1977)

  K^- ^{12}C not calculated:

  - uncertain initial state of K meson $l_K = 1, 2, 3$
  - 4 nucleons in s-orbit , 8 nucleons in p-orbit
  - final state hyperon interactions

Λt correlation studies.. the background

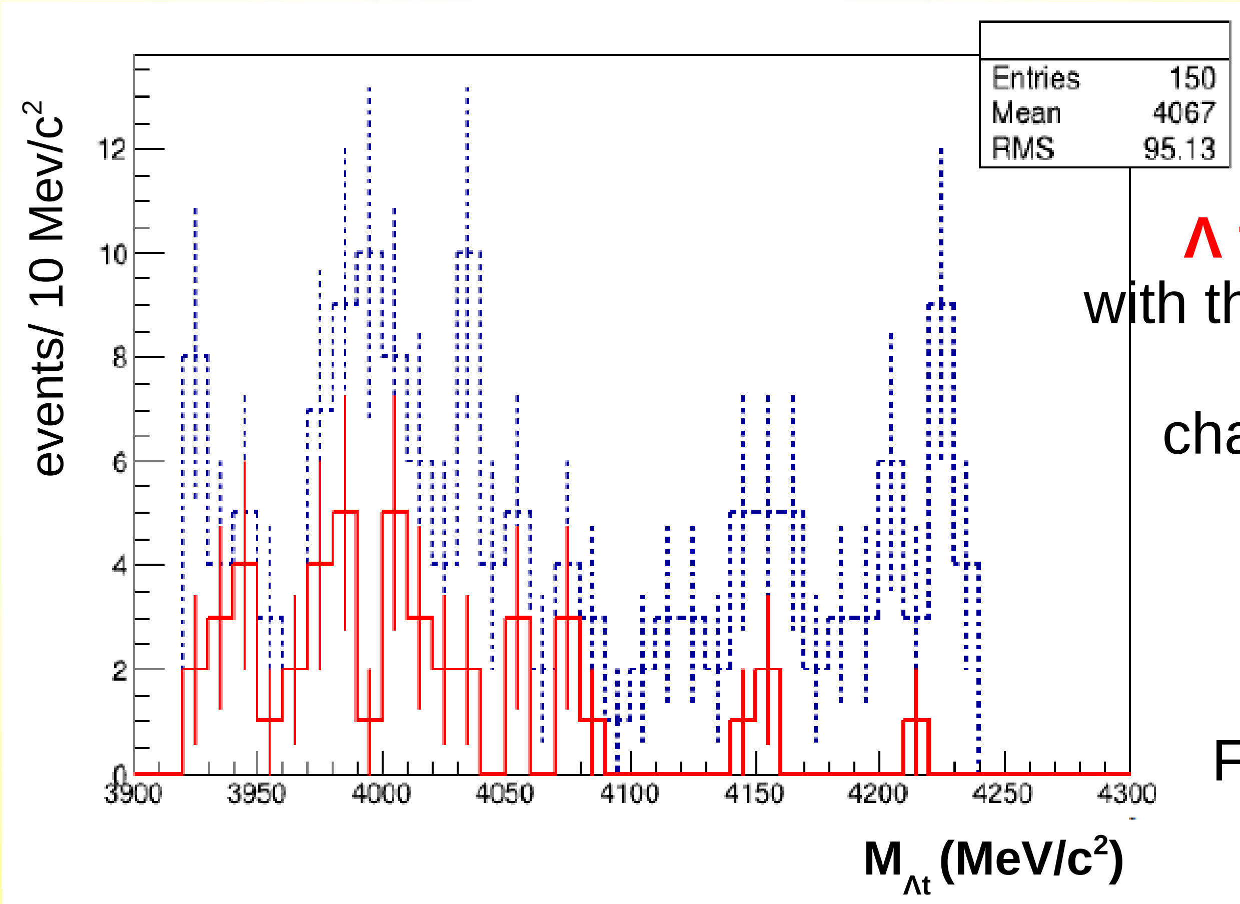

Λ t - p vertices are searched with the same selection criteria for **p**

characterized by lower energy due tu:

BE of the absorbing α
+
FSI of Y/t with the residual

Red points – events containing an **extra proton** (not possible in pure ^4He)

→ **K^- ^{12}C captures in isobutane**

MC simulations: K^- 4NA in ^{4}He at-rest

$$E_i = E_f = \sqrt{m_\Lambda^2 + P^2} + \sqrt{m_t^2 + P^2} = 4221 \mathrm{MeV/c^2} \rightarrow$$

$$|\mathbf{P}| = |\mathbf{p}_\Lambda| = |\mathbf{p}_t| = 711.7 \mathrm{MeV/c}$$

kinematics is closed

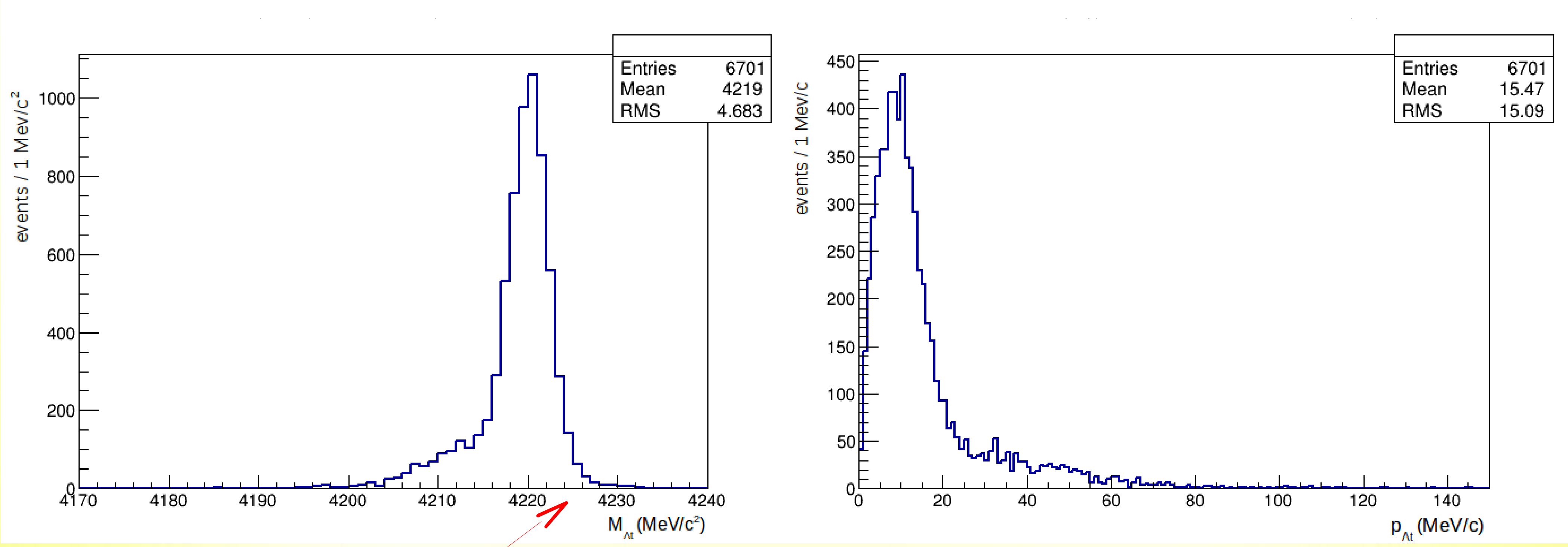

Lower mass threshold

MC simulations: K^- 4NA in ^{4}He in-flight

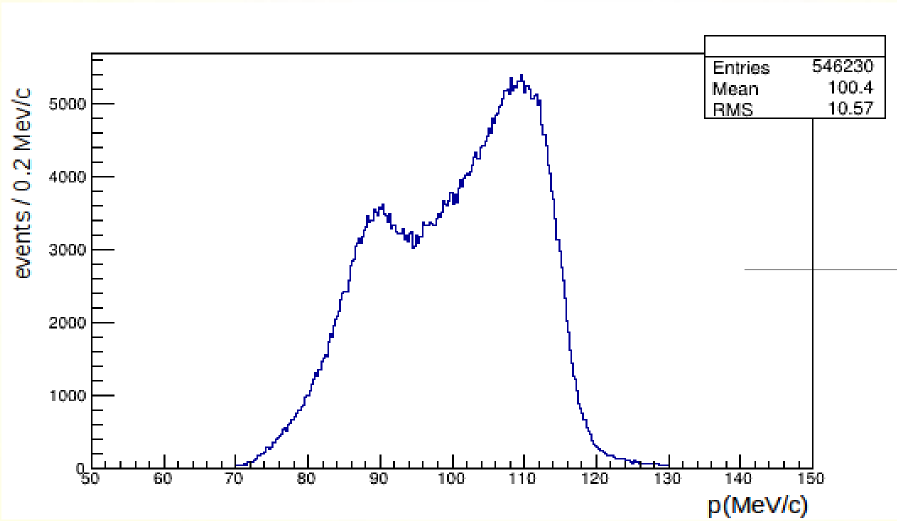

Measured **K^-** momentum at the last point of the track
(in absorption events)
used as an input for the simulation

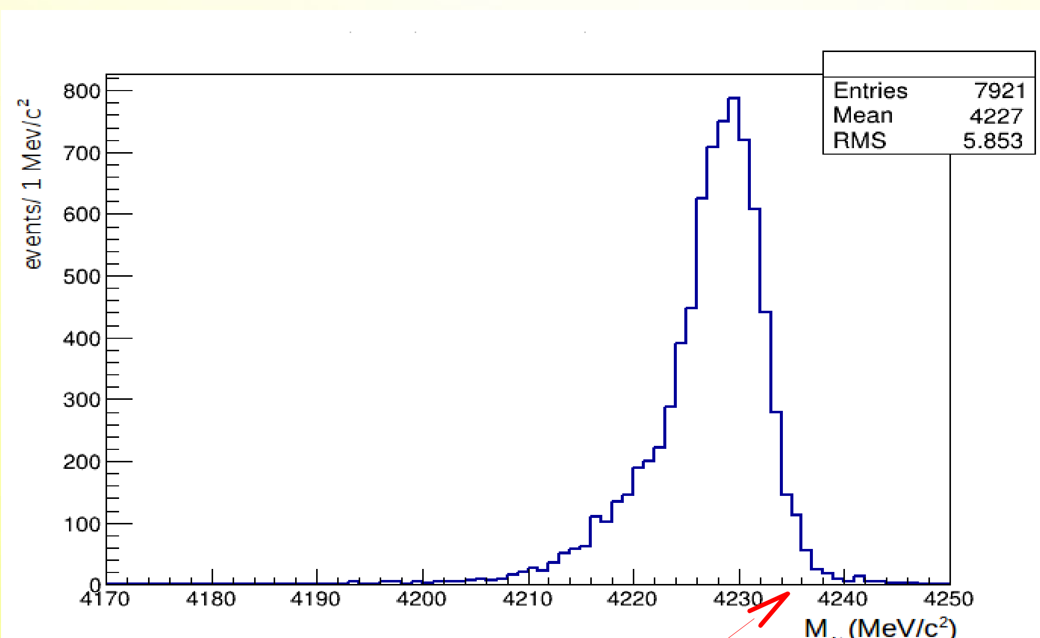

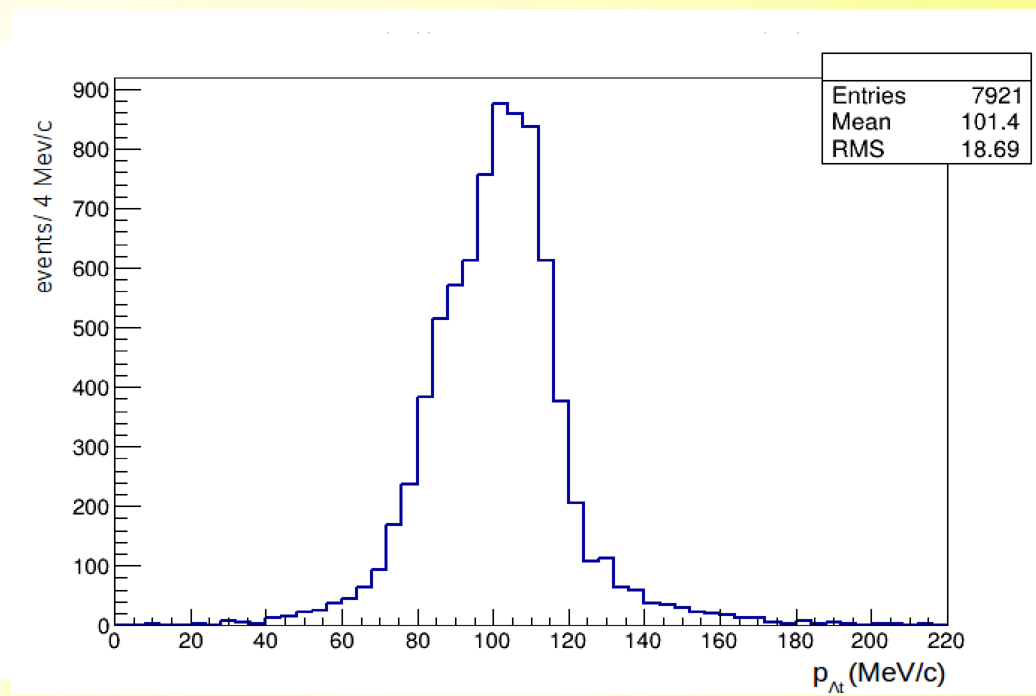

higher mass threshold

Λt correlation studies in ^{4}He from the DC gas

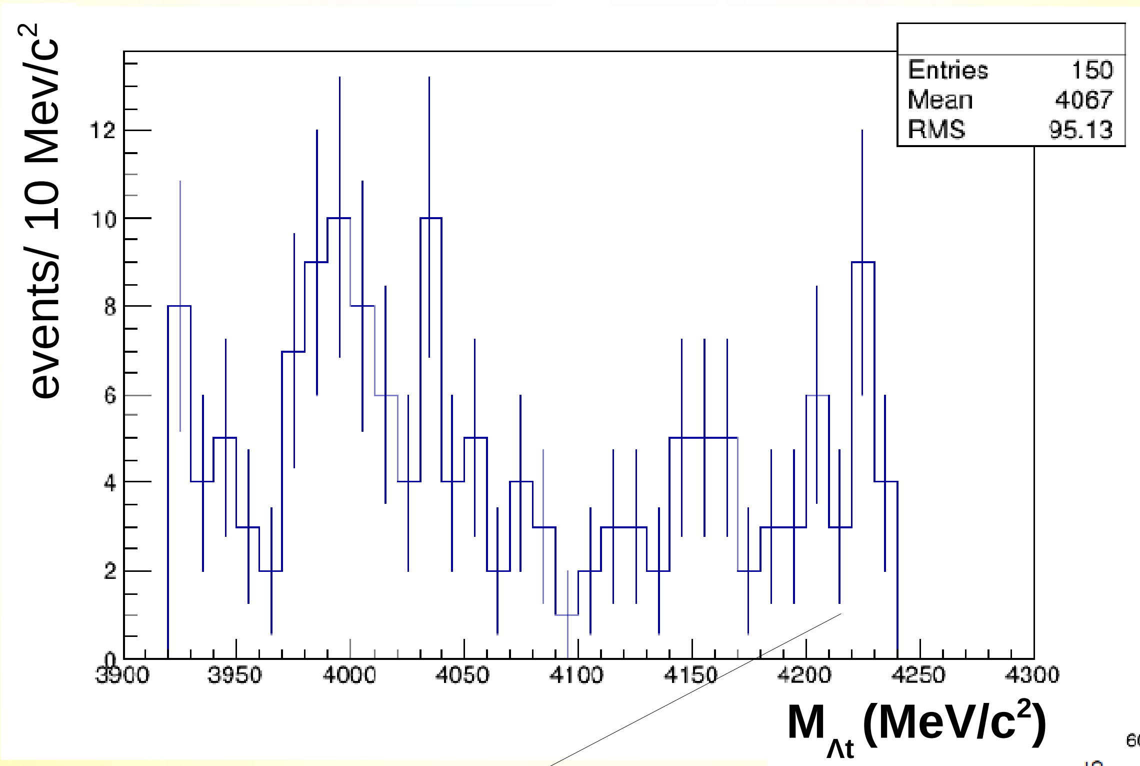

back-to-back Λt events

from 4NA

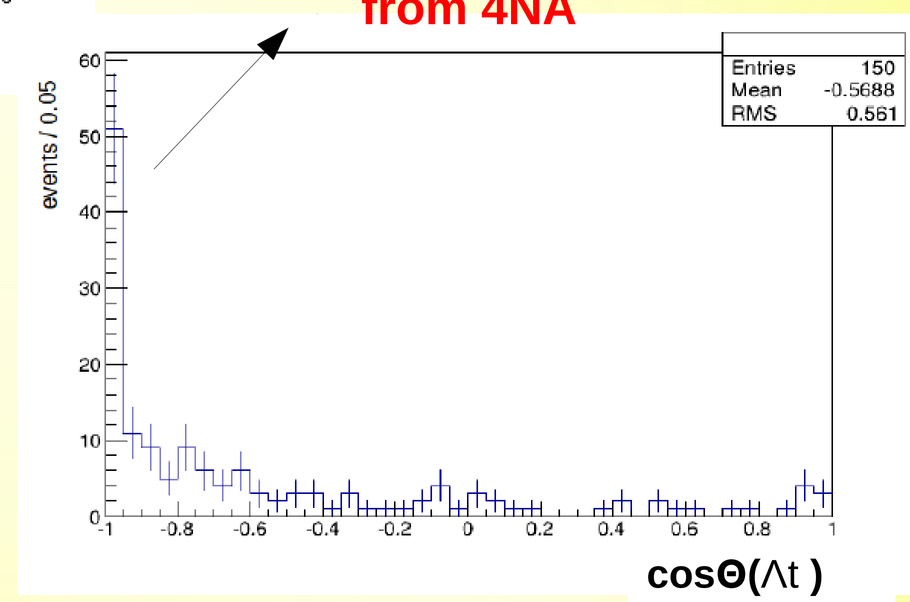

4NA process :

- **highest part of invariant mass spectrum**
- **back-to-back topology**

Λt correlation studies in ^{4}He from the DC gas

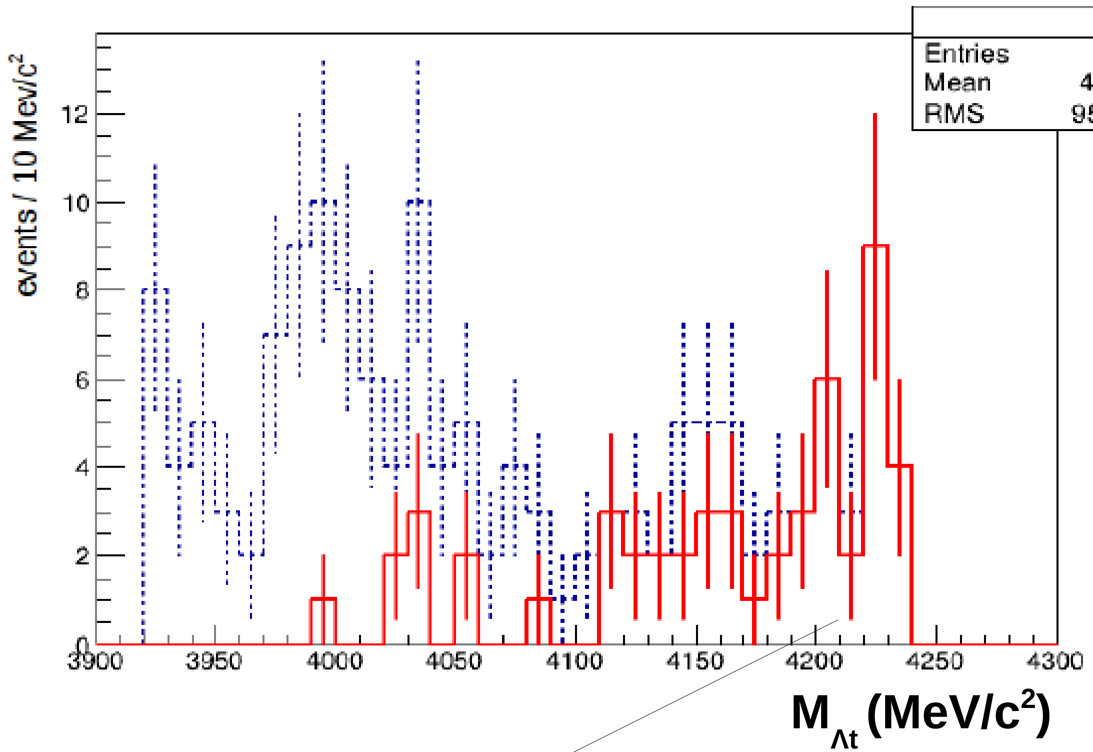

red line -
back to back events
($\cos\Theta_{\Lambda t}$) < -0.95

4NA process :

- highest part of invariant mass spectrum
- back-to-back topology

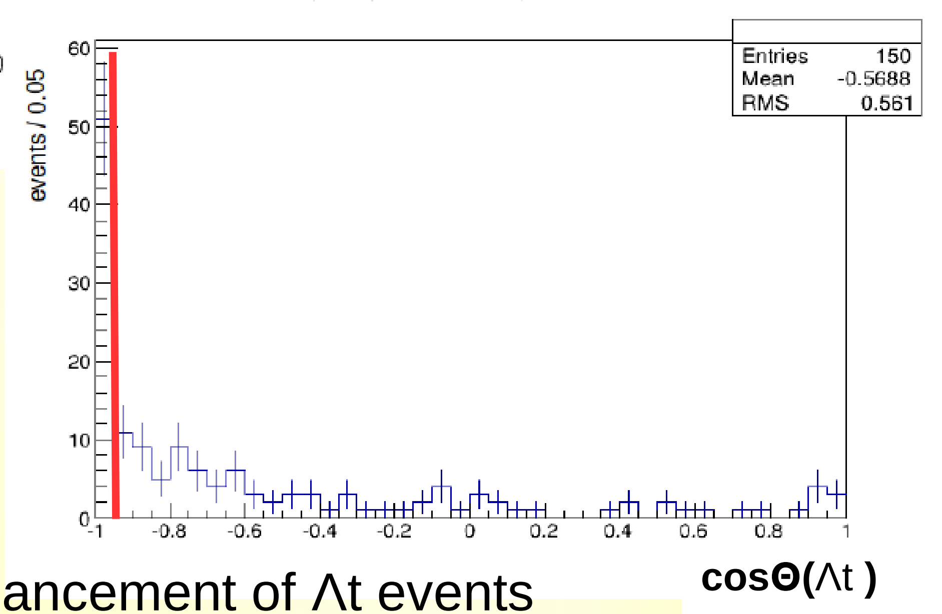

Clear back-to-back enhancement of Λt events

BR calculation

$$\mathbf{BR} = \frac{N(\Lambda t)_{tag,fit} \; / \; eff(\Lambda t)_{tag} \; / \; BR(\Lambda \rightarrow p\,\pi^-)}{N(K^+_{\ tag}) \cdot \%K_{stop}}$$

$$N\,(K^+_{\ tag}) = L_{lum} \times \sigma_{e+e- \rightarrow \Phi} \times BR\,(\Phi \rightarrow K^+K^-) \times c_{tag}$$

$BR(\Lambda \rightarrow p\,\pi^-) = (63.9 \pm 0.5)\ \%$

$L_{lum} = 1.74\ fb^{-1}$

$\sigma_{e+e- \rightarrow \Phi} = 3.1\ \mu b$

$BR\,(\Phi \rightarrow K^+K^-) = (48.9 \pm 0.5)\ \%$

$C_{tag} = 0.2585 \pm 0.0002$

Obtained by MC

$K_{stop,gas} = (0.161 \pm 0.004)\ \%$

Cross section calculation

$$\sigma = \frac{N(\Lambda t)_{tag,fit} \;/\; eff(\Lambda t)_{tag} \;/\; BR(\Lambda \rightarrow p\,\pi^-)}{N(K^+_{\;tag}) \cdot \%K_{DECAY} \cdot L_{material} \cdot n_{centers,m}}$$

$$n_{centers,m} = \frac{N_{AV}}{A_{material}} \cdot \rho_{material}$$

$N_{AV} = 6.022 \cdot 10^{23}$ - Avogadro number

$A_{gas} = 4.003$ g – atomic weight of ^{4}He

$\rho_{gas} = 0.4271\ 10^{-3}$ g/cm^3 from which 4He partial density was obtained

L_{gas} = sum of lenghts of 5 cm to take care of the kaon decay

Mean K- momentum at hadronic absorption in-flight

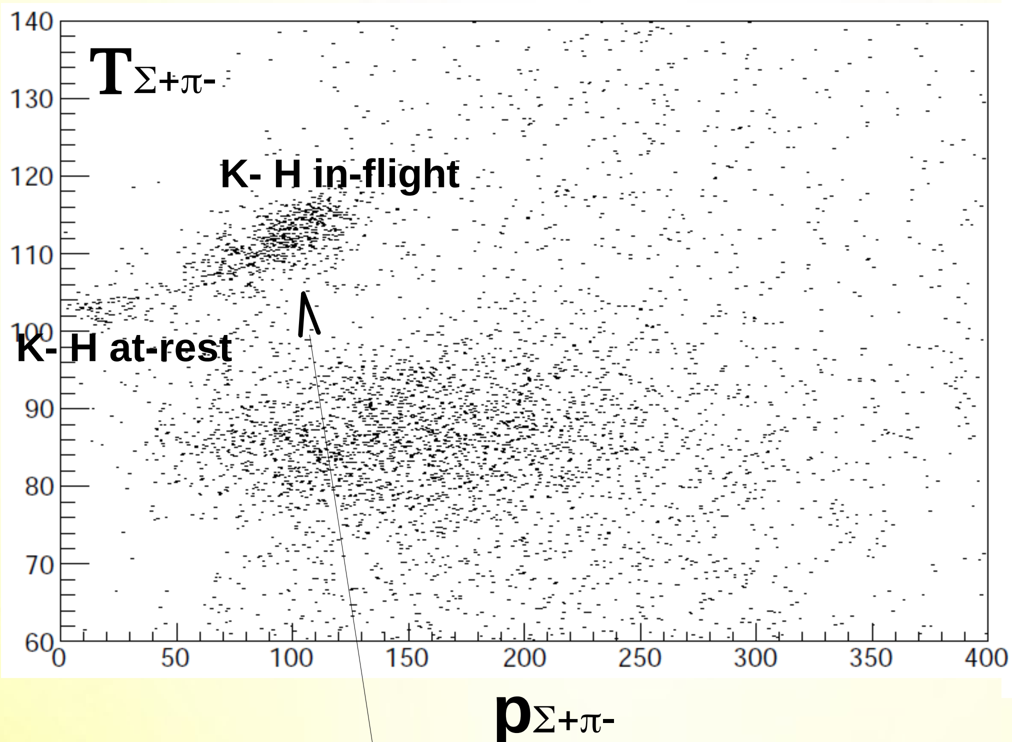

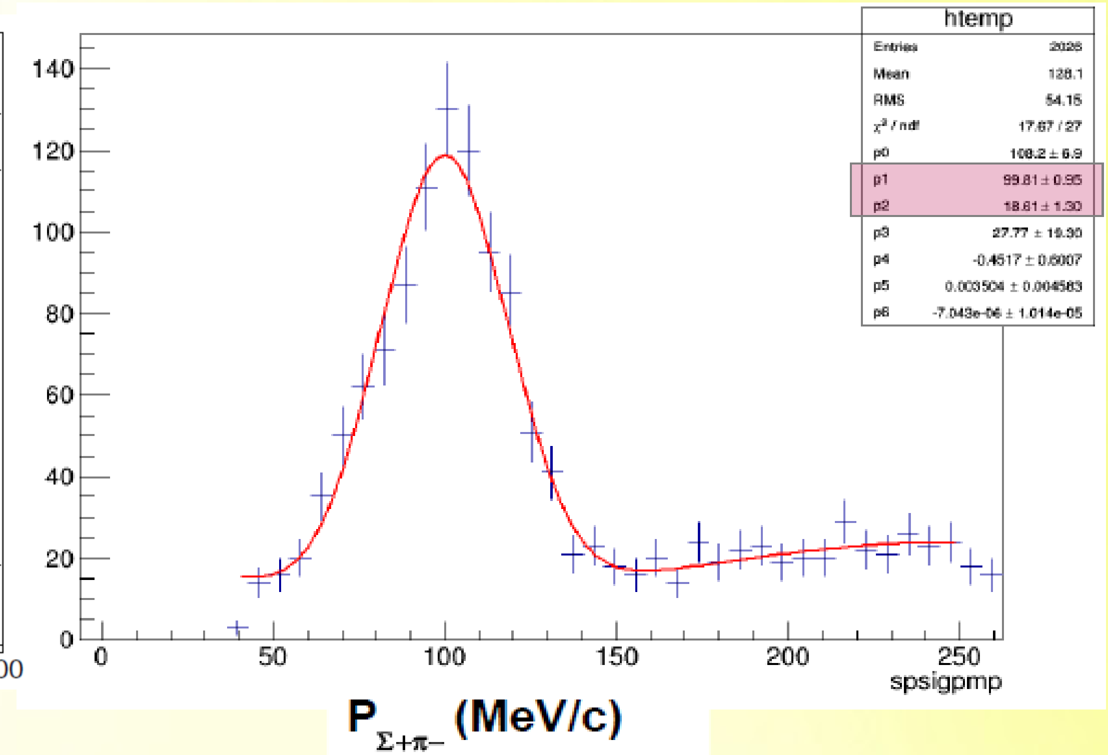

K- momentum when interacting in-flight in the DC gas, obtained by fitting the Σ+π- momentum spectrum, from K- H absorptions (H from C4H10), Gaussian + polinomial fit.

Advantages:

- Pk not dependent on the hadronic channel,
- high statistics
- good resolution

$P_K = 99.81 \pm 18.81$ MeV/c

Mean K- momentum at hadronic absorption in-flight

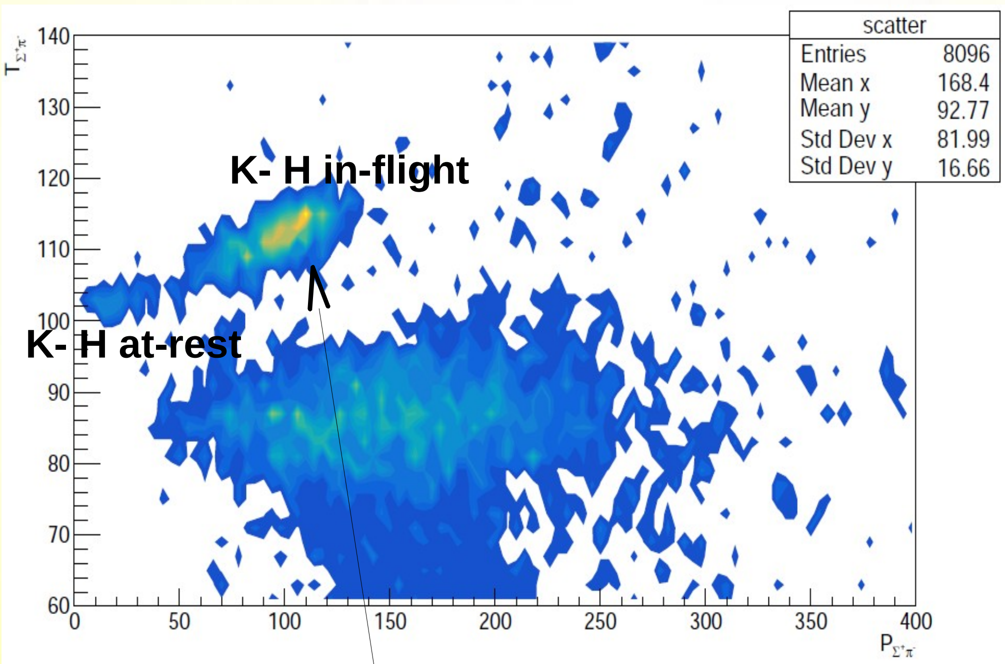

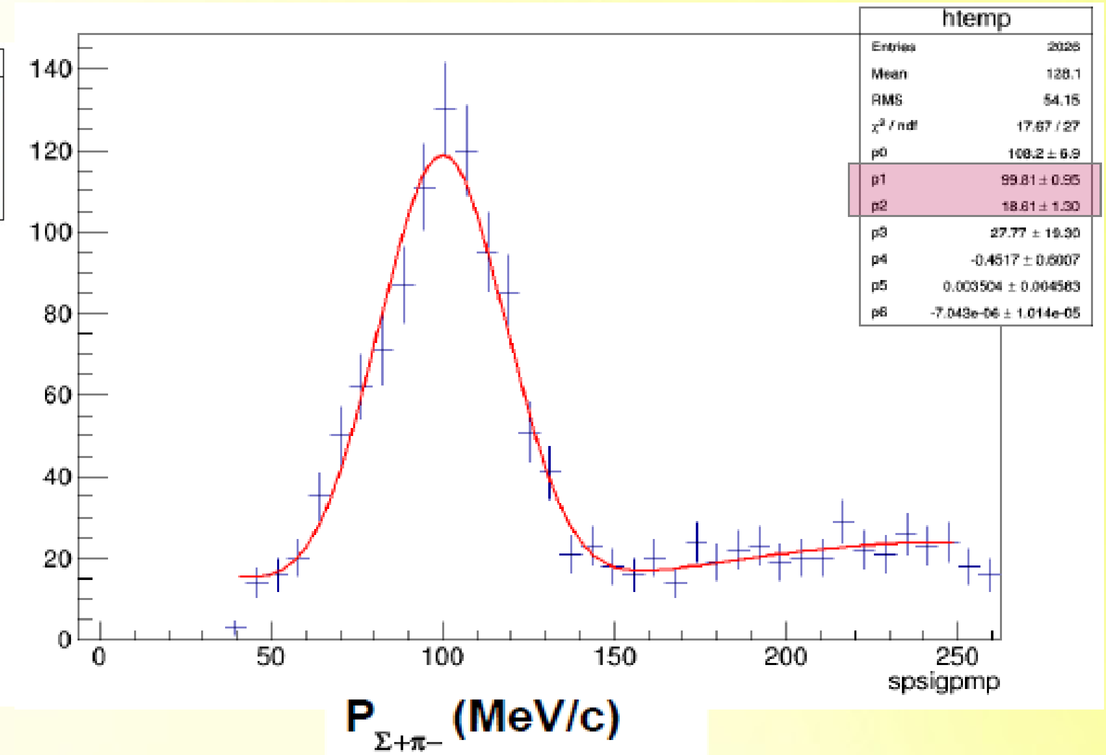

K- momentum when interacting in-flight in the DC gas, obtained by fitting the Σ+π- momentum spectrum, from K- H absorptions (H from C4H10), Gaussian + polinomial fit.

Advantages:

- Pk not dependent on the hadronic channel,
- high statistics
- good resolution

$P_K = 99.81 \pm 18.81$ MeV/c

Λt invariant mass geometric + reconstruction acceptance

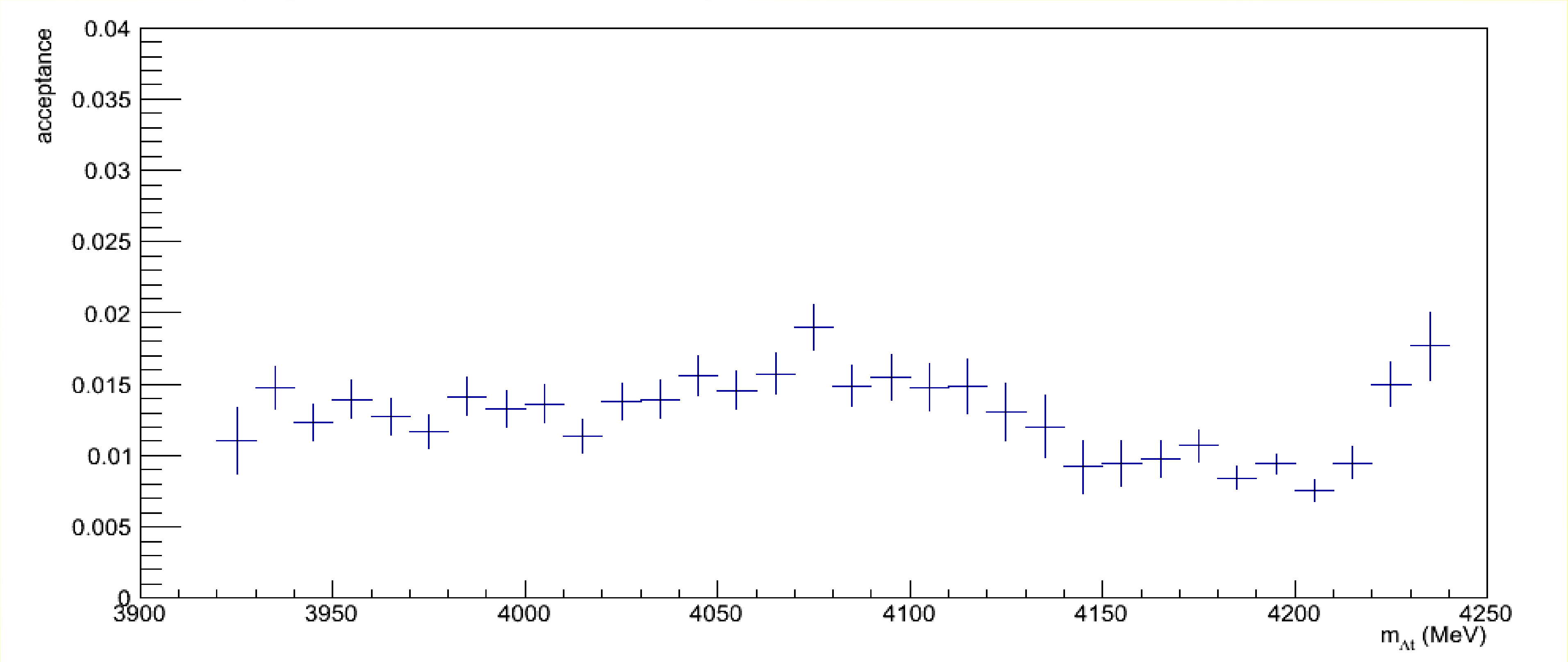

Obtained by simulating: K- 4NA absorptions on 4He (at-rest + in-flight)
K- 4NA absorptions on 12C (at-rest + in-flight) w. o. final state
K- 4NA absorptions on 12C (at-rest + in-flight) with final state of the lambda

In order to cover all the available phase space,
correlations mantained by conserving energy and momentum.
2.5 * 10^5 simulated events.

Λt invariant mass geometric + reconstruction acceptance corrected

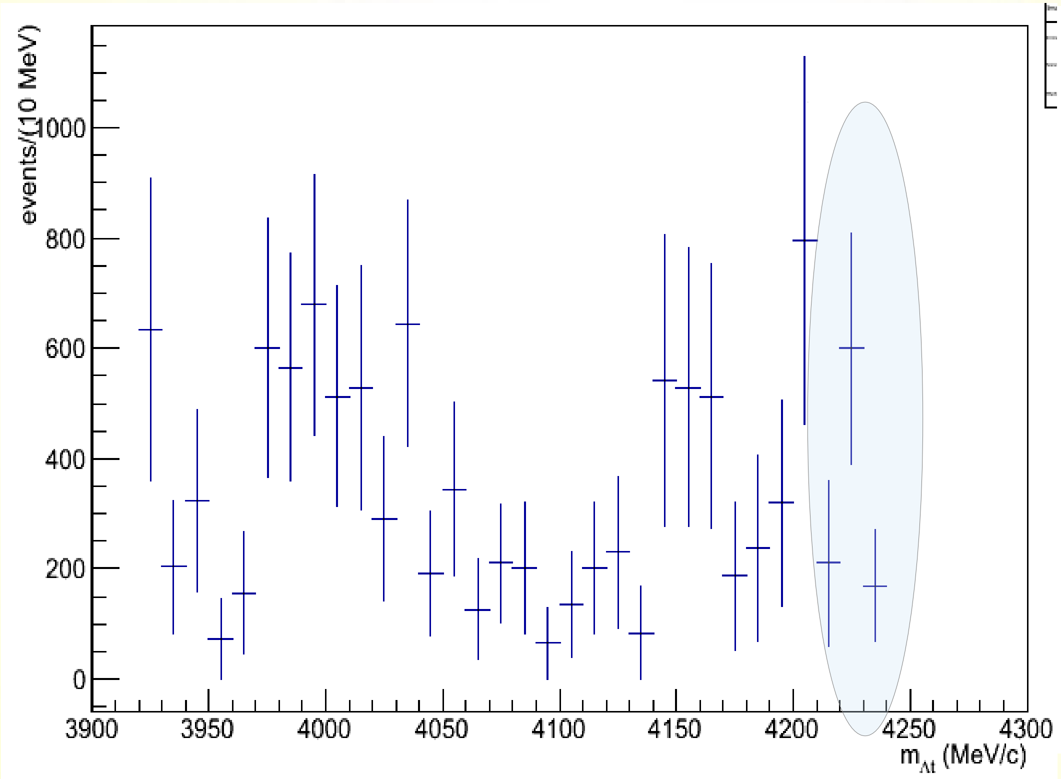

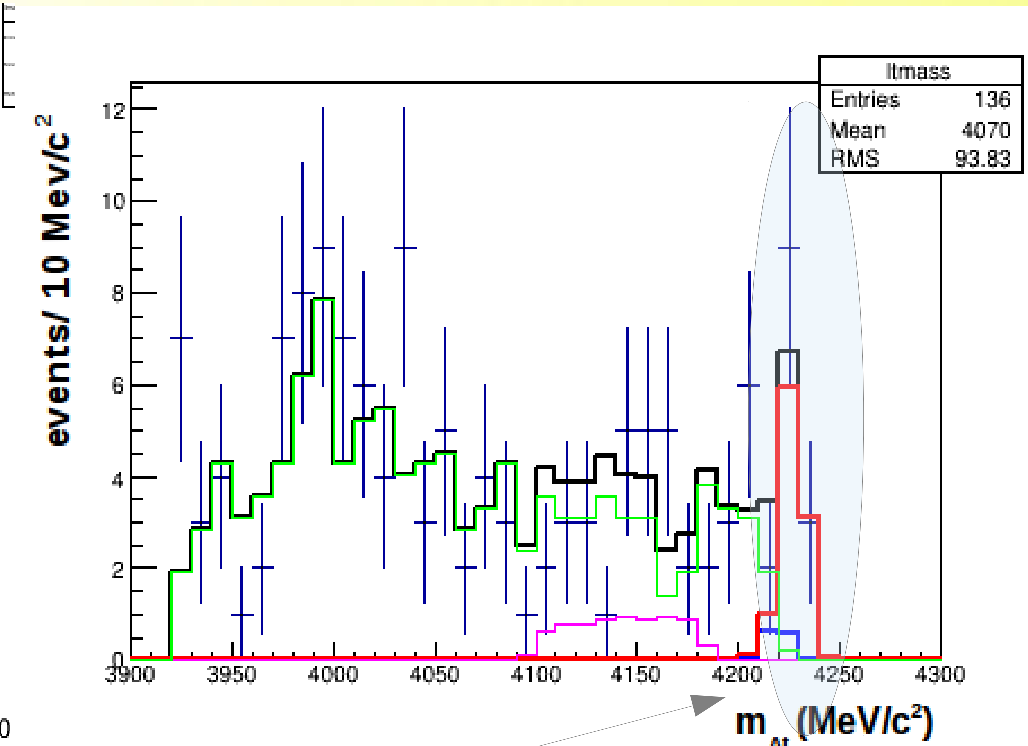

K- 4NA absorptions on 4He in-flight

Not significantly distorted